ИЗМЕРИТЕЛЬНАЯ ТЕХНИКА

Number 9, September, 1960
Translation Published April, 1961

OF MICHIGAN
MAY 22 1961
ENGINEERING LIBRARY

SOVIET INSTRUMENTATION AND CONTROL TRANSLATION SERIES

Measurement Techniques

(The Soviet Journal *Izmeritel'naya Tekhnika* in English Translation)

■ This translation of a Soviet journal on instrumentation is published as a service to American science and industry. It is sponsored by the Instrument Society of America under a grant in aid from the National Science Foundation with additional assistance from the National Bureau of Standards.

SOVIET INSTRUMENTATION AND CONTROL TRANSLATION SERIES

Instrument Society of America Executive Board

Dr. Ralph H. Tripp
President
J. Johnston, Jr.
Past President
Philip A. Sprague
President-elect-Secretary
Henry J. Noebels
Dept. Vice President
E. A. Adler
Dept. Vice President
Adelbert Carpenter
Dept. Vice President
Nathan Cohn
Dept. Vice President
Francis S. Hoag
Dept. Vice President-elect
John C. Koch
Treasurer
Nelson Gildersleeve
Dist. I Vice President
H. Kirk Fallin
Dist. II Vice President
John R. Mahoney
Dist. III Vice President
F. R. Gilmer
Dist. IV Vice President
Milton M. McMillen
Dist. V Vice President
Otto J. Lessa
Dist. VI Vice President
J. Howard Park, III
Dist. VII Vice President
Roy Horton
Dist. VIII Vice President
Robert C. Mann
Dist. IX Vice President
Kenneth S. Vriesen
Dist. X Vice President
John J. McDonald
Dist. XI Vice President

Headquarters Office

William H. Kushnick
Executive Director
Charles W. Covey
Editor, ISA Journal
Herbert S. Kindler
Director, Tech. & Educ. Services
Ralph M. Stotsenburg
Director, Promotional Services
Ira S. French
Director, Public Relations

ISA Publications Committee

Charles O. Badgett, *Chairman*

Jere E. Brophy	George A. Larsen	Joshua Stern
Dr. Enoch J. Durbin	Thomas G. MacAnespie	Frank S. Swaney
Prof. Richard W. Jones	John E. Read	Richard A. Terry

Translations Advisory Board of the Publications Committee

Jere E. Brophy, *Chairman*

T. J. Higgins	S. G. Eskin	G. Werbizky

■ This translation of the Soviet Journal *Izmeritel'naya Tekhnika* is published and distributed at nominal subscription rates under a grant in aid to the Instrument Society of America from the National Science Foundation. This translated journal, and others in the Series (see back cover), will enable American scientists and engineers to be informed of work in the fields of instrumentation, measurement techniques, and automatic control reported in the Soviet Union.

The original Russian articles are translated by competent technical personnel. The translations are on a cover-to-cover basis and the Instrument Society of America and its translators propose to translate faithfully all of the scientific material in *Izmeritel'naya Tekhnika*, permitting readers to appraise for themselves the scope status, and importance of the Soviet work. All views expressed in the translated material are intended to be those of the original authors and not those of the translators nor the Instrument Society of America.

Publication of *Izmeritel'naya Tekhnika* in English translation started under the present auspices in August, 1959, with Russian issue No. 1 of Jan.-Feb. 1958. The program has been continued with the translation and printing of the 1959 and 1960 issues which are monthlies.

Transliteration of the names of Russian authors follows the system known as the British Standard. This system has recently achieved wide adoption in the United Kingdom, and is currently being adopted by a large number of scientific journals in the United States.

Readers are invited to submit communications on the quality of the translations and the content of the articles to ISA headquarters. Pertinent correspondence will be published in the "Letters" section of the ISA Journal. Space will also be made available in the ISA Journal for such replies as may be received from Russian authors to comments or questions by American readers.

1960 Volume Subscription Prices:

Per year (12 issues), starting with 1960, No. 1

General: United States and Canada	$25.00
Elsewhere	28.00
Libraries of nonprofit academic institutions:	
United States and Canada	$12.50
Elsewhere	15.50
Single issues to everyone, each	$ 6.00

1958 and 1959 issues also available. Prices upon request.

See back cover for combined subscription to entire Series.

Subscriptions and requests for information on back issues should be addressed to the:

Instrument Society of America
313 Sixth Avenue, Pittsburgh 22, Penna.

Translated and printed by Consultants Bureau Enterprises, Inc.

Copyright © 1961 by the Instrument Society of America

EDITORIAL BOARD OF IZMERITEL'NAYA TEKHNIKA

G. D. Burdun *(Editor)*
I. I. Chechik *(Asst. Editor)*
V. I. Ermakov
N. M. Karelin
M. I. Levin
G. N. Sharonov
L. M. Zaks
M. K. Zhokhovskii

Measurement Techniques

A translation of Izmeritel'naya Tekhnika, a publication of the Academy of Sciences of the USSR

Russian Original Dated September, 1960

1960, No. 9, pp. 727-816 April, 1961

CONTENTS

	PAGE	RUSS. PAGE
LINEAR MEASUREMENTS		
Measuring the Waviness of Frictionless Bearing Races. V. V. Matveev, A. N. Puzyr'kov and V. L. Ryaskov	727	1
Determining the Roughness of Casting Surfaces. V. N. Levitskii	729	3
Errors in Determining Regular Undulations of Cylindrical Surfaces. Z. P. Grozinskaya	730	3
Frequency Characteristics of Feeler Profilometers. A. I. Boyarov	733	5
Automatic Control of Dimensional Accuracy in Internal Grinding. Hua Ch'ang-ken	735	7
Investigating Errors in Optical Dividing Heads. L. Ya. Gustyr'	739	10
MEASUREMENTS OF MASS		
Hydrostatic Weighing of Liquids in Containers of Complex Shape. L. P. Stepanov	742	12
Elimination of Errors in Loaded Piston Scales Due to the Leakage of Liquid Through the Gaps. V. N. Gramenitskii	744	13
MEASUREMENT OF TIME		
Dynamic Accuracy of Trigger Regulators with Unstable Pulses. V. A. Shpolyanskii	747	16
MECHANICAL MEASUREMENTS		
A Machine for the Calibration and Checking of Dynamometers up to 50 Ton-Wt. O. N. Fofanov	756	22
A Bell Differential Manometer DKFM. M. D. Gafanovich and B. Ya. Gorodetskii	758	23
An Autocompensated Thermal Vacuum Gauge. V. I. Bakhtin and V. N. Mikhailin	760	25
Measurement of Accelerations by Means of Piezoelectric Transducers Working in Strain-Gauge Equipment. B. A. Glagovskii	762	26
Scales with Transverse Graduations. S. N. Basovich	764	28
THERMOTECHNICAL MEASUREMENTS		
The Use of Alternating Currents for Calibrating Commercial Optical Pyrometers. Yu. Ya. Donde and M. A. Pisarevskaya	766	29
ELECTRICAL MEASUREMENTS		
Design of Temperature Error Compensation Circuits in DC Volt-Hour Meters. I. V. Khakhamov	769	31
Compensation for Temperature Effects in the EMF of Potentiometer Standard Cells. A. Ya. Shramkov	772	33
Measuring Impedances by Means of Oscilloscopes. K. P. Mikhailovskaya	775	35
An Amplitude-Phase Indicator with an Alternating Action of the Compared Voltages. L. Ya. Mizyuk	778	38
Frequency Errors of Rectifying Instruments with Blocking Capacitors. E. N. Kurilov and L. A. Sinitskii	782	41

CONTENTS (continued)

	PAGE	RUSS. PAGE
Rewinding Output Transformers. I. G. Luk'yanchuk	784	42
A Lamp for Lighting Electrical Measuring Instrument Scales Under Test. M. Sh. Kapnik and A. S. Sergeev	785	43
HIGH AND ULTRAHIGH FREQUENCY MEASUREMENTS		
Slotless Measuring Lines. A. I. El'kind	786	44
The Study of High-Q Quartz Crystal Plates. A. G. Smagin	792	48
Measuring the Complex Reflection Factor of Dielectric Materials. D. I. Mirovitskii, G. G. Valeev, and I. F. Budagyan	796	51
Utilization of the Standard Frequency of 100 kc Transmitted Over the Radio. V. Ya. Volodarskii and A. G. Nikitin	799	53
ACOUSTICAL MEASUREMENTS		
Investigation of Soundproof Coverings for Sound-Measuring Cabinets. A. N. Rivin and L. Z. Pronenko	800	54
LIQUID AND GAS FLOW MEASUREMENTS		
Symmetrical Constant Pressure-Drop Flow Gauge. D. N. Ulezko	803	56
PHYSICOCHEMICAL MEASUREMENTS		
An Ultrasonic Recorder of the Level of Liquids. B. A. Syvak and V. A. Nosov	805	57
ESSAYS AND REVIEWS		
An Automatic Measuring Converter Based on the Hall Effect.	807	58
MATERIAL RECEIVED BY THE EDITORIAL BOARD		
Experience of Developing Departmental Inspection Networks and Instrument Repair Depots. M. S. Bril'.	810	60
Organizing the Work of Sections According to the Type of Measurements. N. V. Malinin.	812	62
INFORMATION		
Measuring Equipment at the Industrial Exhibition of the Hungarian People's Republic.	814	63
Collection "New Measuring Instruments and Methods of Checking Them" (No. I).	816	64

LINEAR MEASUREMENTS

MEASURING THE WAVINESS OF FRICTIONLESS BEARING RACES

V. V. Matveev, A. N. Puzyr'kov and V. L. Ryaskov

Translated from Izmeritel'naya Tekhnika, No. 9, pp. 1-2, September, 1960

The Saratov bearing plant produced an instrument for measuring the waviness of bearing raceway surfaces [1]. The instrument's schematic is shown in Fig. 1. The tested race 3 is placed on a mandrel 1 which is fixed in centers 2. During measurements, race 3, together with the mandrel 1, rotates at a speed of 0.3 rpm. Motor 4 turns a pulley through a worm reduction gear, which drives mandrel 1 and race 3, by means of a V-belt pulley 5, firmly fixed to the front end of center mandrel 1 and 2, and then through a dog race 3 and a washer, which is secured to the mandrel by a stop screw.

Measuring rod 7, of the differential capacitance transducer 8, rests on the bottom of the raceway. The cylindrical surface of mandrel 1, on which the U-shaped bracket 6 rests, serves as a basis for measuring the waviness of the race. The lower ends of this bracket carry semicircular pertinax bearings 9. One of the bearings is rigidly fixed and the other attached to a spring parallelogram. The upper end of the bracket is fixed by means of a bent flat spring 10 to stand 11. Base block 12 is fixed on a square rod between the two supports of the bracket. The block can be moved horizontally, together with the transducer fixed to it, along the mandrel axis and secured by means of a set screw in any position, depending on the position of the tested race. Base 12 carriers a bracket 13 to which transducer 8 is fixed on a spring parallelogram. Bracket 13 is equipped with screws for a rough and precise displacement of transducer 8 in the vertical direction.

The back end of the rotating center 2 carries a disk 15 which is 300 mm in diameter and serves as a base for a circular paper chart. The recording on the chart is made by the spark method with an electric device 16, whose frame carries a pertinax arm 17 with a metal needle 18. A constant gap of 0.5 mm is maintained between the current carrying arc 19 and needle 18. The end of needle 18 travels along the surface of disk 15 at a constant distance of 0.5 mm from it. The two gaps are designed to provide a continuous sparking from the current carrying arc 19 to disk 15. When disk 15 is rotated and needle 18 displaced along its surface, a point trace of the measured surface profile is recorded on the chart.

The schematic of the waviness recorder is shown in Fig. 2.

The main units of the electrical part of the instrument consist of a high frequency generator, electronic amplifier, voltage stabilizer, high-tension generator, and a moving coil recording instrument.

In the middle, zero, position of the capacitor plate the bridge is balanced. The deviation of the plate from this position produces, across the measuring diagonal of the bridge, a voltage which is fed through a matching transformer TB_1 to the input of a two-stage resistance-capacity coupled amplifier. The amplified signal is fed through the output matching transformer TB_2 to rectifier Rc and moving coil instrument G. The gain is controlled in three steps by switching resistors R_6 and R_7. When tubes are changed the resulting difference in gain is compensated by means of resistor R_5.

The amplifier and the generator are fed from the kenotron rectifier through a filter consisting of a choke L and two capacitors C_{14} and C_{15}. In order to stabilize the gain, a heavy negative feedback and a ferroresonance stabilizer are used.

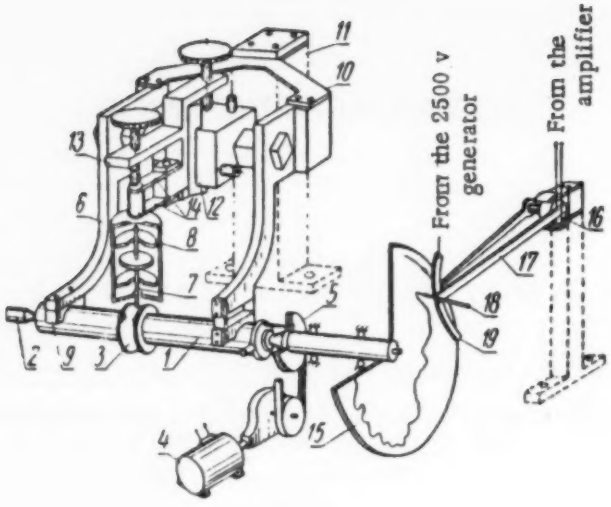

Fig. 1.

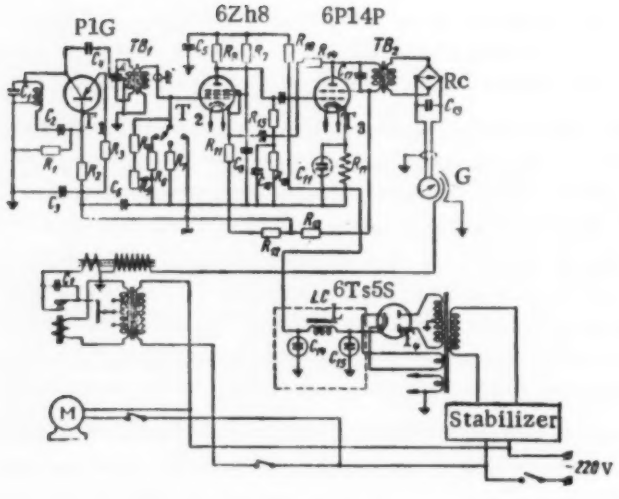

Fig. 2.

In order to reduce the effect of the shunting distributed capacitance of the screened connections, the high frequency generator is mounted in the metal jacket of the transducer. The generator uses a germanium transistor, type P1G, in a Hartley grounded emitter circuit. The input transformer TB_1 is mounted on the same chassis as the generator. In order to avoid stray coupling the transducer, generator, and transformer are separated by metal screens. The generator operates at 20 kc, thus making it possible to use a minature capacitative transducer. At the same time, this frequency does not require special screening of the equipment. The mean gap between the transducer capacitor plates is ~ 0.7 mm. The instrument magnification is 12000.

The metallic body of the transducer carries in separate compartments the high frequency generator, and the amplifier. The measuring effort of the transducer amounts to 30 ± 5 g/wt. The radius of curvature of the measuring probe is 2.5 mm.

The instrument has three magnifications of 4000, 6000, and 12000 with measuring ranges equal respectively to ± 15, ± 10, and ± 5 μ.

The error of the instrument's magnification is determined by means of block gauges certified with an accuracy of ± 0.05 μ.

The waviness meter recording is analyzed by means of a combined scale rule.

LITERATURE CITED

[1] Author's certificate No. 118989 dated July 3, 1959.

DETERMINING THE ROUGHNESS OF CASTING SURFACES

V. N. Levitskii

Translated from Izmeritel'naya Tekhnika, No. 9, p. 3, September, 1960

Present methods of die and "lost wax" casting provide blanks which approach completed articles in their accuracy of linear and angle measurements and surface roughness.

It is impossible to use successfully for the control of their surfaces opticomechanical profilographs, since they are designed to operate over very clean surfaces. The application of a double microscope, type MIS-11, is also limited.

Below we provide the description of a simple attachment to a measuring microscope BMI. This attachment has been used for checking the roughness of cast surfaces up to 150 mm long.

A special detail 1 is fixed to the protruding part of the objective (see figure). Holder 2 of the attachment carries an extensometer 3 whose measuring rod has a phonograph needle 4 fixed to it. The roughness of the surface of detail 7 is evaluated by the intermittent probing method, with the needle being alternately lowered and lifted. The microscope stage 6 is displaced by means of micrometer screw 5. The height of the undulations is determined from the extensometer 3 readings and the frequency of measurements along the profile from the micrometer 5 indications.

Thus, readings are taken at discrete points and the profilogram is plotted on millimetric paper.

ERRORS IN DETERMINING REGULAR UNDULATIONS OF CYLINDRICAL SURFACES

Z. P. Grozinskaya

Translated from Izmeritel'naya Tekhnika, No. 9, pp. 3-5, September, 1960

The accuracy of measuring regular waviness of details is affected by their shape and the inaccuracy of their setting. The degree to which these errors affect the results depends to a great extent on the method of checking. Below we compute the error in measuring the waviness of the external surface of cylindrical details according to the methods shown in Fig. 1. In all instances, when the effect of one of the errors due to the geometrical shape is considered, the other errors are ignored.

Method A. According to this method, the rest 1 and the probe 2 are fixed in a rocking holder and can only follow the variations of the measuring surface in the vertical plane. The existence of eccentricity of the external measuring surface, with respect to the measuring plane, leads to errors, since the geometrical center of the controlled surface will vary its position with respect to the rest and the probe. It is assumed that the rest remains stationary, and that the continuity of the contact between the rest and the contolled surface is achieved by a vertical displacement of the axis of the detail with respect to the rest (Fig. 2). Here K is the point of contact of the rest with the measured surface; E and C are the points of contact of the probe with the surface for different positions of the geometrical center of the measured detail with respect to the axis of rotation, which is being displaced along the line I – I. The arc along which the geometrical center is being nominally displaced is 00'; and a is the value of the error due to eccentricity:

$$a=KH-KM.$$

From ΔOKH and ΔO'KM we have:

$$KH=\sqrt{R^2-(A-e)^2},$$

$$KM=\sqrt{R^2-(A+e)^2},$$

$$a=\sqrt{R^2-(A-e)^2}-\sqrt{R^2-(A+e)^2}.$$

It will be seen from the above expressions that the error decreases with an increasing radius of the measured detail, and increases both with a rising distance between the rest and the probe and with a rise in the eccentricity.

The effect of the ellipticity on the accuracy of measurements is determined from the following computation (Fig. 3):

$$a=OO'+r-R,$$

where r and R are the minor and major half axes of the ellipse.

From ΔOMK and ΔO'MK we have

$$OO'=\sqrt{R^2-A^2}-\sqrt{r^2-A^2},$$

when

$$a=\left(r-\sqrt{r^2-A^2}\right)-\left(R-\sqrt{R^2-A^2}\right).$$

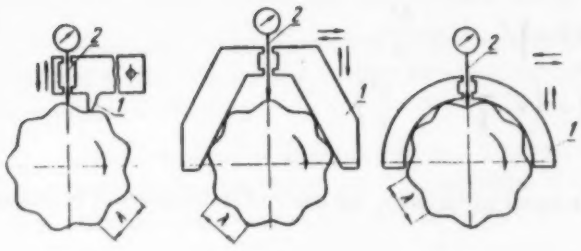

Fig. 1.

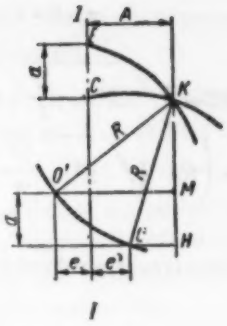

Fig. 2.

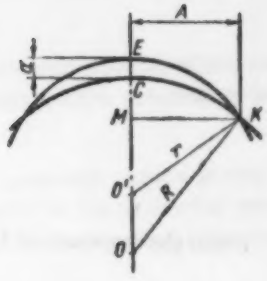

Fig. 3.

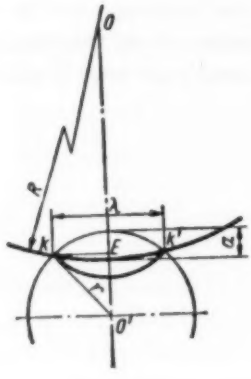

Fig. 4.

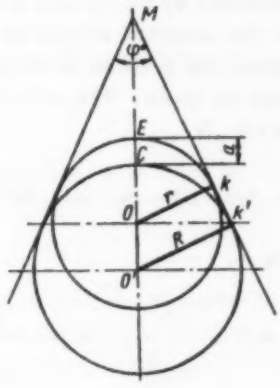

Fig. 5.

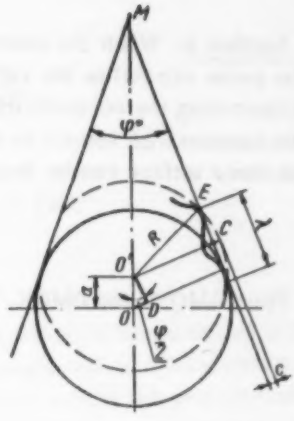

Fig. 6.

The error rises with increasing ellipticity and decreases with a decreasing distance between the rest and probe.

When the waviness is measured by means of method a and the radii of the rest and the probe are approximately the same, they will contact continuously all the points of the surface, and as the result of this, the determination of the waviness will depend on the spacing of the waves and the distance between the rest and the probe.

If the distance between the rest and the probe is a multiple of the wave spacing and the radius of the rest is smaller than that of the valley between the waves, the waviness cannot be detected, since when the rest is at the crest of waves or in the valley between them, the probe will be in a similar position, i.e., the difference in the vertical position of the rest and probe will remain constant. When the distance between the rest and probe is equal to an uneven number of half-waves, a double wave amplitude will be recorded, since when the rest is at a crest the probe will be in a valley and vice versa.

In the remaining instances, when the distance between the rest and probe does not satisfy condition $A = (2n + 1)\,\lambda/2$, or when the wave spacing is variable, the instrument readings will not correspond to the actual size of the waviness, since when the rest is at the crest or in the valley the probe will be in some intermediate position.

In order to eliminate the above errors, some of the instruments have a very large radius of the rest (from 200 mm to ∞). Then the rest slides over the crests of the waves, and the measurements are made from a theoretical line passing through the crests of the waves of the measured surface. Such an increase in the radius of the probe decreases the error but does not eliminate it completely. The error is then determined by the following relationship (Fig. 4) where K and K' are points of contact of the rest with the measured surface; λ is the wave spacing; and a is the error.

$$a=R+r-OE-O'E,$$

$$OE=\sqrt{R^2-\frac{\lambda^2}{4}},\quad O'E=\sqrt{r^2-\frac{\lambda^2}{4}},$$

$$a=\left(R-\sqrt{R^2-\frac{\lambda^2}{4}}\right)+\left(r-\sqrt{r^2-\frac{\lambda^2}{4}}\right).$$

When the waviness of flat surfaces is measured and r is equal to infinity, the error of measurement becomes:

$$a=R-\sqrt{R^2-\frac{\lambda^2}{4}}.$$

Method B. When the waviness is measured by means of a rest in the shape of a prism (Fig. 1), the rest and the probe can follow the variations of the measured surface in two planes (the horizontal and the vertical), thus eliminating the eccentricity effect, since the position of the geometrical center of the measured surface remains constant with respect to the rest and the probe. The relation of the measurement error to ellipticity of the measured surface can be derived from Fig. 5:

$$a=CM-ME;\ CM=MO'-R;\ ME=MO-r.$$

From $\Delta MO'K$ and ΔMOK, we obtain:

$$MO'=\frac{R}{\sin\frac{\varphi}{2}},\quad MO=\frac{r}{\sin\frac{\varphi}{2}},$$

$$a=\left(\frac{1-\sin\frac{\varphi}{2}}{\sin\frac{\varphi}{2}}\right)(R-r).$$

It will be seen that the error increases with a decreasing angle of the prism.

Figure 6 shows the case of the largest error in measuring waviness when each side of the prism touches the surface at two points. The value of this error is determined by the following relation:

from $\Delta OO'D$:

$$a=\frac{OD}{\sin\frac{\varphi}{2}},\quad OD=R-O'C,$$

from $\Delta O'EC$:

$$O'C=\sqrt{\frac{D^2}{4}-\frac{\lambda^2}{4}},$$

$$OD=\frac{D}{2}-\sqrt{\frac{D^2}{4}-\frac{\lambda^2}{4}}.$$

Hence:

$$a=\frac{D-\sqrt{D^2-\lambda^2}}{2\sin\frac{\varphi}{2}}.$$

From the expression thus obtained, it will be seen that the error increases with a decreasing angle of the prism, an increasing wave spacing and a decreasing diameter.

Waviness can be determined most accurately, and the effects of ellipticity and eccentricity eliminated, if the rest touches the surface in discrete points only, which are placed on a theoretical surface determined by the crests of the waves.

Such a method is shown in Fig. 1c. The rest can follow the position of the measured surface in two directions thus eliminating the effect of eccentricity of the measured surface with respect to the measuring surface. It is obviously necessary in this case to make a circular rest of the appropriate size for each size of the measured detail, which is only justifiable in large-scale mass-production.

FREQUENCY CHARACTERISTICS OF FEELER PROFILOMETERS

A. I. Boyarov

Translated from Izmeritel'naya Tekhnika, No. 9, pp. 5-7, September, 1960

The profile of industrially produced surfaces has a complex shape and consists of irregularities with different spaces, including waviness. At a constant speed of probing, i.e., a constant rate of displacement of the transducer with respect to the surface, alternating currents arise in the electrical part of the profilometer or profilograph, and the frequency of these currents is proportional to the speed of transducer movement and inversely proportional to the spacing of the irregularities. It is obvious that the reading of the instrument will depend on its frequency characteristic.

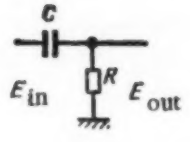

Fig. 1.

The necessity of standardizing the frequency characteristics is recognized by all the specialists in the measurement of surface roughness, since the publication of the recent works on this subject in the Soviet Union, and this has resulted in the drafting of a standard for the basic parameters of profilometers and profilographs.

If the frequency characteristic of a probing instrument has a sufficiently sharp incline in the low frequency range, and if its position can be displaced by the operator (with respect to frequency) either up or down, such an instrument becomes to a certain extent, a harmonic analyzer and provides more information on the surface under test than the existing types of instruments.

The basic factor which determines the shape of the frequency characteristic of the instrument as a whole, in the low-frequency range, is its electrical amplifying and converting section, which includes high-pass filters required for eliminating irregularities with large spacings.

According to GOST 2789-59 (State Standard) several basic lengths have been specified for measuring surface roughness, namely 0.08, 0.25, 0.8, and 2.5 mm, thus determining the maximum irregularity spacings measured by profilometers. Surface irregularities with spacings greater than the above should not be measured by the respective instruments.

With a probing speed of 0.5 mm/sec (the speed of displacement of the transducer in the "Kalibr-VÉI" instrument) and spaces of 0.08 and 2.5 mm, frequencies of 6.3 and 0.2 cps are obtained. In practice, for such low frequencies it is possible to use an RC high pass filter of a fairly complex design, which consists of capacitances and ohmic resistances. Filters containing inductances cannot be used, since their dimensions and weight would considerably exceed those of the whole instrument. The simplest RC filter (Fig. 1) consists of series connected capacitors C and ohmic resistors R. The frequency characteristic of such a filter is shown in Fig. 2

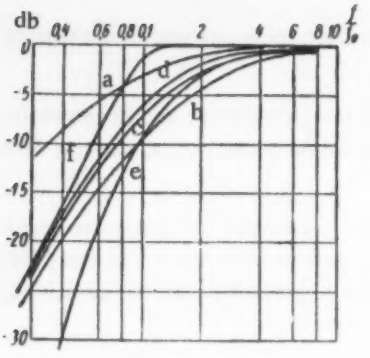

Fig. 2. a) One section; b) two sections, $\gamma = 1$; c) two sections, $\gamma = 4$; d) two sections, $\gamma = \infty$; e) three independent sections; f) RC filter with an amplifier.

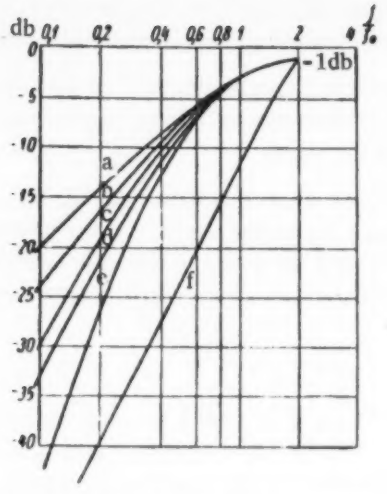

Fig. 3. a) One section; b) two sections, $\gamma = 1$; c) two sections, $\gamma = 4$; d) two sections, $\gamma = \infty$; e) three independent sections; f) RC filter and amplifier.

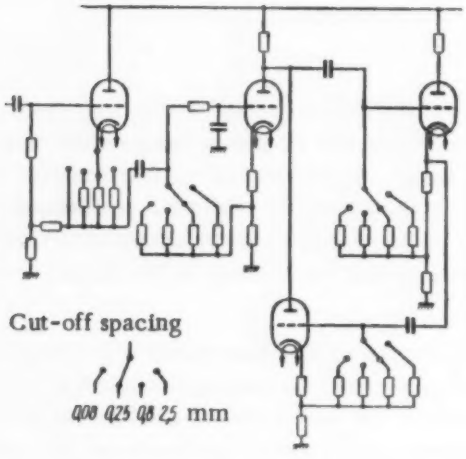

Fig. 4.

(curve a). In Fig. 2, the logarithms of the ratio f/f_0 are plotted along the x axis, where f_0 is the tuning frequency of the RC filter which is given by the formula:

$$R = X_c = \frac{1}{2\pi f_0 C},$$

where R is the ohmic resistance of the RC filter; X_C is the reactance of the capacitor; C is the capacity; the transfer constant A is plotted along the y axis and expressed in db:

$$A = 20 \lg \frac{E_{out}}{E_{in}},$$

where E_{in} is the voltage at the input of the filter; E_{out} is the voltage at the output of the filter.

By connecting several sections in series it is possible to obtain frequency characteristics with a sharper cut-off at low frequencies. Curve b in Fig. 2 corresponds to a two-section filter with similar sections, and curve e to a three-section filter with three independent sections. By keeping the time constants of the sections of an RC filter constant and increasing the ohmic resistance between the input and output of each section, it is possible to improve the frequency characteristic of the filter. Figure 2 (curve b, c, and d) represents the frequency characteristics of two-section RC filters with sections which have the same time constants, but different ratios γ of their ohmic resistances (also see Fig, 3, curves b, c, and d).

For the convenience of comparing different RC filters, their characteristics (Fig. 3) have been displaced in such a manner that the points corresponding to the decrease of the transfer constant by 1 db coincide.

The selection of the −1 db point as a reference for the pass band boundary is arbitrary. In transmission practice, − 3 db points of the frequency characteristic are normally taken as the pass band limits. We think that since a measuring device is under consideration, it is more accurate to use the − 1 db point of the frequency characteristic. The − 1 db point of the frequency characteristic should correspond on the linear scale to the chosen standard length.

In analyzing curves a, b, c, d, and e (Fig. 3), it is possible to arrive at the following conclusion: When the difference between the "critical" * frequency and the frequency which has to be filtered out is relatively small (one or two octaves), all the above characteristics differ but little from each other, and it is only when the difference is large, of the order of 4 octaves or more, that the characteristics begin to differ. Thus, the defect of the above RC filters consists in the small slope of their characteristic near the critical frequency, i.e., the insufficiently pronounced separation of the low frequencies or irregularities with wavelengths close to the basic wavelength. This defect can be eliminated by using more complicated RC filters which contain, in addition to the RC sections, also amplifying devices. Figures 2 and 3 (curves f) show the frequency characteristics of one such filter. Curve f in Fig. 3 differs considerably from those of ordinary RC filters. Filters with such characteristics provide a sufficiently pronounced separation of frequencies which are close to the critical frequency. The transfer constant at very low frequencies for these filters is the same as for the simple two-section RC filter (12 db per octave). The sharp bend in the curve near the critical frequency which is required for a pronounced separation of low frequencies is attained by means of a negative feedback.

Figure 4 shows the schematic of one of the filters with an amplifier. The frequency characteristic of the filter is given in Figs. 2 and 3 (curves f). The instrument has a switch for four cut-off spacings of 0.08, 0.25, 0.8, and 2.5 mm.

Conclusions. Simple RC filters are considerably inferior in their characteristics to filters with amplifiers, but they are much simpler than the latter type. In view of the fact that an RC filter with an amplifier and characteristic similar to the one shown in Fig. 3 (curve f) is complicated and equal in size to the whole amplifying device of a portable workshop probing instrument, it is advisable in standardizing the frequency characteristics of filters to adopt, for portable instruments with an error exceeding ± 15%, simple two-stage RC filters with a coefficient $\gamma = 3 - 4$; and for precision instruments, with an error smaller than ± 15%, filters with amplifiers. Moreover, the slope of the characteristic of these filters at frequencies below the critical should be the same as for RC filters with two similar sections (12 db per octave).

A further, more detailed, study of the frequency characteristics of complex filters with amplifiers is required. This problem should be solved by developing a filter with an amplifier which is as simple and reliable as possible.

AUTOMATIC CONTROL OF DIMENSIONAL ACCURACY IN INTERNAL GRINDING

Hua Ch'ang-kẽn

Chinese Peoples' Republic

Translated from Izmeritel'naya Tekhnika, No. 9, pp. 7-10, September, 1960

In order to provide an automatic control of dimensional accuracy in grinding, a method of limiting the displacement of the carriage to which the grinding wheel is fixed, is normally used.

Measurements are carried out according to this method in the following manner. First, the grinding wheel nears the surface of the machined detail at a high speed. As soon as the initial stress is obtained the high-speed drive is changed to the rough working drive which remains in operation until the cam fixed to the dial and rotating with it operates a microswitch, which transfers the operation from rough to accurate grinding, whose duration is fixed by means of a time relay. Following this operation, the grinding wheel is dressed. Next. the finish grinding starts, at the end of which a second cam, which is placed at a certain distance from the first, closes a

* By "critical" frequency, we shall understand henceforth a frequency at which the transfer constant decreased by − 1 db.

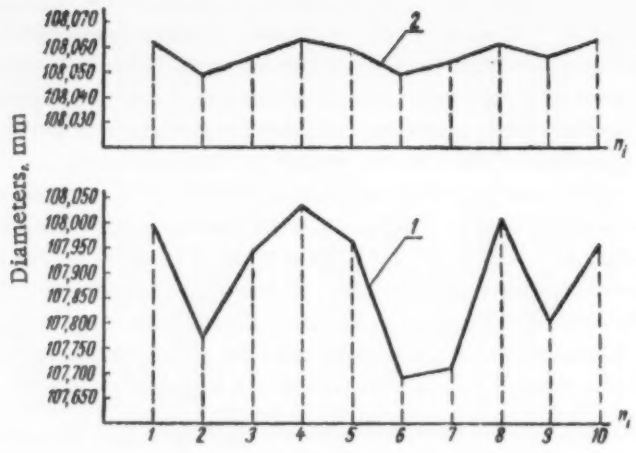

Fig. 1. 1) Ring diameters before machining; 2) ring diameters after machining.

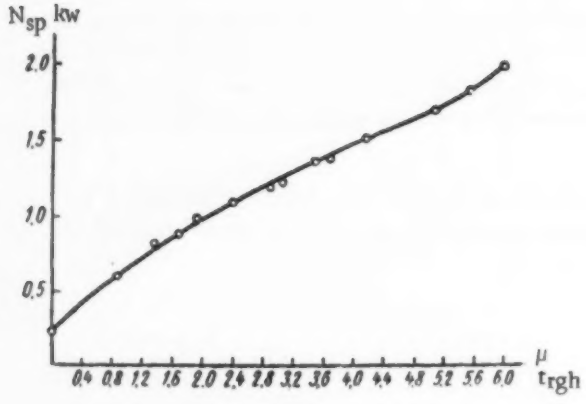

Fig. 2.

microswitch, leading to the widthdrawal of the wheel and the ring and the beginning of a new cycle of operations.

In this method, the position of the cutting edge of the tool is, in fact, being measured. The accuracy of this method of measurement is affected by the following factors: the basic surface diameter of the machined ring, wear in the adjusting tools, wear in the grinding wheel during the finishing grinding, properties of the material used, variations of the tolerances, etc.

This method of controlling ring grinding provides a dispersion of the order of 0.02 mm in their diameters. This dispersion is affected to a considerable extent by the initial allowance which amounts to 0.30 mm (Fig. 1; along the x axis, the ordinal numbers of the rings are plotted, and along the y axis, their diamaters). Hence, the elimination of this effect is an important factor in improving the accuracy of machining.

The variations in the allowance for the rings affect the size of the thermal and stress deformations of the machining system, which in turn affect the accuracy of the ring diameters. According to the experimental data obtained [1], an increase in the depth of cooled grinding does not affect, to any considerable extent, the temperature of the rings. Therefore, we shall only examine henceforth the effect of the deformation due to stresses.

After the first double operation of the grinding wheel, the following equation holds:

$$t_{rgh}+y_0=t_1+y_1.$$

after the second:

$$t_{rgh}+y_1=t_2+y_2. \qquad (1)$$

after the n-1th

$$t_{rgh}+y_{n-2}=t_{n-1}+y_{n-1}.$$

after the nth

$$t_{rgh}+y_{n-1}=t_n+y_n.$$

By adding the left and the right hand sides of these equations, we obtain a new equation which after transformations becomes:

$$y_i=it_{rgh}+y_0-\sum_{i=1}^{n}t_i, \tag{2}$$

where t_{rgh} is the value of the rough transverse feed, set on the dial for one double operation of the grinding wheel; y_0 is the initial displacement under pressure of the wheel's cutting surface; y_i is the displacement of the cutting surface of the wheel after the ith double operation from the beginning of the rough feed; t_i is the actual value of the rough feed after the ith double operation of the grinding wheel.

In the right hand side of (2), the value of t_i, due to the number of double operations, is variable for a transient grinding process. The number of double operation depends on the allowance and is calculated from the beginning of the rough feed up to the instant when the first cam trips the microswitch. Hence, the value of y_i, which is a function of t_i, is also variable. As the compression of the wheel increases, the value of t_i tends to that of t_{rgh}, and for a sufficiently large working allowance, the value of t_i becomes equal to t_{rgh}. In practice, however, the rough feeding operation stops before the stable condition of grinding is reached when $t_i < t_{rgh}$. Under this condition, variations in the allowance produce different deformations due to stress, and also affect the accuracy of determining the position of the cutting surface of the wheel. Thus, the problem is reduced to establishing conditions under which the relatively insufficient allowance does not affect the position of the cutting surface of the grinding wheel at the end of the rough grinding.

Equation (1) can be written in a general form:

$$t_i=k\,(t_{rgh}+y_{i-1}), \tag{3}$$

where k is the cutting ability coefficient of the grinding wheel and represents the relative thickness of metal cut in one double operation per unit displacement of the grinding wheel.

By substituting t_{rgh} in (3) for t_i (for a stable state) we shall obtain for i = 1:

$$y_0=\frac{t_{rgh}(1-k)}{k}. \tag{4}$$

Equation (4) provides the required condition for eliminating the effect of allowance variations on the accuracy of measuring the position of the cutting surface of the wheel at the end of the rough grinding, when the allowance is insufficient for attaining a stable state of grinding under normal conditions. The equation represents the relation of the initial tension y_0 to the rough feed t_{rgh}. Under production conditions, requirement (4) can be attained by means of a power relay, which switches over from the high speed approach of the grinding wheel to the rough grinding condition. If an initial tension is established by means of the relay equal to that required for a grinding depth of t_{rgh} per double operation, the rough grinding will proceed under stable state conditions. Moreover, the variations in the allowance will not affect the accuracy of determining the position of the wheel's cutting edge at the end of the rough grinding, i.e., they will not affect the accuracy of the ring dimensions.

Figure 2 shows an experimentally obtained relation between the power of the relay required for attaining a stable operating condition and the value of the rough feed (let us call it the optimum condition), at which the variations in the allowance do not affect the accuracy of measuring the position of the wheel's cutting surface at the end of the rough grinding.

The experimental curve was plotted in the following manner.

After the operation preceding the grinding, 15 rings were specially selected with working allowances which would provide stable grinding under any conditions. The experiment was carried out on an 1GP3 automatic

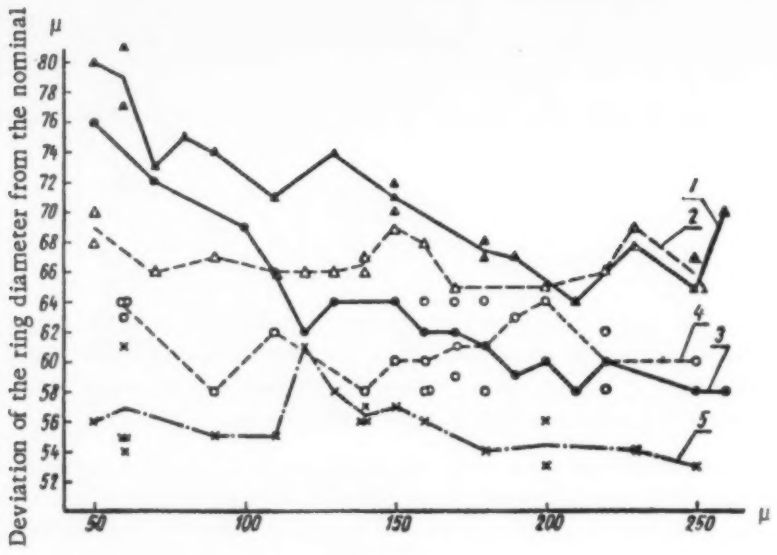

Fig. 3.

line for machining hardened steel, ShKh15 rings of 108 mm in diameter on a machine type 02S33 with a grinding wheel Eb80S1K of 70 × 50 × 20 mm. The relation of the required power to the corresponding rough feed was obtained for each ring. The values of the rough feed were measured on the dial and the power was set by a wattmeter. The point on the y axis corresponds to the power required for the free running of the wheel.

Figure 3 shows the experimental data obtained in investigating the effect of the allowance on the accuracy of measuring rings at different ratios of set powers and rough feeding values.

In curves 1 (for a stable power of N_{sp} = 0.90 kw, rough feed of t_{rgh} = 4.58 μ/db. op.; a number of precise operation of n_{pr} = 8; and a finishing feed of t_{fn} = 3.15 μ/db. op.) and curve 3 (for N_{sp} = 0.90 kw; t_{rgh} = 5.33 μ/db. op.; n_{pr} = 8; and t_{fn} = 3.15 μ/db. op.) the allowance for rough grinding was less than 130 μ and considerably affected the final diameters of the gound rings. The degree to which the allowance affects the diameter depends on the relation between the set power and the value of the rough feed. If the rough grinding is carried out at the optimum condition shown by curve 2 (for N_{sp} = 1.6 kw; t_{rgh} = 4.58 μ/db. op.; n_{pr} = 8; and t_{fn} = 3.15 μ/db. op.) and curve 4 (for N_{ps} = 1.73 kw; t_{rgh} = 5.33 μ/db. op.; n_{pr} = 8; and t_{fn} = 3.15 μ/db. op.), the effect of the allowance on the ring diameters is considerably reduced. In this instance, the dispersion of the ring diameters does not exceed 6 μ (without taking into consideration the errors due to the wear in the adjusting tools, and variations in the external basic surface of the rings).

It will be seen from curve 5 of Fig. 3 (for N_{ps} = 1.60 kw; t_{rgh} = 4.58 μ/db. op.; n_{pr} = 0; t_{fn} = 3.15 μ/db. op.) that it is possible, under optimum conditions, to grind rings without passing through the precision stage. The roughness of the surface is not increased and the dispersion of dimensions increases very little. It should be noted that the accuracy of measuring the cutting surface position is affected very little by the finishing grinding.

Conclusions. With the above method of measuring under optimum conditions, it is almost possible to completely eliminate the effect of allowance variations on the accuracy of the ground ring diameters.

2. On grinding machine 02S33, and similar machines, it is possible to grind details without subsequent precision grinding, thus raising the productivity of the grinding process.

LITERATURE CITED

[1] A. A. Matalin, "Investigating the grinding temperature of steel details," from the collection: Quality of Surfaces and the Life of Machine Parts [in Russian] (NIS-LIÉI, 1956).

[2] S. S. Volosov, An Automatic Control of the Accuracy of Dimensions in Grinding [in Russian] (Mashgiz, 1958).

INVESTIGATING ERRORS IN OPTICAL DIVIDING HEADS

L. Ya. Gustyr'

Translated from Izmeritel'naya Tekhnika, No. 9, pp. 10-12, September, 1960

A Leitz optical dividing head was chosen by the Novosibirsk State Institute of Measures and Measuring Instruments (NGIMIP) for their investigations.

This head is described in [1] and is one of the most precise angle measuring devices with a double-sided readout. The setting of the spindle is made by the mutual position of two marks located at the opposite ends of the same diameter. The double-sided readout reduces the effect of the dial eccentricity with respect to the head to an error of the second order, thus providing, with respect to this component, foolproof handling of the instrument. The high accuracy is achieved also by rolling bearings which consist of hardened bushes and a sphere between which rotate many calibrated balls. All the balls make contact and provide a smooth movement of the bearing.

The reading errors were investigated by comparing the angles of a 18-sided prism by means of an autocollimator with the angles of rotation of the head [2].

The results of these investigations are shown in Fig. 1.

In determining the law of error distribution along the dial scale we assumed that large period distributions are subject to one of the following laws [3]:

$$\delta = A \sin 2\varphi, \quad \delta = A \sin 4\varphi, \quad \delta = A \sin 6\varphi,$$

where φ is the angular interval between the dial diameters.

It will be seen from Fig. 1 that the dial errors of the head under investigation follow approximately the law:

$$\delta = A \sin 2\varphi.$$

The theoretical curve of error distributions is shown in Fig. 2.

In our investigation we aimed at finding the maximum error which could arise in using the head. Since in comparing the head readings with the 18-sided prism the measurements were not continuous along the dial of the head, but were taken at certain points only, spaced by 20°, the maximum error of the head could have been missed under these conditions (the experimental points of the sine wave could have been missed). The question arises, therefore, to what extent the error of the head has been revealed by this method.

The ratio of the discovered error to the maximum will vary with the value of the initial count. The dial can best be checked if one of the counts coincides with the minimum and the other with the maximum error. The dial error will then be represented by the algebraic difference between the ordinates at 45 and 135°.

A smaller accuracy will be obtained when the counts fall into the intervals of (35°, 45°), (135°, 145°) and (45°, 55°), (125°, 145°) which correspond to the initial counts of (15°, 25°), (5°, 15°).

Let us assume that the initial count may fall at any point in the interval (15°, 25°). Then the discovered error of the dial will be expressed as the algebraic difference between the ordinates in the intervals (35°, 45°) and (135°, 145°).

In these intervals the equation of the curve $\delta = A\sin\varphi$ has the form:

$$\delta = A \sin 2(35° + \alpha), \quad \delta = A \sin 2(135° + \alpha),$$

where $0 \leq \alpha \leq 10°$.

The error thus discovered is:

$$\delta = A \sin 2(35°+\alpha) - A \sin 2(135°+\alpha) = 1.97\, A \cos(10°-2\alpha).$$

Taking the derivative with respect to α

$$\delta' = 2A \cdot 1.97 \sin(10°-2\alpha)$$

and equating it to zero:

$$\delta' = 0; \quad \sin(10°-2\alpha) = 0,$$

we obtain $\alpha = 5°$.

The second derivative is:

$$\delta'' = -4 \cdot 1.97\, A \cos(10°-2\alpha) < 0.$$

Thus, the function in question has but one extremum, at point $\alpha = 5°$, which is a maximum. At points $\alpha = 0°$ and $\alpha = 10°$, the function $\delta = 1.97A\cos 10°$ acquires its minimum value of 1.93 A in the interval of $0 - 10°$.

Hence, if the initial count falls within the interval (15°, 25°), not less than 1.93A/2A = 97% of the total error will be found. If the initial count falls within the interval (5°, 15°), the equation of the error found in this case has the form:

$$\delta = 1.97\, A \cos(10°-2\alpha),$$

i.e., in this case also 97% of the total error of the dial diameters are found.

The error of the above method of measurements depends mainly on the inaccuracy of setting the opposite ends of the dial lines. This error was investigated separately and its root-mean-square value was found to amount to 1.17".

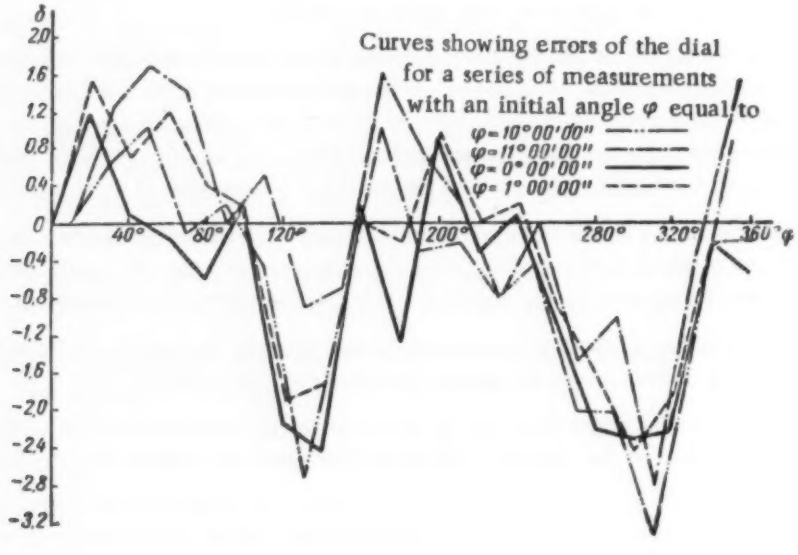

Fig. 1.

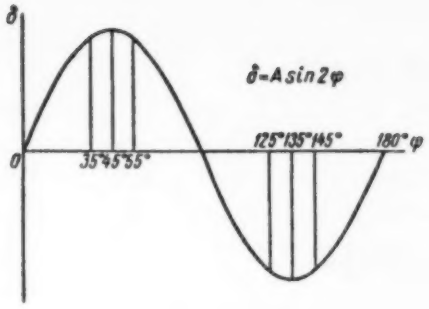

Fig. 2.

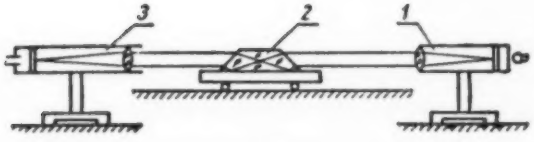

Fig. 3.

The total error of this method of measurement amounts to:

$$\sigma = \sqrt{1.17''^2 + 0.23''^2 + 0.19''^2} = 1.21'',$$

where 0.23" is the root-mean-square error allowed in certifying the autocollimator and 0.19" is the root-mean-square error of setting and reading by the eyepiece micrometer.

When the dial was checked on a 36-sided prism, its error was found to be similar to the one previously measured.

The maximum error of the dial, as it was found in examining the operation of the head, lies within 5".

It should be noted that the use of an 18-sided prism is most suitable precisely for an error distribution according to the law $A\sin 2\varphi$. For another distribution of errors the use of an 18 sided prism provides results which amount to the smaller part of the total error.

In addition to the reading errors the linearity of the working surface of the base was also checked.

The checking was carried out by means of a collimator 1 (Fig. 3), a Dove prism 2, and a telescope 3. The collimator and the telescope were fixed in a stationary position, but the Dove prism was fixed to the base of a sine rule, which had a distance of 100 mm between its rollers, and moved along the base surface under test.

As the result of this check it was found that the maximum deviation of the base from linearity did not exceed 5.2 μ. The linearity was measured in two positions of the rule along the width of the base.

The data obtained by this method of studying an optical dividing head showed that the tested Leitz head satisfies the tolerances provided by GOST 9016-59 for optical dividing heads of the ODG-5 type.

LITERATURE CITED

[1] N. P. Sobolev, Optics in Metal Working Machines [in Russian] (Mashgiz, 1958).

[2] A. K. Kutaya, editor, Reference Book on Engineering Production Control [in Russian] (Mashgiz, 1956).

[3] V. Ya. Eidinov and L. N. Logacheva, Izmeritel'naya Tekh. 6 (1957).

MEASUREMENTS OF MASS

HYDROSTATIC WEIGHING OF LIQUIDS IN CONTAINERS OF COMPLEX SHAPE

L. P. Stepanov

Translated from Izmeritel'naya Tekhnika, No. 9, pp. 12-13, September, 1960

The journal "Izmeritel'naya Tekhnika" (No. 1, 1960) carries V. G. Tseitlin's article entitled "A new principle of hydrostatic weighing of liquids."* This article deals with the weighing of liquids in a cylindrical container which is a particular case of a more general treatement suggested and worked out by the D. I. Mendeleev All-Union Scientific Research Institute of Metrology. The weighing of the liquid in the container is based on measuring the hydrostatic pressure on an immersed body of a special shape, whose cross sections by horizonal planes are proportional to the cross sections of the liquid by the same planes.

The instrument and the vessel in which the amount of liquid is to be measured are shown in the figure. The particles of the liquid of the same density are ranged in horizonal layers; hence, the hydrostatic force acting on the instrument can be represented by the formula:

$$p=\int_0^H f\gamma dx, \tag{1}$$

where p is the hydrostatic force acting on the instrument; f, the cross section of the body of the instrument by a horizonal plane N-N, placed at height x from the bottom of the vessel; γ, the weight of a unit volume of liquid at height x from the bottom of the vessel; H, the height of the liquid level.

On the other hand, the weight of the liquid in the vessel can be calculated from the formula:

$$P=\int_0^H F\gamma dx, \tag{2}$$

where P is the weight of the vessel; F, the difference of the cross sectional areas of the vessel and the instrument cut by plane N-N.

It was pointed out that the areas of cross sections f of the instrument are proportional to areas F of the liquid in the vessel:

$$F=kf. \tag{3}$$

where k is the coefficient of proportionality.

By inserting (3) in (2), and taking into consideration (1), we have:

$$P=k\int_0^H f\gamma dx \tag{4}$$

* See English translation.

or

$$P=kp. \qquad (5)$$

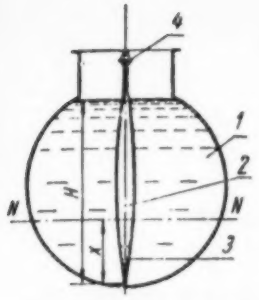

1) Vessel with the liquid; 2) cigar-shaped body of the instrument; 3) heavy end piece; 4) adjustable weights.

The latter formula indicates that the weight of the liquid in the vessel is proportional to the hydrostatic force, which acts on the immersed body. Hence, by measuring the force p it is possible to find the weight of the liquid. It is possible to measure the hydrostatic force by various methods, for instance, by suspending the immersed body from the arm of a balance.

One of the instances when instruments working on the above principle can be used consists of measuring oil products in stationary containers of cylindrical, spherical, or any other shape. It is also possible to use these instruments in tankers.

The advantage of the above method of measurements consists in the fact that in measuring the mass of liquid, it is not required to determine either the volume or the density of the liquid and the result remains correct even with heterogeneous substances. The latter property is very important in certain cases, as for instance, when measuring oil products in the summer in stationary vessels, when owing to heating by the sun, the upper layers of the oil become considerably lighter than the lower ones. If the instrument is made of a material whose temperature coefficient is similar to the one of the container, a temperature compensation of the error due to the expansion of the vessel is obtained.

The above method of measurements was tested out on an instrument intended for measuring the quantity of oil products in railroad (similar type) tank cars. According to the prevailing rules the tank cars travel completely filled with oil; the possible variation of the liquid level amounts to some 50 cm. An instrument which floated in the oil was designed; its center of gravity was always placed below the center of the volume of its immersed part. The measurement consists in finding the required weights for making the instrument float almost touching the bottom of the tank car. The weight of the instrument with its weights is equal to the hydrostatic force and proportional to the weight of the oil product.

In testing, the instrument was immersed in the liquid in the middle of the tank car opening. The ring shaped weights were selected in such a manner that the instrument was floating, but with an additional weight of 1 g touched the bottom of the tank; this can be easily checked by pressing on the instrument from the top. For the instrument in question, one gram of its own weight corresponds to 22 kg weight of the oil product in the tank or ~ 0.05% of the total mass of the liquid. The results thus obtained were compared with those obtained by the usual methods of measurement, namely by the height of the level and density of a sample.

The tests revealed a high sensitivity of the instrument and consistency of measurements, i.e., qualities which provide for small measurement errors if the instrument is properly made and calibrated.

It is relatively easy to make measurements with an error of some 0.5%. For this purpose it is sufficient to measure the hydrostatic force p with an error not exceeding 0.1%, and make an immersion body (of circular cross section) with a diameter tolerance of ± 0.1% which corresponds to a tolerance for the cross sectional area of the instrument of ± 0.2% and will determine the cross sectional area of the vessel with an error not exceeding 0.2-0.3%.

Conclusions. The above method of hydrostatic weighing of liquids is useful for vessels of any shape and provides accurate results irrespective of the density variations along the height of the vessel. Instruments working on the basis of the above principle can be recommended in the first instance for measuring oil products.

ELIMINATION OF ERRORS IN LOADED PISTON SCALES DUE TO THE LEAKAGE OF LIQUID THROUGH THE GAPS

V. N. Gramenitskii

Translated from Izmeritel'naya Tekhnika, No. 9, pp. 13-15, September, 1960

Reference loaded-piston scales, types OGV-1 and OGV-2, with maximum measures of 1000 and 2000 kg, respectively, are used for control of sample liquid and gas measures, by the "weighing" method, for checking reference weights up to 2000 kg, and for precision measurements of the mass of various liquids in flow measuring, and for other special equipments.

The scales are produced in two versions: portable (Fig. 1) which have a manometric column (a piston manometer) and are mounted directly onto the power piston; and stationary (Fig. 2) which have their manometric column placed on a separate table and coupled to the power piston.

Mass M of the body weighed on these scales is determined from the formula:

$$M = Km\frac{\rho_1(\rho_2-\rho_3)}{\rho_2(\rho_1-\rho_3)}, \quad (1)$$

where m is the mass of the weights placed on the cylinder of the manometer for balancing the body whose mass is to be determined; ρ_1, ρ_2, and ρ_3 are, respectively, the density of the measured body, the weights, and of air; for the portable scales $K = (F_1/F_2) - 1$; for the stationary scales $K = F_1/F_2$.

F_1 and F_2 are the effective areas respectively of the power and manometric pistons.

In determining the mass of the body on these scales, two balances are obtained: the first one for unloaded scales, and the second one with the tested body placed on the platform of the scales.

When these scales are certified and checked a method of determining K (repeated loading of the scales with 2-nd grade weights) and m is used which makes the scale error equal ±0.01% to ± 0.005% of the measured value depending on the use to which the scales are put.

In order that the error should not exceed these limits, it is necessary that, during the time between the weighing of the unloaded scales and the placing of the load on the platform, the pressure in the liquid should remain unchanged in the column between the power and the manometer pistons. However, in the loaded piston scales, as well as in all measuring instruments using unsealed pistons, the working liquid leaks continuously during the operation of the instrument through the gaps between the piston and the cylinder. Therefore, the power piston slowly drops and the level separating the working liquids (kerosene and castor oil) in the dividing chamber rises.

The lowering of the power piston does not change the pressure of the liquid column between the pistons in the portable scales, since in these scales the manometric column, which is placed immediately above the power piston, drops together with it.

In the stationary scales, however, when the power piston drops, the height of the liquid column changes, and, hence, the pressure in the column varies. This variation, however, is so small that its effect can be neglected even for very precise measurements.

The level of the liquid separation inside the instrument can have a greater effect on the measurement accuracy which can become as large as the specified tolerance for a prolonged operation of the instrument without rebalancing with an unloaded platform and with a sufficiently large gap between the manometer piston and the cylinder.

It can easily be shown that the additional measurement error in this case will be:

$$\Delta M = -(\rho_4-\rho_5)F_1\Delta l, \quad (2)$$

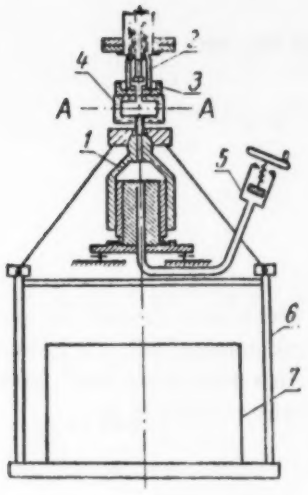

Fig. 1. Schematic of the loaded piston portable scales. 1) Power piston (beaker); 2) manometric column; 3) trap; 4) dividing chamber; 5) liquid press; 6) frame; 7) body whose mass is to be determined.

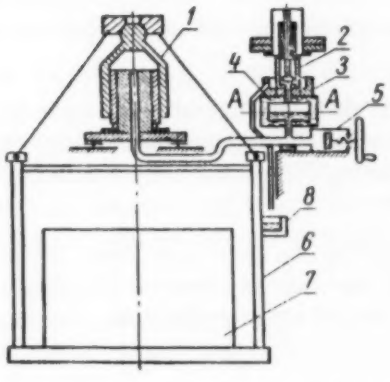

Fig. 2. Schematic of the loaded piston stationary scales. 1) Power piston (beaker); 2) manometric column; 3) trap; 4) dividing chamber; 5) liquid press; 6) frame; 7) body whose mass is to be determined; 8) trap.

where ρ_4 and ρ_5 are respectively the density of castor oil and kerosene; ΔH is the variation in the dividing level of the liquids.

Equation (2) determines the additional absolute error of loaded piston scales, whose origin is due to an inherent property of systems with unsealed pistons, namely the flowing-out of the liquid through the gaps.

The value of ΔM for prolonged work on the scales without repeated rebalancing in an unloaded state can attain tens of grams which cannot be tolerated in view of the precision required from the loaded piston scales.

In order to reduce this error the gap between the piston and cylinder was made very small; this however led to a rise in hydraulic friction between the piston and the cylinder and a prolongation of the balancing. Moreover, it was recommended not to let large intervals of time elapse between the balancing of the unloaded scales (calibration of the scales) and the weighing of the bodies on the platform.

In certain special cases when especially great precision was required the scales were calibrated twice, before and after weighing, thus making it possible to determine the value of ΔM experimentally and apply the required corrections to the measurements.

These steps provided the accuracy specified for the reference loaded piston scales, but made the use of the scales more difficult.

In order to eliminate completely the additional error due to the leakage of the liquid it is necessary to make the dividing chamber with a determined horizonal cross section area,and make traps for the liquid flowing out through the gaps.

The conditions which should be met by the diameters of the dividing chambers can be obtained on the basis of the following considerations.

During the operation of the scales, after a certain time elapses following the calibration of the scales, the dividing level A-A of the liquids rises in the dividing chamber by an amount ΔH (not shown in the figure), and the pressure of the liquid on the power piston (beaker) in the upwards direction as the result of this increases by:

$$\Delta P=(\rho_4-\rho_5)\, g\Delta H.$$

At the same time the force acting on the power piston from below increases by:

$$\Delta G_1=(\rho_4-\rho_5)\,(F_1-F_3)\, g\Delta H,$$

where F_3 is the area of the dividing chamber cross section at level A-A.

The weight of kerosene accumulated in trap 3 during this time will be:

$$\Delta G_2 = \rho_5 F_3 g \Delta H.$$

Assuming that $\Delta G_1 = \Delta G_2$ we have:

$$F_3 = \frac{\rho_4 - \rho_5}{\rho_4} F_1. \quad (3)$$

In the stationary scales (Fig. 2) the traps for collecting liquid which leaks through the gaps between the manometric cylinder and piston are placed not only at the manometric column, but also at the platform, and the kerosene can freely flow from the first into the second trap through a connecting pipe. In this instance the variation in the force acting on the power piston with a changing dividing level will be·

$$\Delta G_1' = (\rho_4 - \rho_5) F_1 g \Delta H.$$

Assuming similarly to the preceding case that

$$\Delta G_1' = \Delta G_2,$$

we obtain

$$F_3 = \frac{\rho_4 - \rho_5}{\rho_5} F_1. \quad (4)$$

Providing conditions (3) and (4) are kept it becomes possible to eliminate the effect of the leaking liquid on the accuracy of measurements.

Moreover, the construction of dividing chambers according to the above formulas will make it possible to increase the tolerance for the gap between the manometer piston and the cylinder thus not only facilitating the technology of lapping the piston to the cylinder, but also improving the operational properties of the scales by reducing the balancing time.

For scales which are in use and have not the facilities for meeting the above conditions, but require high precision measurement, for instance in checking reference weights, the traps and dividing chambers can be made on the spot, with the chamber dimensions corresponding to Eqs. (3) and (4). The chambers should be made of plexiglas.

Below we give the cross-sectional area of dividing chambers calculated from (3) and (4) for scales type OGV-1 and OGV-2.

Type of scales	Cross-sectional area F_3, cm^2
OGV-1 (portable)	6.2
OGV-1 (stationary)	7.3
OGV-2 (portable)	12.4
OGC-2 (stationary)	14.6

In the calculations it was assumed that: $\rho_4 = 0.97$ g/cm^3; $\rho_5 = 0.82$ g/cm^3; $F_1 = 40$ cm^2 (for OGV-1 scales) and $F_1 = 80$ cm^2 (for OGV-2 scales).

LITERATURE CITED

[1] V. N. Gramenetskii, "Precision instruments for measuring pressure, force and mass, based on the application of unsealed pistons," Information Leaflets VNIIK IRD-18, No. 128 [in Russian] (1957).

[2] M. K. Zhokhovskii, The Theory of Designing Instruments with Unsealed Pistons [in Russian] (Mashgiz, Moscow, 1959).

MEASUREMENTS OF TIME

DYNAMIC ACCURACY OF TRIGGER REGULATORS WITH UNSTABLE PULSES

V. A. Shpolyanskii

Translated from Izmeritel'naya Tekhnika, No. 9, pp. 16-21, September, 1960

In the present work, we study the effect of the excitation pulse instability on the trigger regulator characteristics, which is of interest from the metrological point of view.

There exist [1] statistical studies of this effect based on the assumption that the variations in the pulse amplitude with time can be represented by a certain determined function of time.

The present article deals with the dynamic problem of the effect of the pulse instability (the speed of pulse variations is comparable with the speed of the transient decay in the system). At the same time the value of the pulse is considered as a random function of time due to a chaotic modulation of a pulse train.

For the first time such a problem was examined in its most general form for an arbitrary dynamic system in [2]. In this work a somewhat different method developed by S. M. Rytov is used for a direct investigation of fluctuations in self-oscillatory systems of the Thompson type, and applied for determining the limiting width of a spectral line of a tube generator [3]. The advantages of the above method amount in practice to the fact that it provides, by means of symbolic equations and the correlation theory, relatively simple solutions of the problem without solving the general equation of Fokker-Planck for the probability of transition.

The solution of the problem, in the general form, provided sufficiently simple relations of the root-mean-square deviation of the amplitude and the daily variation to the instability of the pulse (dispersion of the modulating function) for any trigger regulator.

The above expressions also provide a qualitative evaluation of the accuracy and noise resistance of trigger regulators of various types and indicate in each concrete case the means of improving accuracy.

Let us first examine the nature of the variations of the excitation pulse magnitude in trigger regulators from the point of view of statistical characteristics. These variations are due in various types of trigger regulators to different reasons: the instability of the torque of the escapement wheel in mechanical regulators, variations in the supply voltage, and contact resistance in electrical contact systems, drifting of the transistor parameters in contactless circuits of trigger regulators, etc. A detailed examination shows that, in all these cases, we deal to a greater or smaller extent with random processes. Let us illustrate this assertion on a less obvious example of the variations of the escapement wheel torque due to the nonuniformity of the drive gear ratio.

For any arbitrary mechanism variations with time in the escapement wheel torque can be represented by the expression:

$$m_x(t) = m_{x0} + \sum_{r=1}^{R} m_{xr} \sin(n_r t - \varepsilon_r), \qquad (1)$$

where m_{x0} is the mean value of torque; m_{xr} is the amplitude of the alternating components of torque, which are determined by the profile of the gearing and the play in wheels and pinions; ϵ_r are the phases of the alternating components determined by the initial position of the wheels.

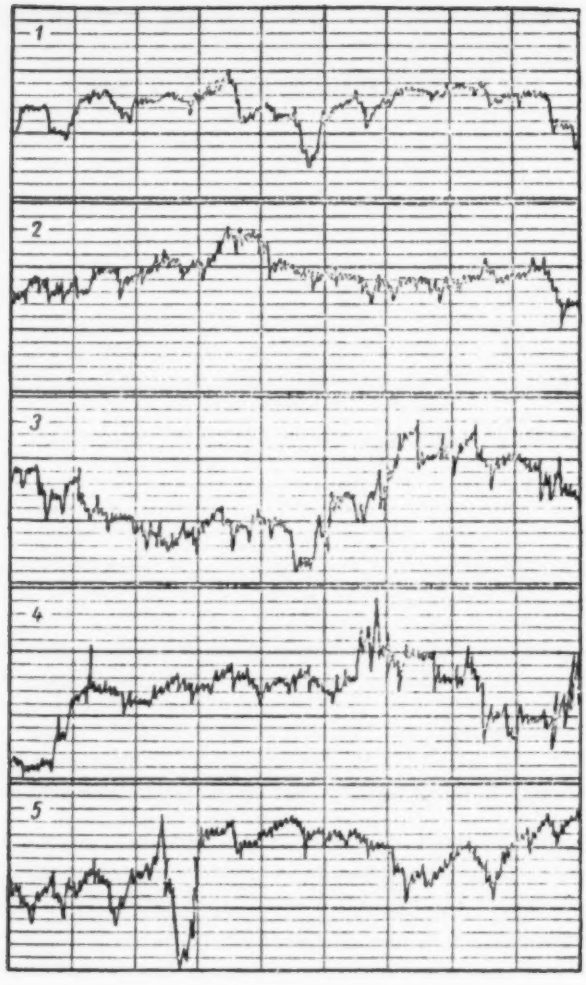

Fig. 1.

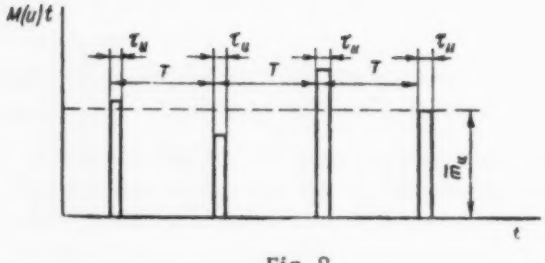

Fig. 2.

It is obvious that m_{xr} and ϵ_r are random quantities and m_{xr} follows a normal distribution law with $M[m_{xr}] = 0$*, and ϵ_r has an equal probability over segment $[0,2\pi]$. Then the variations of the torque of the escapement wheel [4] can be considered as a normal stationary random process of the type of (1).

Figure 1 shows the curves of the torque variations in an escapement wheel of five different "Volga" watches recorded on a microdynagraph. The shape of the above curves confirms in a graphic manner the conclusions we have arrived at.

It should also be noted that in the case of a pronounced regularity of $m_x(t)$ variations we can formally regard the process determined by (1) with a fixed m_{xr} and ϵ_r as a particular case of a random process with a spectral density of:

$$S(n) = \frac{\pi}{2} \sum_{r=1}^{R} m_{xr}^2 [\delta(n-n_r) + \delta(n+n_r)], \qquad (2)$$

where δ (n) is the Dirac function.

* $\overline{M[...]}$ is the symbol of mathematical expectation.

Thus, the excitation pulse train is modulated in a general case by the amplitude of a random function $\gamma(t)$, in the above particular case $\gamma(t) = m_x(t)$. Figure 2 shows such a pulse train, moreover, for the sake of simplicity the negative pulses of the return torque are not shown; τ_u is the pulse duration; T is the cycle interval which in the above case coincides with the period of self-oscillations, and $\overline{m_u}$ the mean value of the pulsed torque. From the above, it will be seen that we are dealing with a discrete (pulsed) random process.

In order to simplify the problem a little, it can be assumed that the random amplitudes of any pair of train pulses are independent, and the pulse process can be considered as a result of a second order* pulse amplitude modulation (PAM) of a pulse train by an interference of the type of white noise. In actual systems the spectrum of the pulse variations can be considered uniform only in a certain range of $n'' - n'$ where $n' = \min(n_r)$ and $n'' = \max(n_r)$ are the excluding frequencies. However, it is shown below that in the majority of cases examined by us this fact is not essential.

The power spectrum of this process is determined in a general case [4] by the expression of the form:

$$F(n) = \frac{2}{T} |g(n)|^2 \left\{ \sigma^2 [1 + \psi_1(n)] + \frac{2\pi}{T} \overline{m_u}^2 \sum_{r=-\infty}^{\infty} \delta\left(n - \frac{2\pi r}{T}\right) \right\}. \tag{3}$$

where g(n) is the spectral density of a single pulse; $\overline{m_u}$ is the mean value of the random pulse amplitudes; σ^2 is the dispersion of the random amplitudes.

$$\psi_1(n) = 2 \lim_{N \to \infty} \sum_{i=1}^{2N} \left(1 - \frac{i}{2N+1}\right) \rho_i(iT) \cos inT, \tag{3a}$$

where in turn $\rho_i(iT)$ is the correlation coefficient of the random pulse amplitudes.

If $\sum_{i=1}^{\infty} |\rho_i(iT)|$ is converging, the limit of (3a) exists and $\psi_1(n)$ determines the spectral density of the process. Taking into account that in our case $\rho_i(iT) = \sin iT\Delta / iT\Delta$ we obtain from (3) the following expression for the power spectrum of the process:

$$F(n) = F_\kappa(n) + F_\partial(n), \tag{4}$$

where $F_\kappa(n) = \frac{2}{T} |g(n)|^2 \sigma^2 \left(1 + 2 \sum_{i=1}^{\infty} \frac{\sin iT\Delta}{iT\Delta}\right)$ is the continuous portion of the spectrum;

and $F_\partial(n) = \frac{4\pi}{T^2} |g(n)|^2 \overline{m_u}^2 \sum_{r=-\infty}^{\infty} \left(n - \frac{2\pi r}{T}\right)$ is the discrete portion of the spectrum.

Figure 3 shows the power spectrum of the process represented by expression (4) for the case of $\Delta < \pi/4$. With an increasing Δ range the intervals between the boundary frequencies disappear and the spectrum becomes similar to the one with an infinite range of a modulating interference.

Having examined the statistical characteristic of the excitation pulse instability, let us investigate the effect of this instability on the parameters of the stationary self-oscillations in the regulator.

We shall represent the schematic of the trigger regulator in the form shown in Fig. 4, which is similar to the one used in [5]. In adopting the form of a centered random function $\lambda(t) = m_u(t) - \overline{m_u}$, let us account, in our schematic, for the pulse instability by introducing it formally as an extraneous fluctuation effect $\lambda(t)$.

* In pulse technique the amplitude of each pulse in second order PAM modulation is considered constant during the duration of the pulse and equal to the value of the modulating function at the instant of the pulse leading edge.

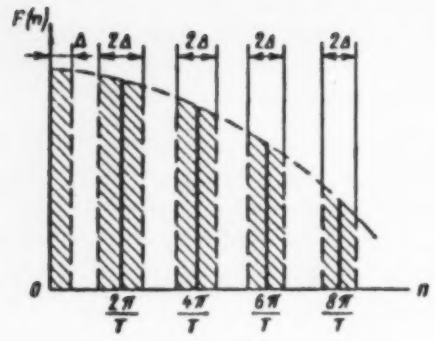

Fig. 3.

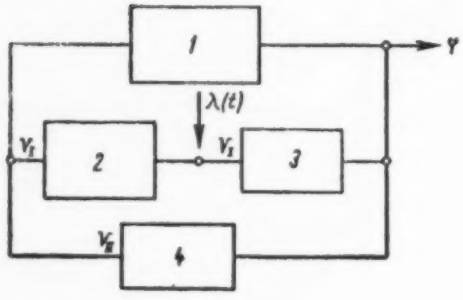

Fig. 4. 1) Linear part of the system; 2) delay element; 3) nonlinear element I; 4) nonlinear element II.

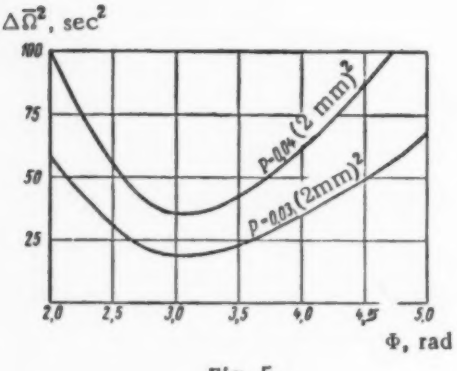

Fig. 5.

The linear part of the system is represented by an equation of the form:

$$\varphi = \frac{k_1}{T_1^2 p^2 + T_2 p + 1}(V_I' + V_{II}), \quad \left(p = \frac{d}{dt}\right), \tag{5}$$

where T_1 and T_2 are the time constants of the oscillating element; k_1 is the static transfer constant.

The nonlinear elements I and II are represented respectively by equations:

$$V_I = f_I(\varphi, p\varphi) \text{ and } V_{II} = f_{II}(\varphi, p\varphi). \tag{5a}$$

and the delay element by an equation of the form

$$V_I' = V_I e^{-p\tau}, \tag{5b}$$

where τ is the time of "pure" delay.

Let us assume that the system's parameters lead to unquenched oscillations which approximate harmonic oscillations. Then it is possible to write:

$$\varphi = -\Phi \cos \xi, \tag{6}$$

where $\dot{\xi} = n_0 + \dot{\psi}(t)$; Φ and ξ are slowly changing functions of time.

Owing to the high selectivity of the linear part of the system in actual triggering regulators the following inequality normally holds:

$$R_0 < 2\Delta, \tag{7}$$

where R_0 is the transmitting range of the linear part of the system tuned to a frequency of $n_0 \approx 2\pi/T$.

If condition (7) is fulfilled the oscillating system will obviously respond in the first approximation to a disturbance with a power spectrum (4) and to the first harmonic of a stable pulsed process modulated by a noncorrelated interference, i.e., to an interference with a correlation function of:

$$R_\lambda(t_1, t) = P\delta(t_1 - t), \tag{8}$$

where P is mean square of the interference.

Now the disturbance $\lambda(t)$ can be represented in the form:

$$\lambda(t) = \lambda^\circ \cos \xi + \lambda^* \sin \xi, \tag{9}$$

where coefficients λ° and λ^* are determined according to the principle of equivalent linearization. Having transformed in a similar manner the nonlinearities (5a) taking into consideration (5), (5b) and (9) and the schematic in Fig. 4 we obtain the following equation for determining the slowly changing functions Φ and ψ:

$$\frac{2}{n_0\Phi}\cdot\frac{\partial\psi}{\partial t}=k_1[(q_I^*+\lambda^*)\sin n_0\tau+(q_I^\circ+\lambda^\circ)\cos n_0\tau]-T_1^2n^2+kq_{II}^\circ+1;$$
$$\frac{2}{n_0}\cdot\frac{\partial\Phi}{\partial t}=k_1[(q_I^*+\lambda^*)\cos n_0\tau+(q_I^\circ+\lambda^\circ)\sin n_0\tau]+n_0(T_2+k_1q_{II}^*). \tag{10}$$

where

$$q_I^\circ=\frac{1}{\pi\Phi}\int_0^{2\pi}f(-\Phi\cos\xi,\ n_0\Phi\sin\xi)\cos\xi d\xi;\quad q_{II}^\circ=\frac{1}{\pi\Phi}\int_0^{2\pi}f(-\Phi\cos\xi,\ n_0\Phi\sin\xi)\cos\xi d\xi; \tag{10a}$$

$$q_I^*=\frac{1}{\pi\Phi n_0}\int_0^{2\pi}f(-\Phi\cos\xi,\ n_0\Psi\sin\xi)\sin\xi d\xi;\quad q_{II}^*=\frac{1}{\pi\Phi n_0}\int_0^{2\pi}f(-\Phi\cos\xi,\ n_0\Phi\sin\xi)\sin\xi d\xi. \tag{10b}$$

Provided in [5] are the values calculated from (10a) and (10b) of coefficients q_I^*, q_{II}^*, q_I^* and q_{II}^* in typical nonlinearities peculiar to the moving and oscillating systems of trigger regulators of various types. Owing to smallness of the pulse fluctuations it is possible to consider that:

$$\lambda^\circ=\Lambda^\circ\nu(t)\ \text{and}\ \lambda^*=\Lambda^*\nu(t), \tag{11}$$

where

$$\Lambda^\circ=\frac{\partial}{\partial\nu}\left[\frac{1}{\pi\Phi n_0}\int_0^{2\pi}m_a(-\Phi\cos\xi,\ n_0\Phi\sin\xi)\cos\xi d\xi\right]\text{and}\quad\Lambda^*=\frac{\partial}{\partial\nu}\left[\frac{1}{\pi\Phi n_0}\int_0^{2\pi}m_a(-\Phi\cos\xi,\ n_0\Phi\sin\xi)\sin\xi d\xi\right]. \tag{11a}$$

By virtue of the same assumption and by eliminating in the solution of (10) the regular components, i.e., taking that:

$$\Phi=\Phi_c+\Delta\Phi\quad\text{and}\quad\xi=\xi_c+\Delta\xi,$$

we obtain by inserting the latter expressions in (10) the following system of stochastic equations, relating the fluctuations of the amplitude and frequency with the pulse instability

$$(p+H)\Delta\Phi=-\frac{\nu(t)}{2\sqrt{Jc}}(\Lambda^c\sin n_0\tau+\Lambda^*\cos n_0\tau);\ p\Delta\xi=\Gamma\Delta\Phi-\frac{\nu(t)}{2\Phi\sqrt{Jc}}(\Lambda^*\sin n_0\tau+\Lambda^\circ n_0\tau) \tag{12}$$

where

$$H=-\frac{n_0}{2}\left[\frac{\partial}{\partial\Phi}(L_2\Phi)\right]_{\Phi_c};\quad\Gamma=-\left[\frac{\partial}{\partial\Phi}(L_1)\right]_{\Phi_c} \tag{12a}$$

J is the moment of inertia of the balance; c is the static stiffness of the spiral, and expressions

$$L_1=k_1(q_I^*\sin n_0\tau+q_I^\circ\cos n_0\tau)+k_1q_{II}^\circ-T_1^2n^2+1;$$
$$L_2=k_1(q_I^*\cos n_0\tau+q_I^\circ\sin n_0\tau+n_0q_{II}^*)+n_0T_2 \tag{12b}$$

determine in turn the stationary condition for a stable pulse when $L_1 = L_2 = 0$ and can be obtained from (10) for $\Lambda^\circ = \Lambda^* = 0$.

The first equation in system (12) is the well-known Langevin equation in the theory of the Brownian movement. This is a relaxation type of equation with a relaxation time of 1/H whose solution for a correlation

function can be written, taking (8) into account as:

$$R_{\Delta\Phi}(t,t_1)=\frac{W^*}{2H}\,e^{-H(t_1-t)}, \tag{13}$$

where

$$W^*=\frac{k_1^2 n_0^2}{4}(\Lambda^\circ \sin n_0\tau+\Lambda^* \cos n_0\tau)\,P. \tag{14}$$

In a stable state condition the mean square of the fluctuation amplitude can be determined from (13) by assuming that $t = t_1$:

$$\overline{\Delta\Phi}^2=\frac{W^*}{2H}. \tag{15}$$

From the latter expression it will be seen that the value of H characterizes the effect of the measured value of the pulse on its amplitude. On this basis it is possible to consider the value of H as the noise-proof coefficient of the regulator (in the theory of oscillations this quantity is known as the increment of the system).

It is interesting to note that the condition of amplitude stability in a stationary state of a trigger regulator is

$$H > 0, \tag{16}$$

which means that the noise suppression of the regulator increases with a rising stability reserve in the system for stable stationary self-oscillations.

When the pulse instability is represented by a regular time function, which is determined by expression (1) and the spectral density (2), the dispersion of the fluctuation amplitude for the r-th harmonic can be obtained by taking into consideration (12) in the form:

$$\overline{\Delta\Phi}^2=\frac{W_r^*}{\sqrt{H^2+n_r^2}}, \tag{17}$$

where

$$W_r^*=\frac{k_1^2 n_0^2}{4}(\Lambda^\circ \sin n_0\tau+\Lambda^* \cos n_0\tau)\,m_{xr}^2.$$

It will be seen from (17) that in this case the value of H has the significance of a noise-proof coefficient. Moreover, it also follows from the same expression that in the case of rapid pulse changes $|n_r \gg H|$ the system does not respond to these variations, and in the case of slow variations $|n_r \ll H|$, it repeats them with a proportionality factor of 1/H. This result becomes understandable physically if one takes into account that the value of 1/H also determines the durations of the transient state of self-oscillations.

The expression for the mean square of the frequency deviations can be obtained from the second equation of system (12) by taking into account (15):

$$\overline{\Delta n}^2=\frac{W^*\Gamma^2}{2H}+\frac{W^\circ}{\Phi_c^2}, \tag{18}$$

where

$$W^\circ=\frac{k_1^2 n_0^2}{4}(\Lambda^\circ \cos n_0\tau+\Lambda^* \sin n_0\tau)\,P. \tag{19}$$

By changing over to a more usual quantity in chronometry, namely the instantaneous daily variation, we obtain:

$$\overline{\Delta\Omega}=\frac{86400}{n_0}\sqrt{\frac{\overline{W^{*}\Gamma^{2}}}{2H}+\frac{\overline{W^{\circ}}}{\Phi_c^2}}. \tag{20}$$

In (20) the first term under the radical determines the daily variation deviations due to the variations of the amplitude caused by the nonisochronism of the oscillations; the second term determines the value of the daily variation deviations due directly to the variations of the pulse magnitude.

Let us now examine some of the characteristic applications of the above formulas.

A trigger regulator with a free lever escapement [6, 7]. Let us assume that the pulse curves are rectangular; that the losses in the strokes are concentrated in the first releasing stroke, and that the moment of inertia of the oscillating system does not change during its interaction with the escapement. Moreover, the oscillating system is assumed to have a constant and linear friction; the returning torque to be expressed by a polynomial of the third order and the wheel balanced.

Expression (12b) for this case will assume the form:

$$L_1=-\frac{(n^2-n_0^2)}{n_0^2}\Phi_c-\frac{(F_u+F_0)\lambda\beta\,\overline{m}_x}{\pi_c\Phi^2}-\frac{\sqrt{\Phi^2-\varphi_1^2(1-S_1^2)}\,\varphi_1}{\pi\Phi}+\frac{3}{4}\sigma_3\Phi^3;$$

$$L_2=-\frac{2\delta}{n_0}-\frac{4\rho}{\pi\Phi}+\frac{2(F_u\lambda-F_0\beta)}{\pi c\Phi^2}-\frac{(\Phi^2-\varphi_1^2)(1-S_1^2)}{\pi\Phi^2}. \tag{21}$$

where λ and β are the pulse and release angles; F_u and F_0, the mean value of the transfer functions for the pulse and release condition; ρ and δ, the damping coefficients of the constant and linear friction; φ_1, the initial release angle; S_1, the impact coefficient; σ_3, the nonlinearity coefficient.

It is possible to obtain for our case from (21) and (12a) the following expressions:

$$H=\delta+\frac{n_0(1-S_1^2)}{2\pi}-\frac{2\overline{m}_x(F_u\lambda-F_0\beta)-c\varphi_1^2(1-S_1)^2}{2\pi n_0 J\Phi_c^2}; \tag{22}$$

$$\Gamma=-\frac{3\overline{m}_x\lambda\beta(F_u+F_0)}{2\pi J n_0\Phi_c^4}-\frac{n_0\varphi_1(1-S_1^2)\sqrt{\Phi_c^2-\varphi_1^2}}{2\pi\Phi_c^3}+\frac{9}{\rho}\sigma_3 n_0\Phi_c^2. \tag{23}$$

and from (14) and (19):

$$W^{\circ}=\left[\frac{(F_u+F_0)\lambda\beta}{2\pi Jcn_0\Phi_c^3}\right]^2 P;\quad W^{*}=\left[\frac{F_u\lambda-F_0\beta}{\pi Jcn_0\Phi_c}\right]^2 P. \tag{24}$$

Then we shall have for the quadratic mean deviation of the amplitude by virtue of (15):

$$\overline{\Delta\Phi}=\frac{(F_u\lambda-F_0\beta)}{\pi_c\Phi}\sqrt{\frac{P}{JcH}}, \tag{25}$$

and for the quadratic mean deviation of the daily variation

$$\overline{\Delta\Omega}=\frac{43200}{\pi c\Phi_c}\sqrt{(F_u\lambda-F_0\beta)^2\Gamma^2+\frac{4}{\Phi_c^4}[(F_u+F_0)\lambda\beta]^2 H}\cdot\sqrt{\frac{P}{JcH}}. \tag{26}$$

Figure 5 shows the relation of the daily variation deviation to the deviation of the torque of the escapement wheel for the trigger regulator with the following parameters: $J = 0.16400 \cdot 10^{-2}$ g·mm·sec^2; c= 0.40465 g·mm; $\beta = 5°40'30''$; $\lambda = 30°40'54''$; $F_0 = 0.06198$; $F_u = 0.22220$; $\delta = 0.01$; $\varphi_1 = 18°10'42''$; $\sigma_3 = 0.0001$; and $\rho = 0.02$.

Trigger regulator of a contactless electrical escapement [8]. Let us examine the system with the following basic assumptions: the pulse curves are rectangular, and the oscillatory system has a constant and linear friction. There are no other disturbances. The degree of lag in the system is considerable and must be taken into account.

The main factor leading to instability in this case is the variation in the supply voltage which can be considered as a normal δ-correlation random process.

Under these conditions expression (12b) will assume the form

$$L_1 = -\frac{(n^2 - n_0^2)}{n_0^2}\Phi_c + \frac{(A-D)\lambda}{\pi\sqrt{J_c}}\sin n_0\tau; \quad L_2 = -\frac{2\delta}{n_0} - \frac{4\rho}{\pi\Phi} + \frac{(A-D)\lambda}{\pi\sqrt{J_c}\,\Phi}\cos n_0\tau, \tag{27}$$

where

$$A = \frac{W_0 W_u B^2 S_0^2}{R+R_0} \text{ and } D = \frac{W_0^2 B^2 S_0^2}{R+R_0}. \tag{28}$$

Here W_0 and W_u are the number of turns in the release and pulse coils; S_0, the equivalent area of the coil; β, the gain of a transistorized stage; B, the magnetic induction in the effective gap; R, R_0, the input resistance of the amplifying stage and the effective resistance of the release coil.

From (27) and (28) we obtain by taking (12a) into consideration:

$$H = \delta, \qquad \Gamma = \frac{(A-D)\lambda}{2\pi J\,\Phi_c^2}\sin n_0\tau, \tag{29}$$

and from (14) and (19):

$$W^0 = \frac{A'}{2\pi J\,\Phi_c}\cdot\frac{\sin n_0\tau}{R+R_0}\left[\left(\frac{W_u\alpha}{1-\alpha} - W_0\right)\frac{1}{R+R_0}\frac{\partial R}{\partial E_n} - \frac{W_u}{(1-\alpha)^2}\cdot\frac{\partial\alpha}{\partial E_n}\right];$$
$$W^* = \frac{A'}{2\pi J}\cdot\frac{\cos n_0\tau}{R+R_0}\left[\left(\frac{W_u\alpha}{1-\alpha} - W_0\right)\frac{1}{R+R_0}\cdot\frac{\partial R}{\partial E_n} - \frac{W_u}{(1-\alpha)^2}\cdot\frac{\partial\alpha}{\partial E_n}\right], \tag{30}$$

where $A' = W_0 B^2 S_0^2$; α, the static gain of the transistor; $\partial\alpha/\partial E_n$ and $\partial R/\partial E_n$ – the slopes of the curves of α and R with respect to the supply voltage.

By inserting (29) in (30), (30a) in (15) and (20) it is possible to obtain in this case expressions similar to (25) and (26).

It follows from (29) that the noise suppression in electrical contactless watches of the type under consideration is determined for the assumed conditions by the coefficient of linear friction δ. The same conclusion was arrived at in [9] experimentally when developing a similar system, and special measures were taken in the design of the ATO-Jungans watch for increasing linear friction in the oscillatory system in order to raise the noise suppression with respect to pulse fluctuations.

Conclusions. As the result of the investigation, expressions were obtained which related the amplitude deviations of the self-oscillations in the regulator and daily variations to the instability of the excitation pulse.

A dynamic study of the question provides the value of the critical rate of variation of the pulse magnitude for which the oscillatory system stops reacting to these variations, which apparently is very important for designing devices of the type of pulse stabilizers and starting units.

The above results can be without further complications applied if required to the case of a correlated pulse envelope providing this fact is taken into consideration when solving equation (12) [10].

LITERATURE CITED

[1] A. M. Torgov, "A dynamic investigation of certain basic types of trigger regulators," Dissertation [in Russian] (MBTU, 1948).

[2] L. Pontryagin, A. Andronov, and A. Vitt, Zhur. Éksp. i Teoret. Fiz. 3, 3 (1933).

[3] S. Rytov, Zhur. Éksp. i Teoret. Fiz. 29, No. 3 (1955).

[4] B. L. Levin, The Theory of Random Processes [in Russian] (Izd. Sovetskoe Radio, 1957).

[5] V. A. Shpolyanskii, Bulletin of the Acad. Sci. USSR, "Automation and Power" Series [in Russian] (1959) No. 6.

[6] A. M. Kuritskii and V. A. Shpolyanskii, Higher Educational Institutions Scientific Papers, "Engineering and Instrument Making" Series [in Russian] (1959) No. 1.

[7] A. M. Kuritskii and V. A. Shpolyanskii, Higher Educational Institutions Scientific Papers, "Engineering and Instrument Making" Series [in Russian] (1959) No. 2.

[8] V. A. Shpolyanskii, Collection of Works of the Scientific Research Institute of the Watchmaking Industry [in Russian] (1959) No. 2.

[9] G. Glaser, Annales Françaisde Chronometric I (1958).

[10] V. A. Shpolyanskii, Bulletin of the Acad. Sci. USSR, "Automation and Power" Series [in Russian] (1960) No. 3.

MECHANICAL MEASUREMENTS

A MACHINE FOR THE CALIBRATION AND CHECKING OF DYNAMOMETERS UP TO 50 TONS

O. N. Fofanov

Translated from Izmeritel'naya Tekhnika, No. 9, pp. 22-23, September, 1960

The machine described inthis article serves to calibrate and check different dynamometers with a specified error of 1-2% including those of a large size and weight; for instance, 50 ton hydraulic crane scales having a mass of 0.5 tons.

The dynamometer which is being calibrated or checked is attached to grips 1 and 2 (see figure). The value of the required force is adjusted by a dial type indicator 3 of dynamometer 4 and the loading is done by means of electromechanical jacks 5, which transmit the effort to grip 2. Weights 6 and 7 connected to beam 8 serve to calibrate dynamometer 4; their total mass amounts to 5 tons. These weights can be periodically placed on the rest of the connecting link 10 by means of the electromechanical jacks 9. Weights 6 and 7 are normally lifted, except for the calibration of dynamometer 4, leaving a gap between the bearing of beam 8 and the rest of link 10. Thus, dynamometer 4 will respond to the same force as grip 1. The calibration by means of the lifting and lowering of weights 6 and 7 is controlled electrically from push-button assembly 11.

The measuring device in this machine used for determining the applied force consists of a mechanical dynamometer calibrated by the method described in [1, 2].

The sensing element of the dynamometer consists of a rod which becomes deformed by the tensile force applied to its ends. The rod carries two sleeves, one inside the other. One end of each sleeve is fixed to an end of the rod. Thus, when the rod is strained, the sleeves move with respect to each other in the direction of the longitudinal axis of the rod. One of the sleeves is attached to a lever which displaces, due to the relative movement of the sleeve, a connecting rod and indicator 3 which is fixed to a bracket mounted on the other sleeve. Thus,each force applied to the rod will correspond to a certain number of divisions on indicator 3.

For the calibration of dynamometer 4,another dynamometer similar to it is placed between grips 1 and 2. Let us call it dynamometer B and denote dynamometer 4 as A. The calibration is carried out by means of a series of repeated operations.

Before placing any loads on the dynamometers A and B, their zero readings are adjusted. Then the operations proceed as follows.

Operation No. 1. By lowering weights 6 and 7 the rest of link 10 is loaded with force P = 5 ton; the absence of any loading on dynamometer B is checked by its zero reading; then a force of P = 5 ton is applied to dynamometer A; the reading $l_{I}^{(a)}$ is taken on dynamometer A; weights 6 and 7 are lifted,force P released, and then both dynamometers are loaded by means of jacks 5 to a force Q_{AI} which corresponds to the reading $l_{I}^{(a)}$; reading $l_{I}^{(b)}$ of dynamometer B is noted. Both dynamometers will be subjected to force Q which is equal to force P within the accuracy of dynamometer A.

Operation No. 2. By lowering the weights,grip 1 is loaded with 5 ton; dynamometer B is then loaded by means of jacks 5 to a force Q_{BII} which corresponds to the reading $l_{I}^{(b)}$; reading $l_{II}^{(a)}$ of dynamometer A which corresponds to force $P + Q_{BII}$ is noted; force P is then lifted and from the reading $l_{II}^{(a)}$ force Q_{AII} is set up which

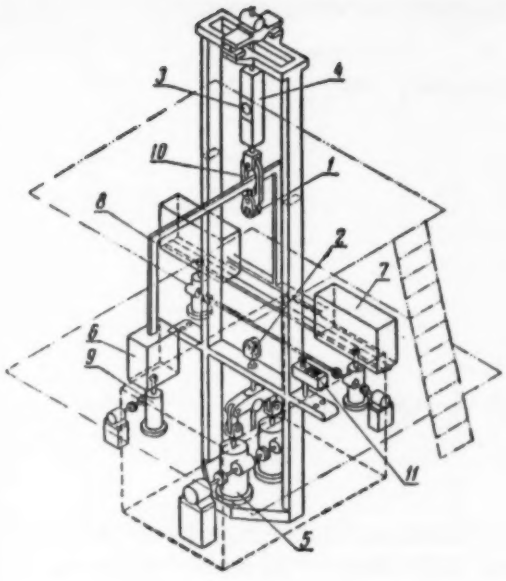

is equal to 2P within the accuracy of reproducing forces by readings $l^{(a)}$ and $l^{(b)}$; the reading of $l_{II}^{(b)}$ which corresponds to force Q_{AII} is noted.

By continuing similar operations it is possible to load the dynamometers up to any force nP and to determine the corresponding readings of their indicating devices.

According to instruction 20-49 [3] the errors of dynamometers with nominal scales must be determined from the deviations of their readings which are obtained for each step by a threefold loading with actual forces. If these deviations do not exceed 0.5% of the measured force, the dynamometer should be considered satisfactory according to the requirements specified for reference dynamometers of grade III. When the forces are reproduced by the method outlined above, the relation between the effective force and the readings of the dynamometer being calibrated are derived in [2] and represented by Eq. (7).

On the basis of the law of adding mean errors [4], the relation will assume the form:

$$l_{m.n}=K_{m.n}\,nP+K_{m.n}\sum_{i=1}^{i=n}\theta_{Pi}\pm\sqrt{(K_{m.n}\sigma_{Qn})^2+(\sigma_{Kn}\,nP)^2} \qquad (1)$$

The deviations in the readings thus obtained are due to errors which are expressed by the terms $K_{m.n}\,\sigma_{Qn}$, and $\sigma_{kn}\cdot nP$. The first one is due to the accumulations of the step by step reproduction errors of the forces and is inherent in the method employed. The second term determines the nominal accuracy of the dynamometer being calibrated at its n-th step of loading. In other words, it represents the quadratic mean of the dispersion of readings providing the actual forces are reproduced with absolute accuracy. Since in practice this condition cannot be fulfilled, any transfer of reference values of forces to working samples will entail errors which will mostly consist (when checked by comparison with a reference instrument) of random errors of the reference instrument. In order to prevent them affecting, to any considerable extent, the accuracy characteristic of the instrument under consideration, it is recommended in [4] to preserve condition:

$$\xi_n<0.3\,\xi_m. \qquad (2)$$

where ξ_n is the error characterizing the accuracy of the reference instrument; ξ_m is the error characterizing the accuracy of the instrument being tested.

In the above method of reproducing the forces, $K_{m.n}\,\sigma_{Qn}$ corresponds to ξ_n. Moreover, their values can only be determined after calibration. It is not necessary to make such a determination if the set accuracy of the dynamometer being calibrated satisfies the specified requirements; in other words, if the sum of errors represented by terms $K_{m.n}\,\sigma_{Qn}$ and $\sigma_{kn}\,nP$ and expressed in the dispersion of repeated measurements does not exceed the tolerance specified for the given dynamometer. This case is the most convenient for the practical application of the above method. It applies to the calibration of dynamometer 4. As the result of periodic calibrations of this dynamometer, during six months, a good consistency of the calibration characteristics of the dynamometer has been established which was preserved during a long period of use (several years) of this machine.

LITERATURE CITED

[1] O. N. Fofanov, Izmeritel'naya Tekhnika, No. 4 (1958).*

* See English translation.

[2] O. N. Fofanov, Izmeritel'naya Tekhnika, No. 12 (1959).*

[3] Instruction 20-39 for the Calibration and Checking of Reference and Working Dynamometers [in Russian] (Moscow, 1954).

[4] M. F. Malikov, Foundations of Metrology [in Russian] (Moscow, 1949).

A BELL DIFFERENTIAL MANOMETER DKFM

M. D. Gafanovich and B. Ya. Gorodetskii

Translated from Izmeritel'naya Tekhnika, No. 9, pp. 23-25, September, 1960

The Khar'kov plant of control and measuring instruments developed and placed in production a contactless primary instrument consisting of a bell differential manometer DKFM intended for measuring pressure differences of noncorrosive gases and the conversion of the readings into electrical signals.

By means of a measuring instrument type VF, the readings of the bell manometer can be remotely received and transformed into pointer indications or chart records.

The bell differential manometer DKFM can be used in conjunction with an electrohydraulic regulator REG and a remote transmitting transducer DZF for automatic control of pressure differences and flow of gases.

The sensing element of the instrument (see figure) consists of a bell 1 partially immersed in oil. The effort arising at the bell under the effect of the measured pressure difference is balanced out by spring 2. The displacement of the bell produces a rotation of frame 3 of the ferrodynamic transducer 4, which converts the angle of rotation into a proportional electrical quantity [1]. Thus, the differential manometer converts the measured pressure difference into an alternating voltage.

The differential manometer mechanism is assembled in a hermetically sealed container 5.

A small tank 6 which is placed in the upper part of the container, houses the measuring units of the instrument. In order to protect them from gas corrosion, the tank is filled to the brim with transformer oil. The bell is connected by means of hook 7 to lever 8 which is fixed to support 9 by means of flat crossed springs 10 which provide a frictionless movement for lever 8. Lever 8 is connected to a balancing spring 2 and a sector 11 which serves to transmit the rotation to the coil of the ferrodynamic transducer by means of gear 12.

The measuring range is changed by varying the number of turns in the working windings and by balancing the spring as well as by the choice of a suitable bell. The setting of the initial position of the bell, that is the zero adjustment, is carried out by means of screw 13.

The lower part of the container has two cavities (traps) for collecting the condensate. The drainage of the precipitate is made through holes plugged with stoppers.

The instrument operates with the larger pressure supplied to the space above the bell and the smaller pressure to the space below it.

The electrical connections to the ferrodynamic transducer are made by means of a hermetically sealed through-socket 14.

Instruments DKFM are made for the following top limits: 4, 6.3, 10, 16, 25, and 40, ± 3.2, ± 5, ± 8, ± 12.5, and ± 20 mm H_2O.

* See English translation.

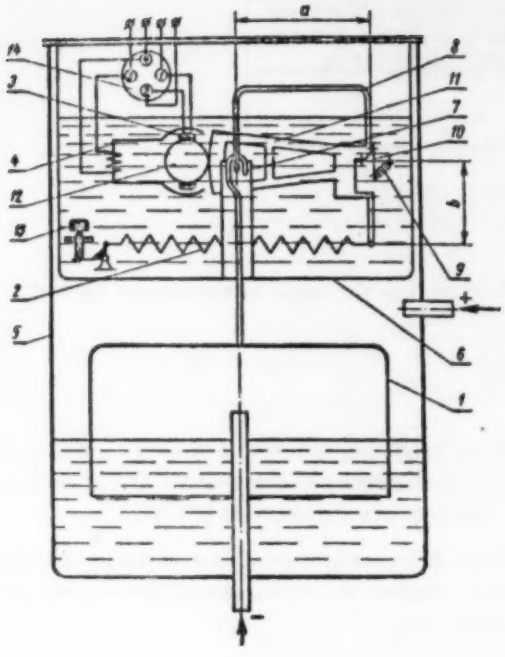

The maximum permissible working pressure in the instrument is 0.5 kg/cm^2.

The accuracy grade of the instrument and the permissible main reading error of the set consisting of the DKFM manometer, and measuring instrument VF are shown in the table.

The feeding of the ferrodynamic transducer is made from the instruments which work in conjunction with the manometer.

The over-all dimensions of the differential manometer are 370 × 300 × 308 mm. Its weight is some 30 kg without the oil.

The basic relation of the bell differential manometer is expressed by the following equation [2]:

$$H=(P_1-P_2)\frac{F-\frac{Sf}{\Phi-S}}{\frac{c(\Phi-S-f)}{\Phi-S}+f(\gamma_1-\gamma_2)}, \qquad (1)$$

where H is the displacement of the bell; P_1 and P_2 are the pressures whose difference is measured; Φ, F, S, and f are areas respectively of the cross sections of the internal cavity of the container, internal cavity of the bell, the tube, which feeds the lower pressure to the instrument and of the walls of the bell; c is the stiffness of the measuring spring; γ_1 and γ_2 are specific gravity, respectively, of the oil and the media above the oil.

In (1) the fraction

$$\frac{F-\frac{Sf}{\Phi-S}}{\frac{c(\Phi-S-f)}{\Phi-S}+f(\gamma_1-\gamma_2)}=A$$

is constant for any given instrument. Thus, the displacement of the bell is related to the measured difference of pressures by a linear expression

$$H=A(P_1-P_2). \qquad (2)$$

Relation (2) has been derived for a balancing spring directly connected to the bell. In the differential manometer DKFM, for the convenience of connecting to the rotating coil of the ferrodynamic transducer, the bell is coupled to the balancing spring by means of a lever (see figure). Owing to a number of constructional devices this drive is sufficiently linear to be able to apply Eq. (2) to the instrument.

In order to obtain a linear relation between the displacement of the bell and the deformation of the balancing spring the following measures were adopted. When the pressure difference is 50% of its maximum, lever a (see figure) is perpendicular to the axis of the bell, and lever b is perpendicular to the axis of the balancing spring. Moreover, the suspension point of the bell from the lever system is horizontally in line with the axis of rotation of levers a and b. The length of the balancing spring is made sufficiently large as compared with the displacement of the end of lever b in the direction perpendicular to the axis of the spring; hence, with an error not exceeding 0.01%, it becomes possible to assume the direction of the spring to be constant with a rotating lever b.

The bell of the differential manometer DKFM is coupled to the moving coil of the ferrodynamic transducer by means of a lever drive. By adopting the notations shown on the figure it is possible to express the

Measuring range, mm H_2O	Grade of accuracy	Permissible main error as read on the measuring instrument, %
10; 16; 25; 40 / ±8; ±12.5; ±20	1.5	±2.0
4; 6.3 / ±3.2; ±5	2.5	±3.0

relation of the bell displacement (or the measured pressure difference) to the angle of rotation of the ferrodynamic transducer coil by the following equation:

$$H = a \sin \alpha. \qquad (3)$$

It will be seen from (3) that the coupling between the above quantities is linear and only for small value of angle α. In the above instrument, the permissible value of the nonlinearity is taken to be 1/5 of the 1.5 accuracy grade of the manometer which amounts to ± 0.3%. This requires a maximum $\alpha = 4°$.

It is useful to note several constructional peculiarities of the differential manometer including the following. The adjustment of the measuring system of the instrument is attained in varying the stiffness of the measuring spring by decreasing or increasing the number of its effective turns.

In order to decrease the variations in the manometer readings due to the hysteresis of the measuring spring, the latter is operated in a condition where its actual extension is 1/5 or 1/6 of its permissible maximum.

As compared with other existing bell differential manometers (KÉP, KÉM, THSK, and others) instrument DKFM has the following advantages. For the same metrological properties and measuring ranges as the above instrument the DKFM manometer is considerably smaller and weighs less; its construction is simple and reliable in use. The DKFM instrument has a high speed of operation and provisions for remote measuring on an indicating or recording instrument.

LITERATURE CITED

[1] M. D. Gafanovich, Izmeritel'naya Tekhnika, No. 10 (1959).*

[2] P. P. Kremlevskii, Flow Meters [in Russian] (Mashgiz, 1955).

AN AUTOCOMPENSATED THERMAL VACUUM GAUGE

V. I. Bakhtin and V. N. Mikhailin

Translated from Izmeritel'naya Tekhnika, No. 9, pp. 25-26, September, 1960

Figure 1 shows the schematic of the electrical circuit of a thermal vacuum gauge, which differs from the normal vacuum gauge VT-2 by its wide range, increased sensitivity and smaller delay in measurements. The thermal emf of its thermocouple manometric lamp LT-2 is fed to the input of a chopper consisting of a standard relay RP-5 (P_1) and then to the input of a three stage amplifier (tubes 6N2P-T_1, and 6P6S-T_2). The thermocouple voltate is converted and amplified by a factor of 35000 and then connected through a step-down (1/50) transformer Tr2 to a rectifier (2× DGTs-24) and used for controlling an output power transistor P4B. The heater of the manometric lamp is connected in series with the 6 v supply voltage to the output of this transistor. The

* See English translation.

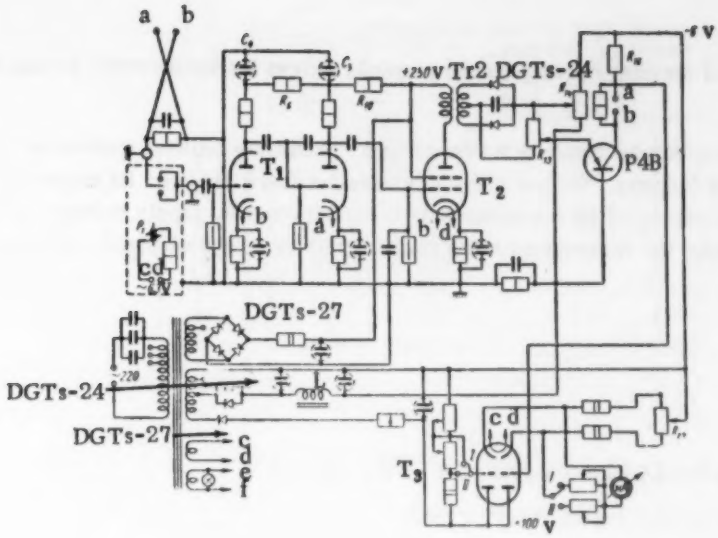

Fig. 1.

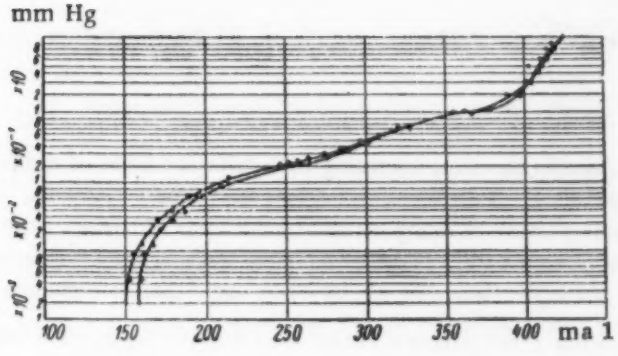

Fig. 2.

decoupling circuits R_6C_4 and $R_{10}C_5$ are provided for improving the dynamic characteristics of the amplifier; owing to these circuits, the ripple factor of the amplified voltage can be reduced to 0.01-0.005. Potentiometer R_{13} is used for tuning the circuit and readjustment tubes are changed. Potentiometer R_{14} provides an adjustment of the initial current of the manometric tube heater, i.e., of the operating temperature of the thermocouple. The gas pressure is measured by the amount of current flowing through the heater. The current is measured in turn by the voltage drop across the standard resistor R_{16} by means of a differential method and the use of triode 6N8 (T_3) and grade 1, 10 μa microammeter M24.

A system of adjustable resistors provides a control of the zero setting and of the sensitivity for measuring the current within the range of pressure variations. The manometer circuit is mounted on the jacket of vacuum gauge VT-2 and is supplied directly from the 220 v source.

Two calibration curves of the autocompensation thermal vacuum gauge which represent the two extreme deviations of the experimental points are shown in Fig. 2. In calibrating the system of manometer VT-2, a sloping oil manometer and a MacLeod type manometer with an error of ± 3 to 4% of the measured value were used. It will be seen from Fig. 2 that the working range of the manometer is 10^{-3} to 10 mm Hg. Its sensitivity increases with a decreasing measured pressure from 6 ma per 1 mm Hg for the range of 1 to 10 mm Hg to 250 ma (for the range of 10^{-2} to 10^{-1} mm Hg) and 1250 ma (for the range of 10^{-3} to 10^{-2} mm Hg). The dispersion of the experimental points with respect to the mean calibration curve does not exceed ± 5% of the measured value. A relatively small deviation between curves taken at different times makes it possible to assume a good stability in the operation of the manometer.

The autocompensated thermal vacuum gauge responds almost instantaneously to rapid variations in the measured pressure.

The above manometer can be conveniently used as a controlling unit for systems of automatic control, regulation and signalling in industry. With a 100% negative feedback between its output and input, the manometer is noise proof; the accuracy of its measurements is not affected by supply voltage variation of ± 15%, it is not necessary to recalibrate the manometer when manometric tubes are changed, and it provides a powerful output signal.

MEASUREMENT OF ACCELERATIONS BY MEANS OF PIEZOELECTRIC TRANSDUCERS WORKING IN STRAIN-GAUGE EQUIPMENT

B. A. Glagovskii

Translated from Izmeritel'naya Tekhnika, No. 9, pp. 26-28, September, 1960

Various acceleration measuring devices, operating with different types of transducers [1, 2] are now being used for measuring acceleration in mechanisms and assemblies and in their elements. Acceleration transducers using for their sensitive elements a ceramic composition on the basis of barium titanate, barium metatitanate and other materials [3] are now widely used. These transducers work in conjunction with other special measuring devices [1, 3] which are made, for their own use, by every organization concerned.

The equipment for measuring acceleration consists of an amplifying circuit, with its supply unit, connected to a recording instrument, for instance, an oscilloscope. Above amplifiers have a relatively high limit at low frequency (of the order of 5 cps)* and are not noise proof, since their wide frequency band includes the commercially used frequencies of 50 and 400 cps.

At the present time equipment which works with various types of strain sensitive transducers is becoming popular in laboratory and industrial applications.

There exist many types of strain measuring devices, which have been developed by different organizations and prove to be satisfactory in use. Strain measuring installations 8ANCh-7M, UTS1-VT-12 and ITU-6 are now being mass produced [4] by our industry.

A strain gauge equipment which operates with a carrier frequency has several advantages: it is highly sensitive, noiseproof, and covers a wide frequency range (down to zero frequency) and has other good properties.

These considerations prompted us to develope a circuit for measuring accelerations based on the standard strain gauge equipment and piezoelectric transducers.

A special attachment has been developed by us to couple the transducer to the strain gauge equipment.**

Figure 1 shows an acceleration measuring circuit for the case in question. The transducer with a barium titanate sensing element is fixed to the structure (detail) under test. The signal is transmitted from the transducer

* The low frequency limit is determined not only by the amplifier, but also by the input impedance of the amplifier, the transducer parameters, the measuring line and other factors.

** The attachments were made under the guidance of T. M. Smirnova, they were adjusted and tuned by Yu. F. Ivanov and I. P. Fil'chenko.

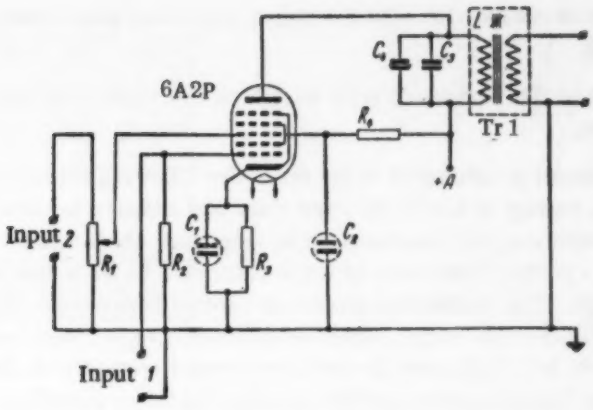

Fig. 1.

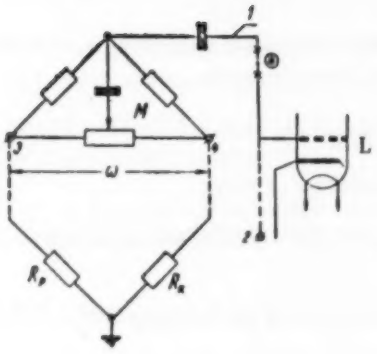

Fig. 2.

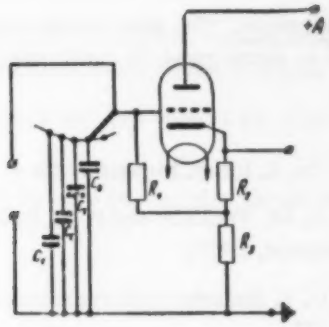

Fig. 3.

to the input stage and from there through a measuring line to the attachment, which is fed by the carrier frequency of the strain gauge equipment. The transducer voltage modulates through the input stage the carrier frequency, which passes through the measuring channel of the strain-gauge equipment (an amplifier and a phase-sensitive device) to the recording instrument.

Of the two types of attachments developed by us, which consist in the first type of an anode modulation stage and in the second type of a mixer stage, the second proved to be the simpler to make and adjust (Fig. 1).

Input 2 is fed by the carrier frequency from the strain-gauge equipment and input 1 by the signal from the transducer transmitted through the input stage. Potentiometer R_1 provides an adjustment of the carrier level.

In transformer Tr1, connected in the anode circuit of tube 6A2P, amplitude-modulated oscillations are produced which have a carrier frequency ω, a lower side band $\omega - \Omega$, and a higher side band $\omega + \Omega$ (where Ω is the frequency of the measured process).

The amplitude modulations are obtained in the same manner as for the operation of the strain-gauge equipment with the transducer bridge connected to the input. The above oscillations, however, by-pass the input bridge M of the strain-gauge equipment (Fig. 2), the bridge is disconnected (unsoldered) from the amplifier 1 input, and are fed directly to point 2. The carrier frequency ω required for the operation of the attachment, is taken from the supply diagonal of the bridge, points 3 and 4. These alterations do not require any modifications of the strain-gauge equipment and can be carried out very quickly both under factory and field conditions by the maintenance personnel.

The batch of attachments, produced by us, was used with piezoelectric transducers* type DU-3 and input stages of equipment ITU-6 which were connected in the manner shown in Fig. 3.

* The transducers were developed and made by V. M. Zubkov.

The transducers DU-3 in conjunction with the output stages and attachments operated with the strain-gauge equipment ITU-6 [5].

The carrier frequency of this equipment is 50 kc, which determined the winding data of transformer Tr1 in the measuring attachment.

The measuring attachment is calibrated in the set in the following sequence: input stage, attachment, strain-gauge equipment. A voltage is fed to the input stage and adjusted to correspond to the fixed values of acceleration obtained in calibrating the transducer. The amplitude characteristic of the channel is obtained either from the readings of a pointer instrument which is connected to the output strain-gauge equipment, or directly from the oscilloscope. The calibration graphs are plotted both for the fixed values of the carrier frequency and for definite positions of the range switch in the strain-gauge equipment. As a rule the sensitivity of the strain-gauge equipment is to high, and the instrument works normally on the second, third or lower sensitivity range, thus providing high operating stability (a larger feedback is used).

The measuring attachment makes it possible to utilize the valuable properties of the strain-gauge equipment and the piezoelectric transducers; including their very low frequency limit, high sensitivity, very low response to noise, etc.

Conclusions. The good results obtained in the use of this attachment for measuring accelerations make it possible to recommend its application in factory and laboratory measurements.

LITERATURE CITED

[1] Yu. I. Iorish, Measurement of Vibrations [in Russian] (Mashgiz, 1956).

[2] A. M. Turichin and P. V. Novitskii, Wire Transducers and Their Technical Application [in Russian] (Gosénergoizdat, 1957).

[3] G. E. Rudashevskii, Piezoelectric Ceramic Vibration Transducers [in Russian] (1956) ITÉIN subject I, No. P-56-477.

[4] A. M. Turichin, editor, Wire Transducer Strain-Gauge Measurements [in Russian] (Mashgiz, 1959).

[5] B. A. Glagovskii and N. Ya. Shtrasfogel', Strain-Gauge Equipment ITU-6 [in Russian] (1959) ITÉIN No. P-59-34/6.

SCALES WITH TRANSVERSE GRADUATIONS

S. N. Basovich

Translated from Izmeritel'naya Tekhnika, No. 9, pp. 28-29, September, 1960

For accurate measurements of segments,including the reading of measuring instruments of the 0.2 and 0.1 grade,transverse scales are used. They help to eliminate the error of determining by inspection by tenths of a graduation.

The transverse scale consists (see figure) or equidistant horizontal lines crossed by perpendicular (vertical) and inclined (transverse) lines (a). The application of scales with transverse graduations provides a reliable evaluations of tenths of a graduation. The reading of such scales is, however, complicated due to their clogging with a multiplicity of lines. In order to clear the scale,the vertical lines are sometimes removed, but this measure only partially solves the problem.

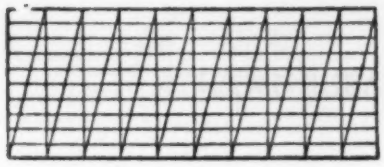

a

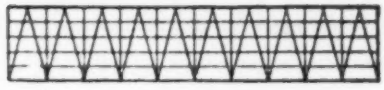

b

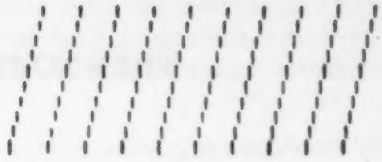

c

d

In order to simplify the scale (a) and make its reading more convenient, we propose to draw vertical lines through the crossing points of the inclined and horizonal graduations and delete all the remaining lines (c).

In order to simplify the reading still further and reduce the size of the scale in the direction of the lines, a similar transformation is applied to scale (b).

Scale (b) has been obtained from scale (a) by reflecting symmetrically about the middle horizonal line the upper half of the scale on the lower one. The results of this simplification are shown in figure d.

The number of intermediate lines depends on the accuracy required and can equal 9 (in c and d) or any other number (for instance 4 or 1).

Contrary to the existing transverse scales,the proposed scale can be used in precision liquid instruments (for instance, areometers and metal alcoholometers).

THERMOTECHNICAL MEASUREMENTS

THE USE OF ALTERNATING CURRENTS FOR CALIBRATING COMMERCIAL OPTICAL PYROMETERS

Yu. Ya. Donde and M. A. Pisarevskaya

Translated from Izmeritel'naya Tekhnika, No. 9, pp. 29-30, September, 1960

When commercial optical pyrometers are calibrated by means of grade 2 temperature lamps, the latter are supplied with direct current. This is due to the greater accuracy attained in measuring direct current which is flowing through the lamps. The feeding of lamps with approximately 20 amp dc is, however, often difficult in factory test laboratories. These difficulties prompted us to look for another solution of this question.

In this instance, it appears to be most expedient to feed the lamps with a stabilized sinusoidal current although this involves a certain reduction in the accuracy of measuring the current which flows through the lamp.

It will be shown that the reduction in accuracy is small and permissible.

In view of the above, the electric lamp plant at Moscow made, in 1958, a universal installation for calibrating optical pyrometers by means of grade 2 temperature lamps, which operated both with dc and ac.

It will be seen from the electrical circuit of the installation (see figure) that the temperature lamp L_1 (type LT-1) can be fed either with dc or ac. The selection of the current is made with a plug-in connector P_1.

The part of the circuit intended for operation on dc does not differ in any way from the existing circuits, which are being produced by our industry.

The ac part of the installation is supplied from 220 v mains through a sinusoidal ferroresonating voltage stabilizer St, an autotransformer AT (type LATR-1) and a step down transformer Tr2 (220/10 v). The current of the temperature lamp is controlled by means of autotransformer AT and partly by rheostats $R_1 - R_3$, which are mainly used for dc control.

The current flowing through the lamp is measured by means of an electrodynamic ammeter type ÉLA (grade 0.2, vernier 5 amp scale) connected to the circuit through an instrument transformer Tr1 (20/5 amp).

The data in the certificates provided by the VNIIK (All-Union Scientific Research Institute of the Committee of Standards, Measures and Measuring Instruments) for grade 2 dc calibrated temperature lamps together with lens and glass PS-5 are used for operating the equipment. Moreover, in calibrating optical pyrometers by means of the above equipment with an alternating current there can arise an additional error due not only to the lowering of the accuracy of electrical measurements, but also to the possible (apparently very small) difference in the calibration of temperature lamps with an alternating as compared with a direct current.

Without considering the possible differences in the calibration of temperature lamps by means of direct or alternating currents, let us dwell on the reduction in the accuracy of measuring the current flowing through the lamp, since this is the controlling factor.

If a grade 0.2 ammeter with a full scale deflection of 20 amp is used without corrections, the maximum absolute error amounts to ± 0.04 amp. If a grade 0.1 instrument is used or corrections are applied this figure can be lowered considerably. The accuracy of the instrument with a vernier scale amounts to about 0.5 of a vernier graduations and hence equals ± 0.02 amp.

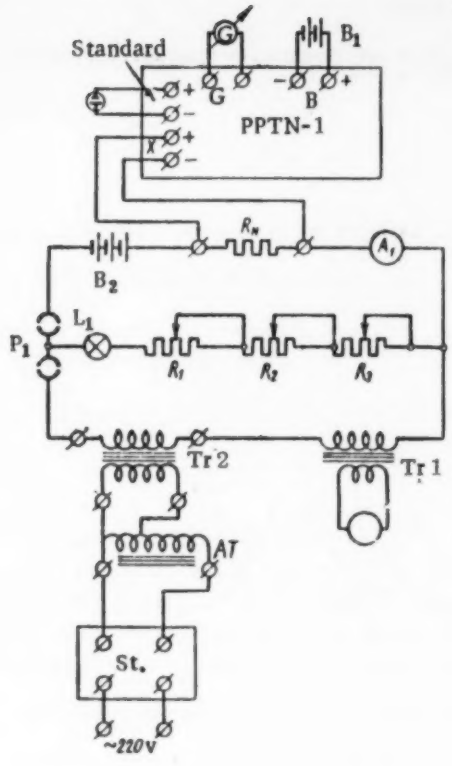

The error of the instrument current transformer as a rule is small and, if a correction is made for it in measurements, it need not be considered in analyzing the errors.

Evaluating tentatively the maximum error which could be obtained in single measurements of the current through the lamp by means of the above equipment at ± 0.04 amp, we find from the calibration curve of the temperature lamp used that this error corresponds to ± 6° in the range of 900-1000°C and gradually drops to ± 2.5° in the range of 1700-1800°C.

It is obvious that this accuracy of measuring the current through the temperature lamp is completely acceptable for the calibration of commercial optical pyrometers, and it will decrease only slightly the overall accuracy of the calibration whose computation is given in [1].

In order to confirm experimentally the possibility of calibrating commercial optical pyrometers with alternating current, we calibrated by means of the above equipment an LT-1 temperature lamp both with alternating and direct current and compared the results (see table).

The calibration was made with reference optical pyrometer grade 2, type OP-48.

In this calibration, eight measurements were made for each point and their arithmetic mean entered in the table. Moreover, the table also gives the mean value for all the dc and ac measurements made by any given current value.

Current flowing through the lamp, amp	ac calibration results, °C					dc calibration results, °C				
	№ 1	№ 2	№ 3	№ 4	mean value	№ 1	№ 2	№ 3	№ 4	mean value
8.06	899	896	905	900	900	903	902	905	906	904
8.66	—	—	999	998	999	—	—	999	1000	1000
9.47	1101	1099	1102	1102	1101	1103	1103	1105	1107	1105
10.29	—	—	1197	1196	1197	—	—	1195	1198	1197
11.41	—	—	1299	1298	1299	—	—	1300	1298	1299
12.58	1399	1399	1402	1402	1401	1400	1399	1404	1406	1402
13.94	—	—	1504	1502	1503	—	—	1506	1507	1507
15.25	1597	1592	1597	1595	1595	1592	1593	1597	1600	1596
16.90	—	—	1704	1706	1705	—	—	1704	1706	1705
18.33	1797	1792	1797	1797	1796	1792	1793	1791	1797	1793

The analysis of the results shows that the discrepancies obtained between calibration of the lamp with alternating and direct currents are insignificant.

The dispersion of the different measurements made with alternating and direct currents are about the same.

Conclusions. In calibrating commercial optical pyrometers in factory test laboratories it is advisable to use for the supplies of temperature lamps a stabilized sinusoidal current. A certain lowering of the accuracy due to this method is completely permissible in the calibration of commercial instruments.

LITERATURE CITED

[1] Methods of Measuring Temperature in Industry, edited by A. N. Gordov [in Russian] (Metallurgizdat, 1952).

ELECTRICAL MEASUREMENTS

DESIGN OF TEMPERATURE ERROR COMPENSATION CIRCUITS IN DC VOLT-HOUR METERS

I. V. Khakhamov

Translated from Izmeritel'naya Tekhnika, No. 9, pp. 31-33, September, 1960

The Leningrad electromechanical plant has developed a range of moving coil dc volt-hour meters for normal voltage of 25 to 800 v intended for a relative estimation of the work of electrolytic shops in the aluminum producing industry. The permissible temperature error of the meters for various measuring ranges amounts to 0.5 to 0.8% per 10°C in the range of 0 to 40°C and the specified short-term overload (10 min) capacity of the meters amounts to 300% of the nominal voltage.

The schematic of the measuring mechanism of the meter is given in Fig. 1.

The turning moment of the moving coil meter is determined [1] from

$$M_{tr} = k_1 i_0 B, \tag{1}$$

where i_0 is the current flowing through the meter armature; B, the induction in the effective gap of the magnet; k_1, a constant coefficient which depends on the number of turns and design parameters of the measuring mechanism.

The braking moment of the meter is calculated [1] from

$$M_B = k_2 n \gamma B^2, \tag{2}$$

where γ is the conductivity of the disk material; n, the speed of rotation of the moving part; k_2, a constant coefficient which depends on the design parameters of the magnet and the disk.

In a stable state, i.e., when $M_{tr} = M_B$ we have:

$$n = \frac{k_1}{k_2} \cdot \frac{i_0}{\gamma B}, \tag{3}$$

and hence, the relative variation of the speed of the meter's moving part with temperature will be:

$$\frac{\Delta n}{n} = \frac{\Delta i_0}{i_0} - \left(\frac{\Delta \gamma}{\gamma} + \frac{\Delta B}{B}\right), \tag{4}$$

where $\Delta i_0/i_0$ is the relative variation with temperature of the current which flows through the armature; $\Delta\gamma/\gamma$, the relative variation with temperature of the meter brake disk conductivity; $\Delta B/B$, the relative variation with temperature of the induction in the effective gap.

In the above meters, aluminum disks with a temperature coefficient of resistance $\Delta\gamma/\gamma = -4\%/10°C$ are used.

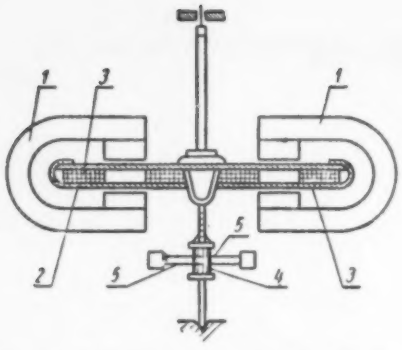

Fig. 1. 1) Permanent magnets; 2) aluminum disk; 3) winding; 4) commutator; 5) brushes.

The meter magnets are made of alloy ANKO-4 which has the value of $\Delta B/B \simeq -0.2\%/10°C$.

The variations, with temperature, of the armature current ($\Delta i_0/i_0$) depend on the condition of operation of the meter winding. When operating with a fixed voltage, i.e., when a meter with a manganin shunt is used, whose impedance is considerably lower than that of the armature, the variations of the current i_0 with temperature will completely depend on the resistance variations of the copper armature, i.e., $\Delta i_0/i_0 \simeq -4\%/10°C$.

In this instance the variations with temperature of the disk conductivity γ are compensated by the variations of the current i_0. The variations of the induction B in the effective gap of the magnet remain uncompensated at a value not exceeding 0.2%/10°C. When working in a condition of a fixed current (a volt-hour meter with a large multiplier resistance) the value of current i_0 does not change with temperature and the error of the meter attains 4.2%/10°C.

In order to eliminate the temperature error in this case, it is necessary to make the current i_0 decrease with a rising temperature in the same proportion as γ and B decrease, i.e., it is necessary to make

$$\frac{\Delta i_0}{i_0} = \frac{\Delta \gamma}{\gamma} + \frac{\Delta B}{B}. \tag{5}$$

For this purpose four circuits were investigated (Fig. 2).

The circuit in Fig. 2a provides a full compensation of the temperature error over a wide range of temperatures, but the power P_m lost in resistor r_m is too large. In fact, we have $r_0 = 80$ ohms, $i_0 = 16$ ma, and with a U = 800 v we obtain $P_m = 10$ w. Moreover, it is difficult to avoid the heating of resistor r_m and the consequent errors due to the heating up of the meter.

The power dissipated in the copper resistance of the Fig. 2b circuit is smaller than that of Fig. 2a, yet the power dissipated in resistor r_m is excessively high (some 400 w).

The Fig. 2c circuit provides a much lower power dissipation in the copper resistors and a lower total power dissipated in the meter.

The main advantages of the circuit in Figs. 2a, b, and c, consist in the linearity of the relations between the temperature and the currents flowing through the various circuits including the armature, which in this case is of great importance. However, the requirements of the relative error at nominal loads and at overloads lead to the necessity of making very large resistors of copper and manganin.

Therefore, the final type of the temperature error compensation in volt-hour meters consisted of semiconductor thermistors in a circuit arrangement shown in Fig. 2d.

The relation of the thermistor resistance to temperature is expressed by the following equation [2]:

$$r_T = Ae^{\frac{B}{T}}, \tag{6}$$

where A and B are constants characteristic of thermistors; T is the absolute temperature.

Thermistors MMT-9, which were used in the volt-hour meters, have the following parameters: B ≃ 2700 ± 10%; the stability of the resistance with time expressed as the change of resistance during 18 months is ±3%; the permissible power per element is 10 mw.

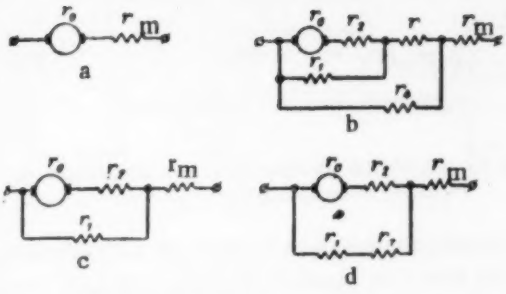

Fig. 2. Sketch a) r_0 is the armature resistance; r_m, multiplier resistance made of copper or nickel and manganin wire; sketch b) r_0, armature resistance; r_1 and r_m, manganin resistors; r_2, nickel and copper resistor; sketch c) r_0, armature resistance; r_1 and r_3, copper and nickel resistors; r_2 and r_4, manganin resistors; sketch d) r_0, armature resistance; r_1, r_2, and r_m, manganin resistors; r_T, thermistor.

The circuit in Fig. 2d provides full compensation of the temperature error in volt-hour meters.

However, the presence of a nonlinear relation to temperature of the resistance r_T leads to a nonlinear variation of the meter temperature error. In the range of temperatures 0 to 40°C the nonlinear part of the temperature error can be calculated from the formula:

$$f_{T2} = \frac{i_0'}{i_0}\left(\frac{r_T''}{r_T'} - \frac{r_T'}{r+r_T} - \frac{r_T'}{r_0+r+r_T+r_3} - \frac{i_0'}{i_0}\right)\times \times \frac{(\Delta T)^2}{2}. \quad (7)$$

where i_0'' and r_T'' are derivatives with respect to temperature of i_0 and r_T, i.e., if for $t = t_0 = 20°C$, $r_T \approx r$, then $f_{T2\ max} \approx 0{,}2\ \%/10°C$.

In case of necessity for improving the linearity of the meter temperature characteristic, over a wider range of temperatures, it is necessary to connect in parallel with resistors $r_0 + r_2$ a shunting resistor, this however increases a little the power consumption of the meter.

It should be noted that in the case of compensation of the temperature error in volt-hour meters, the selection of the thermal inertia of various elements of the circuit becomes important, and in this connection, the circuit with thermistors has considerable advantages as compared with wire resistors.

All the above reasoning, with respect to the thermistors, only holds if the nominal voltage across the meter is assumed large and the effect of the armature resistance on the temperature error can be neglected.

Let us now examine the temperature compensation circuit shown in Fig. 2d for the case when this assumption cannot be made.

Current i_0 which is flowing through the armature is calculated from:

$$i_0 = \frac{U(r_1+r_T)}{r_m(r_0+r_1+r_2+r_T)+(r_1+r_T)(r_0+r_2)}. \quad (8)$$

The temperature error without considering nonlinearity expressed in (7) is according to (4):

$$\frac{\Delta n}{n} = \frac{\frac{r_T}{r_1+r_T}\cdot\frac{\Delta r_T}{r_T} - \frac{r_1+r_T+r_\partial}{r_\partial}\cdot\frac{r_0}{r_0+r_2}\cdot\frac{\Delta r_0}{r_0}}{1+\frac{r_1+r_T}{r_0+r_2}+\frac{r_1+r_T}{r_\partial}} + 0{,}42. \quad (9)$$

If the calculation is made on the basis of a fixed current, i.e., if it is considered that:

$$r_m + \frac{(r_1+r_T)(r_0+r_2)}{r_0+r_1+r_2+r_T} \approx \text{const}. \quad (10)$$

the compensation conditions will be

$$\frac{\frac{r_T}{r_1+r_T}\cdot\frac{\Delta r_T}{r_T}-\frac{r_0}{r_0+r_2}\cdot\frac{\Delta r_0}{r_0}}{1+\frac{r_1+r_T}{r_0+r_2}}+0{,}42=0. \tag{11}$$

Having calculated r_1 and r_2 from (11) and inserted them in (9) we obtain for the case of a nominal voltage of 25 v an overcompensation of $\Delta n/n \simeq 1.0\%$.

It can be shown that the calculation for the condition of a fixed current can be carried out with adequate accuracy (0.1%/10°C) if the nominal voltage of the meter is larger than that across resistors ($r_0 + r_2$) by a factor of at least 40.

It follows from the above that compensation of the temperature error in volt-hour meters with a considerable overload capacity is best attained from the economic point of view by means of a thermistor circuit.

A thermistor circuit provides an adequate linearity of temperature compensation for dc volt-hour meters with a normal error of less than 0.5%/10°C in the temperature range of 20 ± 20°C.

LITERATURE CITED

[1] P. N. Goryunov, S. M. Pigin, and N. N. Shumilov, Electricity Meters [in Russian] (Gosénergoizdat, Leningrad-Moscow, 1951).

[2] I. T. Sheftel', Thermistors [in Russian] (Leningradskii Dom Nauchno-Tekhnicheskoi Propogandy, 1957) No. 3.

COMPENSATION FOR TEMPERATURE EFFECTS IN THE EMF OF POTENTIOMETER STANDARD CELLS

A. Ya. Shramkov

Translated from Izmeritel'naya Tekhnika, No. 9, pp. 33-35, September, 1960

The setting and checking of the operating current in dc potentiometers is attained by means of standard cells and an adjustable resistor. In precision manually controlled potentiometers the variations of the cell emf with ambient temperature is compensated by means of special resistance decades (1 or 2). The required resistance value for a given temperature and emf is set on the decades. This method requires a precise knowledge of the temperature and a periodic setting of new values on the decade with temperature variations.

Below, we describe a method of automatic compensation for the emf variations with temperature by means of wire wound resistors with a positive temperature coefficient (made of copper or nickel).

This circuit is shown in Fig. 1. When the standard cell emf and the voltage drop across resistor R_s are balanced we can write

$$E=I'R_s=I\frac{R_sR}{R_s+R+r},$$

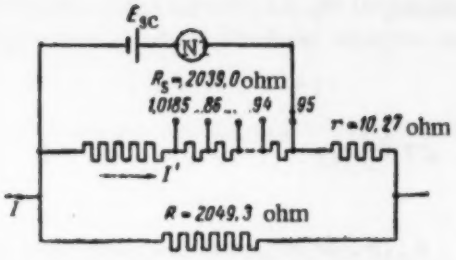

Fig. 1. R_s) setting manganin resistor; R) manganin shunt; r) copper or nickel resistor; NI) null indicator (galvanometer).

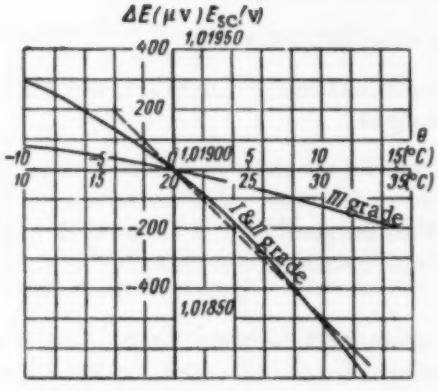

Fig. 2.

when

$$I = \frac{E(R_s + R + r)}{R_s R}. \tag{1}$$

When the temperature deviates from the normal by $\theta = t - 20$, the value of the operating current will be:

$$I_0 = \frac{E_{20}(1+\alpha_m\theta)[R_s + R + r(1+\alpha\theta)]}{R_s R}, \tag{2}$$

where α_m is the temperature coefficient of the standard cell emf (mean for a chosen temperature range); α is the temperature coefficient of the copper or nickel resistor.

The relative error amounts to:

$$\delta = \frac{I_0 - I}{I} = \alpha_m\theta + \frac{r}{R_s + R + r}\alpha\theta. \tag{3}$$

The conditions for temperature compensation are derived from (3) if we assume that $\delta = 0$:

$$-\frac{\alpha_m}{\alpha} = \frac{r}{R_s + R + r} = k. \tag{4}$$

For further calculations, let us denote the shunting coefficient by:

$$\frac{I'}{I} = \frac{R}{R_s + R + r} = n. \tag{5}$$

Solving simultaneously (1), (4), and (5), we find the required resistance:

$$R = \frac{E_{20}}{I}\frac{1}{1-n-k};\quad R_s = \frac{E_{20}}{In};\quad r = \frac{E_{20}}{I}\frac{k}{(1-n-k)n}. \tag{6}$$

Figure 2 shows the curves of the relation of the mean emfs of grade I, II and III standard cells to temperature. For standard cells grades I and II (saturated type) the relation between the emf and temperature is more pronounced than for cells of grade III (unsaturated type). The mean temperature coefficient in the range of 2-30°C (see dotted line in Fig. 2) for grade I and II cells is equal to 50.0 μv per °C ($\alpha_m = -5.0 \cdot 10^{-5}$/°C). For grade III cells the temperature coefficient lies in the range of (6-14) μv per °C [$\alpha_m = -(0.6\text{-}1.4) \cdot 10^{-5}$/°C]. Its mean value can be taken as $1.0 \cdot 10^{-5}$/°C.

For an example, let us calculate a temperature compensating circuit for grade I and II standard cells, assuming that $E_{20} = 1.0195$ v, I = 1 ma and $\alpha = +4.0 \cdot 10^{-3}$ (copper). Let us find the mean temperature coefficient α_m in the range of +20 to +30°C by using a more accurate approximate equation

$$E'_\theta = E_{20}(1 + \alpha'\theta + \alpha''\theta^2), \tag{7}$$

where $\alpha' = -4.0 \cdot 10^{-5}$/°C and $\alpha'' = -1.0 \cdot 10^{-6}$/°C. Equating $E_\theta = E_{20}(1 + \alpha_m\theta)$ and (7) for $\theta_k = 10$°C we find that $\alpha_m = \alpha' + \alpha''\theta_k = -5.0 \cdot 10^{-5}$/°C. The values of the respective resistances calculated from (6) for n = 0.5 in this case will be: R = 2091.3 ohms, R_s = 2039.0 ohms and r = 52.3 ohms.

The error δ' of incomplete compensation due to the nonlinearity of the temperature characteristic of the normal cell emf can be easily calculated if in (2) we take a more accurate quadratic parabolic approximation (7) instead of the linear one. We then have:

$$\delta' = -\alpha''\theta\left(\theta - \frac{\alpha_m - \alpha'}{\alpha''}\right) = -\alpha''\theta(\theta - \theta_k). \tag{8}$$

It will be seen from the above that at points $\theta = 0$ and $\theta = \theta_k$ (second compensation point) there is no temperature error. For the value of $\theta_k = 10°C$ assumed in our example we have

$$\delta' = -1 \cdot 10^{-6}\ \theta(\theta - 10°C). \tag{9}$$

In the range of 15-35°C the error due to incomplete compensation does not exceed + 0.0025 to − 0.008%. At points + 18° and + 22°C ($\theta = \pm 2°C$) this error equals respectively to − 0.0024 and + 0.0016%.

It should be noted that the shunting coefficient n lies in the range of 0.2-0.8.

The setting resistor R_s must include a certain variable part equalto (1.0195 − 1.0185 v) I, which is required for adjusting R_s in the appropriate range when a standard cell is changed.

When a grade III standard cell is used,the compensating resistors for the same conditions as those given above equal to R = 2049.3 ohms, R_s = 2039.0 ohms and r = 10.27 ohms. For these resistance values, which are calculated for a mean temperature coefficient of a standard cell emf, the possible error for grade III standard cells with a maximum or a minimum temperature coefficient does not exceed $\delta' \leq \pm 0.4 \cdot 10^{-5}\theta$, i.e., it will not exceed ± 0.004% per 10°C.

It will be seen from the principle of operation of the above compensation circuit that the residual error due to incomplete compensation is very small and the use of this circuit in potentiometers does not require the knowledge of the standard cell emf at various temperatures. The periodic setting of the operating current by means of a rheostat is, of course, preserved in this method.

Let us also mention the possibility of a temperature compensating circuit on the basis of thermistors. In this case the compensation circuit consists of a series connected manganin resistor and a thermistor which is shunted by another manganin resistor. The voltage drop across this complete circuit balances out the standard cell emf. However, due to the considerable instability of the thermistor resistance with time this method can only be recommended for low grade potentiometers.

Conclusions. The above compensation circuit with copper or nickel resistors can be used both in manually operated and automatic potentiometers. The temperature-sensitive resistors should be placed close to the standard cell so that they should all be at the same temperature.

MEASURING IMPEDANCES BY MEANS OF OSCILLOSCOPES

K. P. Mikhailovskaya

Translated from Izmeritel'naya Tekhnika, No. 9, pp. 35-37, September, 1960

It is possible to determine the modulus z_x and angle φ_x of impedance Z by measuring the phase difference between voltages across the elements of measuring circuit [1].

When this method is used, an effective resistance r_0 (or a capacitance or inductance) is connected in series with the measured impedance. This circuit is connected to a voltage source and the angles α and β, are measured between the voltage across the whole circuit V and respectively the voltages across the reference resistor V_0 and the measured impedance V_x.

From the known value of r_0 and the measured angles α and β it is possible to calculate z_x and φ_x:

$$z_x = r_0 \frac{\sin\alpha}{\sin\beta}; \qquad \varphi_x = \alpha + \beta. \tag{1}$$

The angles can be measured by means of various instruments [2]. The advantages of using an electronic oscilloscope for this purpose consists in its high input impedance and its wide frequency, voltage [3], angle (from 0 to 90°) and modulus range (from fractions of an ohm to tens of megohms).

The technique of measuring phase differences between two voltages of the same frequency, one of which is fed to the horizontal and the other to the vertical axis of the oscilloscope is well known [2, 4].

The errors in measuring angles α and β consist of: finite value of the light spot diameter, finite value of the oscilloscope input impedance, the presence of harmonics in the measured voltages, different phase shifts in the oscilloscope amplifiers [4, 5].

The effect of the last two factors can be neglected [6], hence we shall not consider them any further.

The relative errors in determining the modulus δ_z and the angle δ_φ due to the error in measuring the linear dimensions of the ellipse which is obtained on the oscilloscope screen amount to:

$$\delta_z \simeq \frac{dz}{z} = \frac{1}{z}\left(\frac{\partial z}{\partial \alpha}\, d\alpha + \frac{\partial z}{\partial \beta}\, d\beta\right) = \frac{D_n}{\sqrt{2}\, D_e}\left(\frac{1+\sin\alpha}{\sin\alpha} + \frac{1+\sin\beta}{\sin\beta}\right);$$
$$\delta_\varphi \simeq \frac{d\varphi}{\varphi} = \frac{1}{\varphi}\left(\frac{\partial \varphi}{\partial \alpha}\, d\alpha + \frac{\partial \varphi}{\partial \beta}\, d\beta\right) = \frac{D_n}{\sqrt{2}\, D_e} \cdot \frac{1}{\varphi}\left(\frac{1+\sin\alpha}{\cos\alpha} + \frac{1+\sin\beta}{\cos\beta}\right). \tag{2}$$

here D_n is the diameter of the light spot on the screen, D_e is the effective diameter of the oscilloscope screen (it is assumed that only a part of the ellipse is seen on the oscilloscope screen, a part adequate for determining the angle [5]).

A study of Eq. (2) makes it possible to state that δ_z and δ_φ are at a minimum when $\alpha = \beta$. In practice it is possible to assume a ratio between the sines of angles α and β in the range of 1/2 and 2. This assumption will raise the errors in δ_z and δ_φ respectively by 10 and 20% of their values for $\alpha = \beta$.

The relation of errors δ_z and δ_φ to the value of angle φ_x is represented graphically on Fig. 1 by solid lines for the case when $\alpha = \beta$, $D_n = 0.75$ mm, and $D_e = 100$ mm.

The rise in errors δ_z and δ_φ with a decreasing angle φ_x is obviously unacceptable. It is, however, possible to reduce δ_z and δ_φ by substituting the reference resistance with a reference capacitance or inductance [1] when measuring an impedance with an angle smaller than 45°.

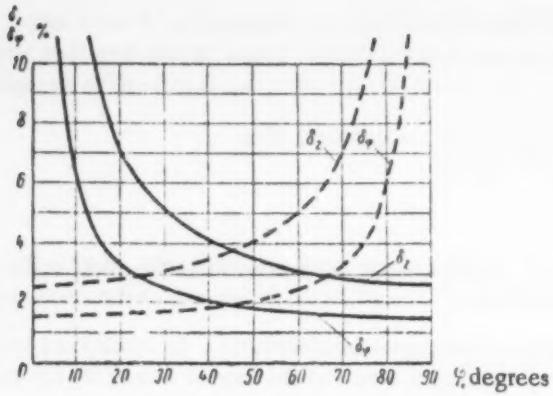

Fig. 1. Curves of the relative errors δ_Z and δ_φ in determining respectively the modulus and angle of the required impedance versus the value of the angle φ_X. It is assumed that $\alpha = \beta$, $D_n = 0.75$ mm and $D_e = 100$ mm. Solid lines represent the case when a reference resistor was used, and dotted lines when a reference capacitance or inductance were used.

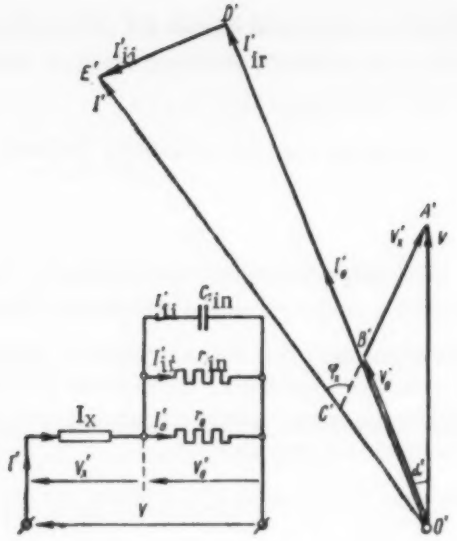

Fig. 2. Schematic and vector diagram of the measuring circuit including the oscilloscope input impedance used for measuring angle α'. r_{in}) oscilloscope input resistance; C_{in}) oscilloscope input capacitance; I') the modulus of the circuit current; I_x) the modulus of the current in the impedance under test; I_0') the modulus of the current in the reference resistor; I_{ir}) the real component of the oscilloscope input current; I_{ii}) the imaginary compent of the oscilloscope input current.

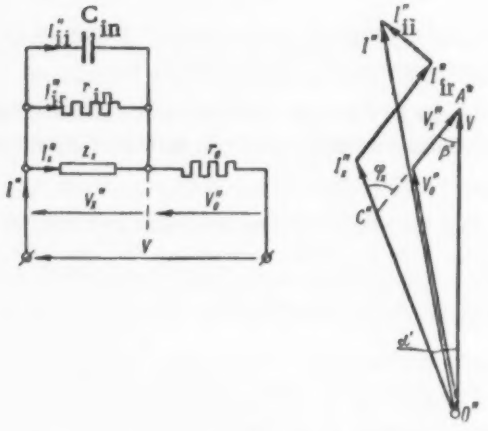

Fig. 3. Schematic and vector diagram of the measuring circuit including the oscilloscope input resistance when measuring angle β".

If a reference capacitance is used when measuring a capacitative impedance and a reference inductance for an inductive impedance the modulus and angle of the measured impedance will be represented according to the vector diagram by the expression

$$z_x = x_0 \frac{\sin\alpha}{\sin\beta}; \qquad \varphi_x = 90° - (\alpha + \beta), \tag{3}$$

where x_0 is the reactance of the reference capacitance or inductance.

When reference capacitances and inductances are used errors δ_Z and δ_φ will also be at a minimum for $\alpha = \beta$, but their relation to φ_X will differ from that obtained with a reference resistance. The latter relations are shown in Fig. 1 by dotted lines.

Thus, for raising the accuracy of impedance measurements reference resistances should be used when the angle of the impedance is $\geq 45°$, and reference capacitances and inductances should be use if this angle does not exceed 45°.

It is recommended to measure in the sequence described below.

Angles α and β should be adjusted with a reference resistor r_0 so that the ratio $\sin\alpha/\sin\beta$ is in the range of 1/2 to 2, and then measured; if the sum of the measured angles is $\geq 45°$, the angle of the required impedance

should be considered equal to that sum and its modulus calculated from (1); if, however, the sum of these angles is < 45°, the reference resistance should be replaced by a reference capacitance or inductance (depending on the nature of the measured impedance) angles α and β should be adjusted and measured and the impedance modulus and angle calculated from (3).

If the above procedure is adhered to, angles in the range of 14 to 65° can be measured directly. Under these conditions, the error of measurements of an impedance by an oscilloscope, which has a D_n = 0.75 mm and D_e = 100 mm, does not exceed 4.2% for the modulus and 2.1% for the angle.

The effect of the finite value of the oscilloscope input impedance consists in the impedance shunting the reference resistor r_0 when measuring angle α and shunting the impedance under test z_x when measuring angle β. If the value of the modulus of the measured impedance is of the same order as the oscilloscope input impedance, this effect cannot be neglected. The effect, however, can be easily corrected.

The measuring circuits and corresponding vector diagrams which take account of the oscilloscope input impedance are shown in Figs, 2 and 3.*

According to the interdependance principle [7] the current I_x'' through the measured impedance, when angle β'' (Fig. 3) is measured, will be equal in magnitude and phase to current I_0' in the reference resistor, when measuring angle α' (Fig. 2), i.e., angle A"O"C" (Fig. 3) equals angle α'.

Hence, angle φ_x of the measured impedance is equal to the sum of angles α' and β'':

$$\varphi_x = \alpha' + \beta''. \tag{4}$$

the modulus of the measured impedance can be determined from the vector diagram in Fig. 2 and Eq. (4):

$$z_x = \frac{r_0 r_e}{r_0 + r_e} \cdot \frac{1}{\sqrt{1 + \left(\omega C_{in} \frac{r_0 r_e}{r_0 + r_e}\right)^2}} \cdot \frac{\sin\alpha'}{\sin\left(\beta'' - \tan^{-1}\omega C_{in}\frac{r_0 r_e}{r_0 + r_e}\right)} \tag{5}$$

Let us denote $\omega C_{in}\frac{r_0 r_{in}}{r_0 + r_{in}} = a$. Then the value of z_x, taking the oscilloscope input impedance into account, will be expressed by:

$$z_x = \frac{r_0 r_{in}}{r_0 + r_{in}} \cdot \frac{1}{\sqrt{1+a^2}} \cdot \frac{\sin\alpha'}{\sin(\beta'' - \tan^{-1} a)} \tag{6}$$

This expression makes it possible to use the above method for measuring impedances with a modulus of the same order of magnitude as the input resistance of the oscilloscope and even higher than that resistance.

If the value of a is small and can be neglected, the modulus of z_x can be calculated from the relation:

$$z_x = \frac{r_0 r_{in}}{r_0 + r_{in}} \cdot \frac{\sin\alpha'}{\sin\beta''}. \tag{7}$$

As an example of such an instance, one can quote oscilloscope ÉO-7 which has an a = 0.00942 at 50 cps for $r_0 = r_{in}$.

Equations similar to (4), (5), and (7) can be obtained when reference capacitances and inductances are used.

* Values referring to Fig. 2 circuit will henceforth be marked as prime ('), and those referring to Fig. 3 circuit as double prime (").

LITERATURE CITED

[1] K. P. Mikhailovskaya, Izmeritel'naya Tekhnika, No. 1 (1959).*

[2] B. P. Aseev, Phase Relations in Radio Technology [in Russian] (Gosénergoizdat, 1958).

[3] V. O. Arutyunov, Electrical Measuring Instruments and Measurements [in Russian] (Gosénergoizdat, 1958).

[4] G. A. Remez, A Course of Basic Radiotechnical Measurements [in Russian] (Svyaz'izdat, 1955).

[5] I. M. Vishenchuk, E. P. Sogolovskii, and B. I. Shvetskii, Cathode-ray Oscilloscopes and Their use in Measurement Techniques [in Russian] (Fizmatgiz, 1959).

[6] V. S. Listvin, Élektroschestevo, No. 1 (1955).

[7] P. L. Kalantarov and L. R. Neiman, Theoretical Foundations of Electrical Technology [in Russian] (Gosénergoizdat, 1948) Part II.

AN AMPLITUDE-PHASE INDICATOR WITH AN ALTERNATING ACTION OF THE COMPARED VOLTAGES

L. Ya. Mizyuk

Translated from Izmeritel'naya Tekhnika, No. 9, pp. 38-40, September, 1960

In ac circuits, one often comes across the problem of comparing two voltages both with respect to amplitude and phase. The error of comparison and the speed of attaining balance depend to a great extent on the type of the indicator used.

At present, for comparing the moduli of voltages differential, indicators are used [1, 2], which are not affected by the phase of the compared signals. For comparing phase angles, various circuits of double channel phase meters are used [3, 4]. The asymmetry of channels which feed the incoming compared voltages to the differential detector or the output phase meter device (trigger, summing circuit) and the zero phase shift of such circuits is an essential defect of these indicators which limits the accuracy of amplitude and phase measurements.

In order to raise the accuracy in comparing alternating voltages one can recommend the use of differential amplitude-phase indicators with alternately acting signals.** The block schematic of the indicator with alternately acting voltages is shown in Fig. 1.

The principle of operation of this circuit consists in feeding by means of any type of commutator (polarized relay in Fig. 1) voltages $u_1 = U_m (\sin\omega t + \varphi)$ and $u_2 = U_{m2} \sin \omega t$ alternately at a repetition frequency of $\Omega << \omega$ to the input of amplifier A_ω which is either aperiodic or tuned to ω. Thus voltage u_{in} which varies in a manner shown in Fig. 2, becomes modulated (more precisely keyed) with respect to amplitude and phase. If the input voltages are not equal in amplitude there appears at the output of the amplitude detector AD an alternating voltage of the modulating frequency. This voltage is picked out by amplifier A_Ω tuned to the

* See English translation.

** A similar circuit was used for amplitude measurements by M. R. Bal'son and Yu. A. Skribnik. M. R. Bal'son [5] erroneously asserts that the defect of this circuit consists in the impossibility of making phase measurements with it.

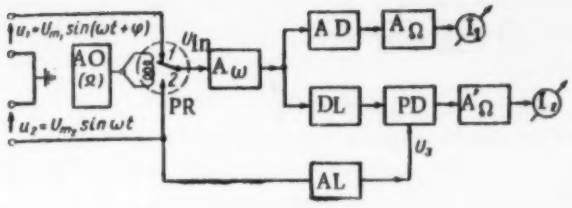

Fig. 1.

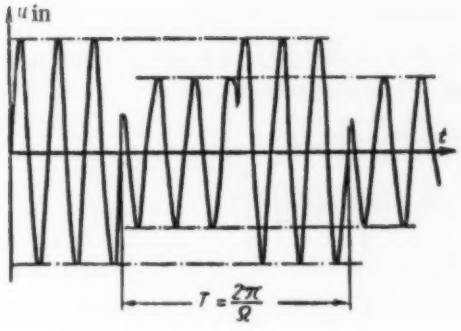

Fig. 2.

keying frequency which is provided by the audio oscillator AO and measured by means of voltmeter I_1 which can consist of a second amplitude detector and a moving coil instrument. It is obvious that for equal frequencies and wave forms of the input voltages the meter reading will be equal to zero irrespective of the phases of these voltages provided their amplitudes are equal.

If the phase angles differ, an alternating voltage will appear at the output of the phase detector PD. This voltage of frequency Ω can be measured by means of amplifier A'_Ω similar to amplifier A_Ω and voltmeter I_2. In order to exclude the effect of amplitude modulation a double-sided limiter DL is included in the indicator phase channel. The controlling (reference) voltage of the phase detector is also limited by the amplifier-limiter AL and can be tapped either in the u_1 voltage circuit or the u_2 circuit (it is better to feed it from the uncontrolled signal circuit).

Let us derive the basic relations which characterize the operation of the amplitude-phase indicator.

With a sinusoidal amplitude and phase modulation the expression for the voltage fed to the input of amplifier A_ω can be written in the form:*

$$u_{in} = U_\omega (1 + m \sin \Omega t) \sin (\omega t + m_\varphi \sin \Omega t), \tag{1}$$

where $U_\omega = \frac{1}{2}(U_{m1} + U_{m2})$; $m = \frac{U_{m1} - U_{m2}}{U_{m1} + U_{m2}}$ is the amplitude modulation factor; m_φ is the phase modulation index which is equal to half the phase difference angle φ expressed in radians.

Let us first examine the amplitude channel of the amplifier. Detector AD of the amplitude channel does not respond to phase modulation and therefore its output voltage will be equal to

$$u_0 = K_\omega U_\omega (1 + m \sin \Omega t) \cos \theta, \tag{2}$$

where K is the gain of amplifier A_ω; θ is the cut-off angle of the detector.

The alternating voltage fed to the input of the amplifier is equal to:

$$u_\sim = mK_\omega U_\omega \cos\theta \sin\Omega t. \tag{3}$$

Voltmeter I_1 receives the voltage:

$$u = mK_\omega K_\Omega U_\omega \cos\theta \sin \Omega t, \tag{4}$$

where K_Ω is the gain of amplifier A_Ω.

When the compared voltages are equal, i.e., when $U_{m1} = U_{m2}$, there is no amplitude modulation and the voltmeter reading is zero.

* This expression does not contradict the underlying principle of operation, since tuned amplifiers are connected to the output of the amplitude and phase detectors, and these amplifiers are tuned to the first harmonic whose amplitude can be easily obtained from an expansion in a series of the rectangular waveform of the envelope which is smaller than the values of m and m_φ by a factor of $2/\pi$.

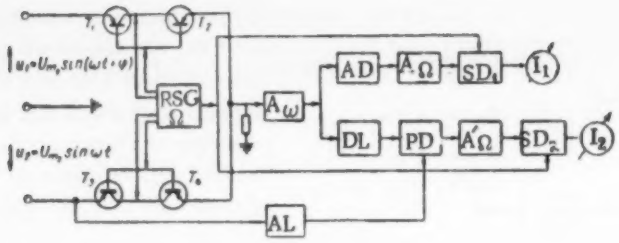

Fig. 3.

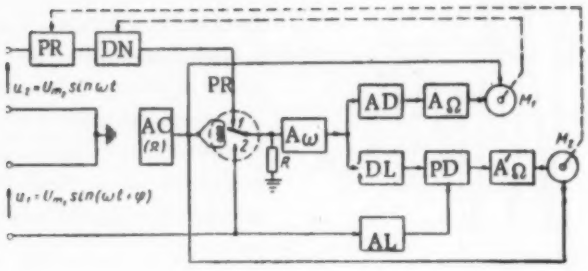

Fig. 4.

In order to obtain a high precision of comparison it is necessary to make the sensitivity of the amplitude channel sufficiently high:

$$S_a = \frac{\partial U}{\partial m} = K_\omega K_\Omega U_\omega \cos\theta \tag{5}$$

so as to provide measurements at modulation factors of 1%. By raising the gain of amplifiers A_ω and A_Ω it is possible to ensure the required sensitivity. Moreover, the gain of the input amplifier should be adequate to provide a powerful signal for the detector.

With a low percentage modulation and a large channel gain the measurement error can increase considerably owing to secondary effects, such as the ac background noise, pick-ups and noise.

In order to pick-up useful signals with frequencies ω and Ω, it is necessary to raise the selectivity of amplifiers A_ω and A_Ω. The selectivity of amplifier A_ω cannot be made too high, since its transients would distort measurements. The selectivity of amplifier A_Ω can be made high. It is only essential to make the tuning of this amplifier stable, otherwise its sensitivity may drop considerably.

If the threshold of sensitivity of the voltmeter δU_1 (it depends on the noise level and background noise in addition to the voltmeter parameters) is known, it is easy to find the minimum voltage which should appear at the output of amplifier A_Ω:

$$U = mK_\omega K_\Omega U_\omega \cos\theta > \delta U_1.$$

The indicator will register a difference in amplitudes if:

$$m > \frac{\delta U_1}{K_\omega K_\Omega U_\omega \cos\theta}. \tag{6}$$

Considering that the relative error of comparison is

$$\delta = \frac{U_{m1} - U_{m2}}{U_{m1}} = \frac{m}{2}, \tag{7}$$

we obtain:

$$\delta < \frac{\delta U_1}{2K_\omega K_\Omega U_\omega \cos\theta}. \tag{8}$$

If the absolute level of the compared voltages is known and the voltage to be fed to the detector assumed, it is easy to determine K_ω and then from (8) also K_Ω for which the required accuracy of measurements is attained. One of the factors which reduces the accuracy of measurements is the error of switching. It is important for the commutator to work stably providing equal durations of switching for each of the two voltages, and to have a small transfer capacitance a property, which for instance is very important at high frequencies. In this respect the semiconductor (transistor and diode) recitifiers deserve special attention.

Let us now consider the phase channel. In excluding amplitude modulation by limiting the signal fed to the phase detector, it is easy to obtain from (1) the alternating component of the voltage at the ouput of the phase detector:

$$u_\sim = K_\varphi m_\varphi \sin \Omega t, \tag{9}$$

where $m_\varphi = \varphi/2$; K_φ is the transfer constant of the phase detector.

The voltage fed to voltmeter I_2, having passed through amplifier A'_Ω which is tuned to frequency Ω and has a gain of K'_Ω, is equal to:

$$u'_\sim = K'_\Omega K_\varphi \frac{\varphi}{2} \sin \Omega t. \tag{10}$$

When the phase difference disappears ($\varphi = 0$) this voltage becomes equal to zero.

The sensitivity of the phase indicator is

$$S_\varphi = \frac{\partial U'_\sim}{\partial \varphi} = \frac{1}{2} K'_\Omega K_\varphi \varphi \tag{11}$$

and can be made adequately high with a suitable choice of K'_Ω.

The error of the phase channel depends not only on the tuned amplifier A', but also on parasitic modulation of the signal which arises due to the difference in the amplitudes of the compared signals and leads to a difference in the leading edges of the pulses fed to the input of the phase detector.

Since it is important with amplitude-phase indicators to know the direction of regulation, it is necessary to connect to the outputs of the phase and amplitude channels phase-sensitive voltmeters, whose reference voltage should be supplied from the oscillator feeding the commutator (relay). Synchronous detectors SD_1 and SD_2 with moving coil instruments I_1, I_2 can be used for such purposes in the amplitude and phase comparing channels respectively (see block schematic of the indicator shown in Fig. 3).

The alternating connection of the compared voltages is made in this instance by means of semiconductor commutators consisting of junction germanium transistors. In order to reduce the effect of the residual voltage a reversed transistor connection is used, i.e., the collector and emitter are interchanged. The required precision of commutation is achieved by a rectangular shape of the reference signal, obtained from a rectangular signal generator RSG (it can consist of a multivibrator or a double-sided limiter).

The independent working of the amplitude and phase channels makes it possible to use an indicator with alternately operating signals in phase and amplitude automatic control circuits of the measured (or reference) voltage. In fact,by connecting at the output of amplifiers A_Ω and A'_Ω reversible motors M_1 and M_2 (Fig. 4) and by choosing an appropriate frequency of commutation, it is easy to make the comparison of voltages automatic. The motor excitation circuits in this instance are fed with voltage of frequency Ω.

The use of an amplitude-phase indicator with alternately operating signals, makes it possible to eliminate the zero drift and asymmetry of channels peculiar to all differential circuits.

With an aperiodic amplifier A_ω the indicator can operate in a wide frequency range. If the response to noise, however, has to be reduced the indicator can be used with a tuned amplifier A_ω. Phase shift and gain variations in amplifier A_ω do not affect either the phase or the amplitude channels of the indicator, since both compared signals pass through the same circuit. With an electromechanical transducer which provides commutation of very weak signals, the amplitude-phase indicator is suitable for comparing voltages with a low absolute level.

An experimental checking of an indicator which employed a polarized relay RP-5 as a commutator showed that it is easy to ensure an accurate comparison of the voltages and phases of the order of 1% and 1° providing the interrupter is carefully adjusted. These values, however, can be improved upon.

If the commutator and the circuit parameters are correctly chosen the amplitude phase indicator with alternagely operating signals can provide a high accuracy of comparison and therefore opens up wide possibilities of lowering the error in measuring alternating voltages, especially at higher frequencies.

LITERATURE CITED

[1] K. B. Karandeev, Electrical Measurement Methods [in Russian] (Gosénergoizdat, 1952).

[2] L. Ya. Mizyuk, Electronic Phase-Insensitive Differential ac Indicators [in Russian] (Nauchnye Zapiski IMA AN UkrSSR, 1955) Vol. 5.

[3] B. P. Aseev, Phase Relations in Radio Technology [in Russian] (Svyaz'izdat, 1954).

[4] F. Terman and J. Pettit, Measurement Techniques in Electronics [Russian translation] (IL, 1955).

[5] M. R. Bal'son, "Methods of eliminating the interrelation between amplitude and phase measurements in complex measuring systems." Bulletin of Technical Information on Geophysical Instrument Making [in Russian] (Ministerstvo Geologii i Okhteny Nedr SSR, Leningrad, 1958).

FREQUENCY ERRORS OF RECTIFYING INSTRUMENTS WITH BLOCKING CAPACITORS

E. N. Kurilov and L. A. Sinitskii

Translated from Izmeritel'naya Tekhnika, No. 9, pp. 41-42, September, 1960

For measuring ac voltages in circuits which also contain dc voltages, blocking capacitors are widely used (Fig. 1).

When measuring low frequencies, for which the reactance x_c of the capacitor C becomes comparable to the effective resistance R, the detected voltage decreases thus leading to errors in the device.

In [1] the following formula is given for determining the error of the instrument at low frequencies:

$$\Delta_f = -\frac{\pi}{R/x_c} = -\frac{\pi}{\omega RC}. \quad (1)$$

The minus sign indicates that the value of the error is negative. The derivation of this formula is not based on sufficiently rigorous premises, and hence, as it will be shown below the error in calculating by means of Eq. (1) is considerable. Therefore, the required capacity determined from this formula is always larger than the minimum permissible.

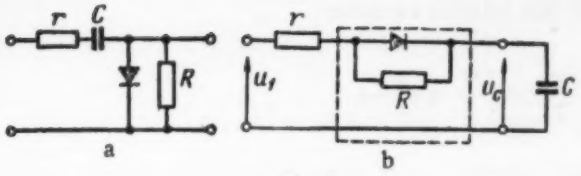

Fig. 1.

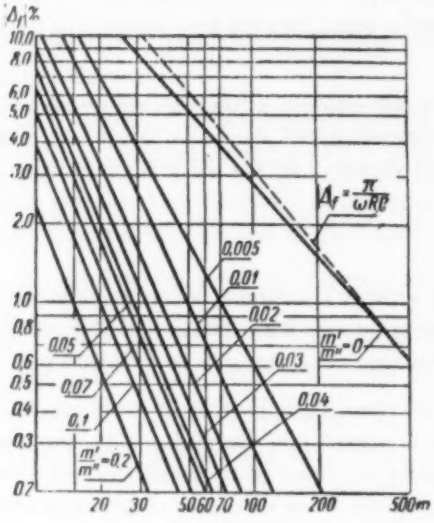

Fig. 2.

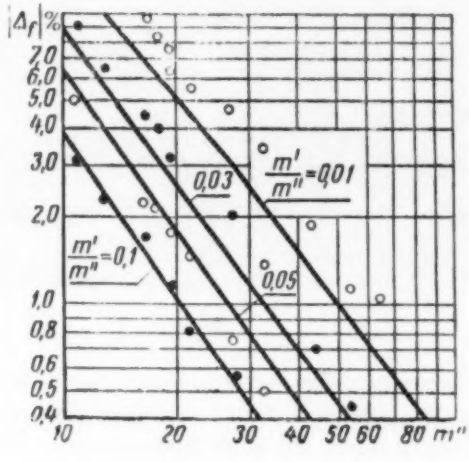

Fig. 3.

For a more precise determination of the error of the rectifying device at low frequencies, let us use the formula for evaluating the dc component of u_0 of the voltage across the capacitance in the rectifier circuit [2] for an external emf $u = U_m \sin(\omega t + \varphi)$:

$$u_0 = \frac{U_m}{\pi} \sin\frac{\Psi}{2}\left[(k'-k'')\sin\left(\frac{\Psi}{2}+\varphi\right)+(k'm''-k''m')\cos\left(\frac{\Psi}{2}+\varphi\right)\right]. \quad (2)$$

where Ψ is the angle which determines the duration of the conducting state of the rectifier;* k' and k" are transfer constants of the quadripole in a no-load condition (Fig. 1b) with a conducting and nonconducting rectifier.

The values of m' and m" are determined from the equalities:

$$m' = \omega R'_{out} C; \quad m'' = \omega R''_{out} C. \quad (3)$$

Here R'_{out} and R''_{out} are the output resistances of the quadripole with a short circuited input for a conducting and nonconducting condition of the rectifier. If m' and m" are sufficiently large, then (2) assumes the following form [2]:

$$u_\infty = U_m \frac{k'm''-k''m'}{m''-m'} \cos\frac{\Psi}{2}. \quad (4)$$

For the circuit under consideration:

$$k' = k'' = 1;\ m' = \left(r+\frac{r_n R}{r_n+R}\right)\omega C;\ \ m'' \simeq (r+R)\omega C,$$

where r_n is the forward resistance of the rectifier.

Equations (2) and (4) can written in the form:

$$u_0 = \frac{U_m}{\pi} m''\left(1-\frac{m'}{m''}\right)\sin\frac{\Psi}{2}\cos\left(\frac{\Psi}{2}+\varphi\right), \quad (2a)$$

$$u_\infty = U_m \cos\frac{\Psi}{2}. \quad (4a)$$

The low frequency error Δf should obviously be determined as:

$$\Delta_f = \frac{u_0-u_\infty}{u_\infty}. \quad (5)$$

* It is assumed that the rectifier starts conducting at t = 0.

By inserting the value of u_0 and u_∞ from (2a) and (4a) into (5) we have:

$$\Delta_f = \frac{m'' - m'}{\pi} \operatorname{tg} \frac{\psi}{2} \cos\left(\frac{\psi}{2} + \varphi\right) - 1. \qquad (6)$$

Figure 2 shows a curve for determining the frequency error calculated from (6) for various values of m" and ratios of m'/m". The angles ψ and φ were calculated for this graph according to the method described in [3]. Dotted lines in Fig. 2 indicate errors calculated by means of (1). It is easily seen that the values of the error determined from this formula correspond to the case of m' = 0 and that the best agreement is attained for large values of m".

In practice, however, m' is never equal to zero owing to the presence of the forward resistance of the rectifier and the internal resistance of the source of the emf. This circumstance should be taken into consideration in all the calculations of such circuits, since even with very small values of m' (of the order of 0.005-0.01) the error is considerably worse than for m' = 0.

Let us illustrate this with an example.

From Eq. (1) it is estimated [1] that in order to keep the error in the circuit below 2%, the value of m' = $= \omega RC$ should be 150. If the finite nature of m' is taken into account, we shall obtain for m' = 0.01 m" from Fig. 2, the required value of m" = 35, i.e., the value of the blocking capacitor can be divided by 4.

Hence, it follows that in calculating rectifier circuits with blocking capacitors it is always necessary to consider the value of parameter m', thus making the capacitor C considerably smaller. It is also possible to decrease the frequency error of such circuits by raising artificially the value of m' by connecting in series with the capacitor or the rectifier a small resistance (without changing the value of the blocking capacitor).

Tests have confirmed the accuracy of the relations thus obtained. Figure 3 shows by means of solid lines the relation of the frequency error to m" obtained by calculation, and by points the one obtained experimentally for values of m' m" = 0.1, 0.05, 0.03, and 0.01, for a crystal diode rectifier D2G. The systematic deviation of the experimental results from the calculated ones for small values of m'/m" is due to these values having been determined with insufficient precision. On the whole the agreement is satisfactory.

LITERATURE CITED

[1] F. Terman and J. Pettit, Measurement Techniques in Electronics [Russian translation] (IL, 1955).

[2] V. P. Sigorskii and L. A. Sinitskii, Élektrichestvo, No. 1 (1959).

[3] V. P. Sigorskii and L. A. Sinitskii, Élektrichestvo, No. 4 (1958).

REWINDING OUTPUT TRANSFORMERS

I. G. Luk'yanchuk

Translated from Izmeritel'naya Tekhnika, 1960, No. 1, p. 42.

In the obsolete automatic electronic potentiometers type ÉPD-07 and bridges types ÉMD-07, ÉMD-207, and ÉMD-237, output transformers sometimes fail. We have established that this is due to the insufficiently good insulation between the windings. In order to eliminate this defect we used empire cloth LKh1, 0.3 mm thick instead of the empire cloth LKhCh2, 0.17 mm thick. When the windings were insulated with two layers of the above cloth, the output transformers worked satisfactorily even when the PÉShO winding wire was replaced by enameled tinned wire. Since their rewinding in September 1959, there were no further failures.

A LAMP FOR LIGHTING ELECTRICAL MEASURING INSTRUMENT SCALES UNDER TEST

M. Sh. Kapnik and A. S. Sergeev

Translated from Izmeritel'naya Tekhnika, No. 9, p. 43, September, 1960

At present, spotlights suitable for illuminating electrical measuring instrument scales under test are not being mass produced.

Normal spotlights are not suitable for this purpose, since they produce bright reflections from the mirror surfaces of the instruments, thus making it impossible to clearly see the position of the pointer.

In the special lamp described in this article and intended for lighting instrument scales in test laboratories (Fig. 1) the requirements are met in the following manner:

1) the scale of the tested measuring instrument is adequately lit;

2) the lighting is diffused, eliminating sharp shadows which hinder the reading of the scale;

3) the mirror of the tested instrument reflects a white diffusing surface instead of a bright source of light, thus providing a convenient background for estimating the position of the pointer;

4) there is no light shining directly into the eye of the operator.

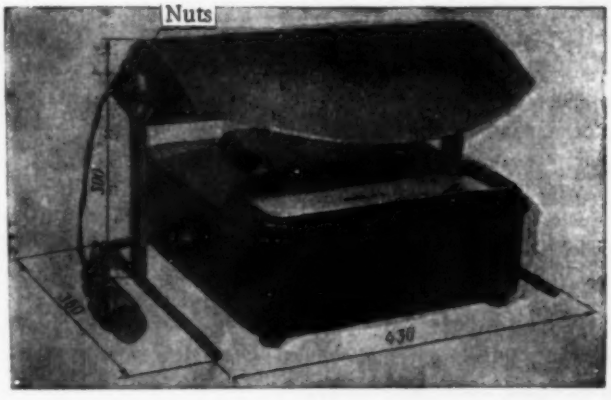

Fig. 1.

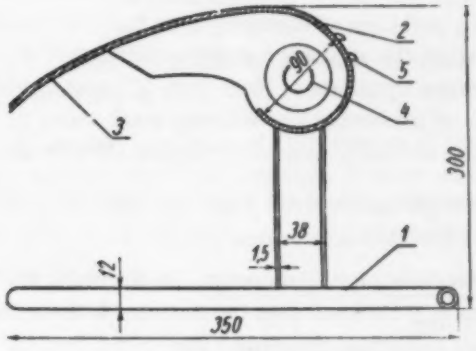

Fig. 2.

The lamp is made of nonmagnetic material and designed for use with instruments of the normal and large size (with a scale up to 300 mm long). It consists of a light frame 1 (Fig. 2) made of brass tubes and a reflector 2. The construction of the frame allows the placing of the lamp with respect to the instrument in a convenient position.

The internal surface of reflector 3 is covered with white paint and reflected from the mirror strip of the instrument providing the desired background.

The shading angle of the lamp can be varied. The fixing of the reflector at different angles to the horizontal plane is achieved by means of springs placed on both sides of the reflector and compressed by special nuts (see Fig. 1).

Two incandescent bulbs 4 (Fig. 2) can serve as a source of light. The power of the bulbs should be chosen to produce adequate illumination without heating up the tested instruments. In order to decrease the heating, a ventilation hole 5 is provided. A fluorescent 15 w lamp can also serve as a source of light. In this case it is necessary to remove the choke coil to a considerable distance from the tested instrument.

HIGH AND ULTRAHIGH FREQUENCY MEASUREMENTS

SLOTLESS MEASURING LINES

A. I. El'kind

Translated from Izmeritel'naya Tekhnika, No. 9, pp. 44-48, September, 1960

Below we examine the use of lines with short-circuiting adjustable devices for measuring the standing wave ratios and load impedances at ultrahigh frequencies. Lines which differ from each other by their methods of coupling are shown in Fig. 1. Some of them have been described in print. This includes line A [1] which evaluates the standing wave ratio of load 1 by the ratio of the maximum and minimum readings (Fig. 1) which are obtained by shifting the short-circuiting device, in a manner similar to a slotted line with an adjustable probe. This line is called a "slotless measuring line." We have used the same name for lines type B and C. Both in [2] and in our own literature an interesting property of line B was noted: the ratio of the maximum and minimum measured standing wave ratio is the square of the standing wave ratio measured with linear detection. This property has been called [2] "standing wave ratio amplification."

The instance of measuring a high standing wave ratio when the line becomes a resonator is examined in [3]. The problems of changing over from the resonance method of measuring [3] to the method of measuring lines, when the measured standing wave ratio decreases, and the differences involved in measuring low standing wave ratios by means of lines with different couplings have not been adequately dealt with in literature. The method of measuring low standing wave ratios by means of lines of the B type has not been described. It is therefore advisable to describe systematically the slotless lines as a special type of instrument.

Relations, which are only applicable to certain types of lines, are indicated by appropriate subscripts in the formula numbers.

Methods of measurement. In discussing the methods of measuring the standing wave ratio from indicator readings it is assumed that the detector follows the square law. The movement of the short-circuiting device produces variations in readings due to two factors. Let us examine them separately.

1. The first factor consists of the displacement of the indicating coupling element with respect to the minima and maxima field distributions in the lines. The form of the distributions in the lines differs with the manner of their excitation.

For instance, in line A the field distribution to the left of the short-circuiting device has the nature of a standing wave and is displaced with the device. The indicating loop always remains in the antinode of the magnetic field (Fig. 1A) and the reading α is only determined by the amplitude of the wave α_k incident to the short-circuiting device. This can be represented taking into account the square law response of the detector as:

$$\alpha = \text{const}\,|a_k|^2. \qquad (1a)$$

The constant represents the coupling of the line with the indicator and its sensitivity.

In line B the field distribution (the standing wave ratio and the position of maxima and minima) to the left of the short-circuiting device is determined by the load (Fig. 1B) contrary to line A in which the load only determines the distribution to the left of the excitation probe.

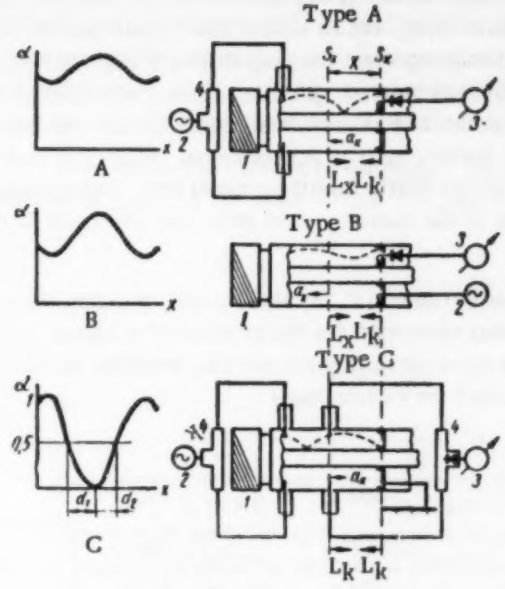

Fig. 1.

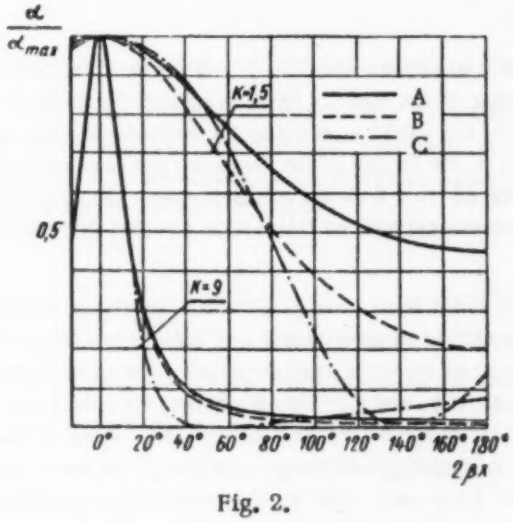

Fig. 2.

The displacement of the indicating loop with respect to a stationary field is equivalent to the displacement of a probe in the slotted lines; the external difference consists in the fact that, in our case, the length of the distribution traversed by the loop is cut off by the short-circuiting device. If the reflection factor L_x of the load is given at a fixed cross section S_x, and the loop is placed in the plane of the short-circuit S_k at a varying distance x from S_x (Fig. 1), the readings may be represented, taking into account the distribution law of the magnetic field along x and the square law of the detector, by the following expression:

$$\alpha = \text{const}\,|a_x(1 - L_x e^{-j2\beta x})|^2, \qquad (1b)$$

where a_x is the amplitude of the wave incident to the load; $\beta = 2\pi/\lambda$ is the attenuation constant.

In line B the standing wave distribution (Fig. 1B) is displaced together with the short-circuiting device with respect to cross section S_x in which the indicating probe is placed. If plane S_k is spaced at a variable distance x from S_k, the detector readings can be represented, taking into account the standing wave distribution law and the square law of the detector, by the expression:

$$\alpha = \text{const}\,|a_k(1 - e^{-j2\beta x})|^2, \qquad (1c)$$

where a_k is the amplitude of the wave incident to the short-circuiting device.

The right hand side of (1c) consists of the square of the standing wave field strength in cross section S_x for an ideal short circuiting device standing wave ratio $K_k = \infty$, $L_k = -1$. In the actual case the following expression holds

$$|a_x(1 + L_x e^{-j2\beta x})|^2 = \left(1 - \frac{2}{K_x}\right)|a_x(1 - e^{-j2\beta x})|^2 + \frac{4}{K_x^2},$$

where $L_k \cong -(1 - 2/K_k)$ is the reflection factor of the short circuiting device. Thus, it will be seen that the correction for the loss in the short circuit of the order of $4K_k^{-2}$ is only important near a node. In the method described below the standing wave curve is not used near the nodes and therefore the second order quantity $4K_k^{-2}$ can be neglected. Factor $(1-2^{-n}K_k)$ is included in the constant.

2. The second factor consists in a resonance variation of the incident wave amplitude when the short circuiting device is moved. This variation is the same in all the types of lines. If plane S_k is placed at a variable distance x from the measuring cross section S_x, the amplitude of the wave incident to the short circuit (a_k) or the load (a_x) can be represented [5] in the form

$$a = \frac{a_0}{1 - L_x L_k e^{-j2\beta x}}, \qquad (2)$$

where a is the actual amplitude of the incident wave (a_x, a_k) if the effect of multiple reflections is taken into account; a_0 is the wave amplitude excluding the above reflections and characteristic of the coupling between the line and the generator and the power of the latter.

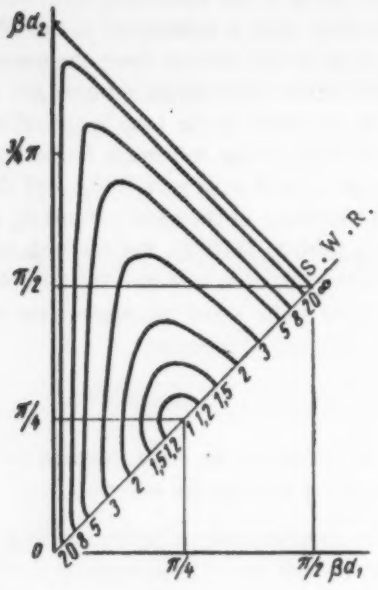

Fig. 3.

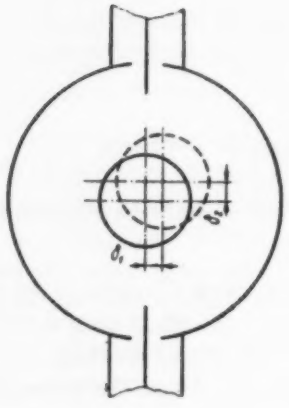

Fig. 4.

When the short circuit is displaced in line A only the second factor affects the reading, but in lines B and C both factors act simultaneously. For instance, when the loop in line B is placed at the maximum distribution created by the load, the field strength in all the distribution points is at a maximum, since in this position of the short-circuiting device, a_x is at a maximum. When the loop is placed to a minimum distribution the general level is also at a minimum. This it the cause of the standing wave ratio amplification in line B [2 and others].

By inserting (2) into (1a, 1b, and 1c) and omitting the constants, we obtain the final expression for the relation of readings α to the position $\underline{x}$ of the short-circuiting device which determine the form of the curves plotted for various lines:

$$A\ \alpha = \frac{1}{|1 - L_x L_\kappa e^{-j2\beta x}|^2} \simeq \frac{1}{|1 + L_l e^{-j2\beta x}|^2}; \tag{3a}$$

$$B\ \alpha = \frac{|1 - L_x e^{-j2\beta x}|^2}{|1 - L_x L_\kappa e^{-j2\beta x}|^2} \simeq \frac{|1 - L_l e^{-j2\beta x}|^2}{|1 + L_l e^{-j2\beta x}|^2}; \tag{3b}$$

$$C\ \alpha = \frac{|1 - e^{-j2\beta x}|^2}{|1 - L_x L_\kappa e^{-j2\beta x}|^2} \simeq \frac{|1 - e^{-j2\beta x}|^2}{|1 + L_l e^{-j2\beta x}|^2}. \tag{3c}$$

The approximate expressions (3) do not account for the fact that the reflection factor of the load L_x in cross section S_x differs from the reflection factor of the load L_l owing to the reflections from irregularities and losses in the length of line between the load and cross section S_x, and the $L_k \neq -1$ owing to the losses in the short-circuiting device. These effects will be taken into account when errors are discussed.

Lines which differ from lines A, B, and C, owing to the interchanging in the positions of generator 2 and indicator 3 (Fig. 1) provide the same readings with the displacement of the short circuit as the respective lines A, B, and C. This is obvious for line B, for the other cases it can be shown either by a similar derivation of the relation of α to $\underline{x}$ or by applying the reciprocity theory for each position of the short circuit when comparing the two lines which differ from each other by the interchanged position of their generators and indicators. By virtue of this reasoning, the methods of determining the standing wave ratio and the load impedance on the corresponding lines, coincide. It should be noted that line B coincides with the circuit for standing wave ratio amplification [2], where instead of the short-circuiting device, the load is moved, which in this case produces the same results. In both cases the characteristic is represented by (3b). In [2] (3b) is given in an approximate form (the right-hand side expression in 3b).

Let us now examine the shape of the characteristics for various standing wave ratios of loads. It will be seen from (3) that the curves obtained in measuring a matched load ($L_l = 0$) on lines A and B degenerate into straight lines, but on line C into an envelope of a standing wave taking into consideration the square law of the detector. When measuring an unmatched load with a low standing wave ratio, the curves of lines A and B have a wavy shape with a smaller difference between the maxima and minima in the case of line A and a larger one for line B. The curve obtained for line B is, in a general case, asymmetrical and always has a node. Figure 2 shows very different curves obtained in measuring the load with a standing wave ratio of 1.5 ($L_l = 0.2$), from those obtained in measuring with a standing wave ratio of 9 ($L_l = 0.8$) which coincide for the chosen scale in the region of the resonance maximum. The two groups of curves approach to each other with a rising standing wave ratio because the resonance variations of amplitude (2) for small displacements of the short circuit are

the same for all types of lines. Owing to the small displacements in this region the first factor which is different for different lines has little effect on the shape of the curves. In the limiting case with a rising standing wave ratio the curves taken for different lines degenerate into the same resonance curve (all the lines become resonators). Therefore, for high Q systems consisting of lines and loads the type of coupling between the line and the indicator has no effect on measurements carried out within the resonance curve bandwidth.

Let us examine the method of measuring the standing wave ratio and the impedance. It will be seen from (3) that line A provides the value of the standing wave ratio from relation:

$$K_l \simeq \sqrt{\frac{\alpha_{\max}}{\alpha_{\min}}}. \tag{4a}$$

line B, from relation:

$$K_l \simeq \sqrt[4]{\frac{\alpha_{\max}}{\alpha_{\min}}}. \tag{4b}$$

The phase φ of the reflection factor can be measured in lines A and B by determining the positions of maxima in two instances: for a connected load and a connected fixed short-circuiting device. In the latter case, the phase of the reflection factor equals $\pm\pi$ and the maximum has a nature of a resonance. From (3a) and (3b) we obtain a relation for determining the phase:

$$\varphi = \pi + 2\beta\,(X_1 - X_0), \tag{4a,b}$$

where X_1 and X_0 are respectively the position of the short-circuiting device in the first and the second case.

The curve obtained for line B has a zero minimum when the probe is in a node of a standing wave. A direct determination of the standing wave ratio in this case is impossible. A simple method can be used in the case of line B for measuring in cross section S_x the characteristic impedance of load Y_l which is related to the reflection factor by the expression

$$L_l = \frac{1 - Y_l}{1 + Y_l}. \tag{4c}$$

The expression for the curve obtained for line B (3b) can be written in the form

$$\alpha = \frac{|1 + Y_l|^2}{|Y_l - j\cot\beta x|^2} = \frac{\text{const}\,(x)}{\text{re}^2 Y_l + (\text{im}\,Y_l - \cot\beta x)^2}. \tag{5c}$$

The numerator of (5c) does not depend on x and does not affect the shape of the curve.

Expression (5c) is obtained from (3b) by inserting (4c) into (3b).

The method of measuring Y_l is based on the fact that the two distances d_1 and d_2 read off the scale of the short-circuiting device and measured from the minimum to the positions corresponding to half the level of the curve (Fig. 1B) fully determine Y_l. The expressions for determining Y_l from the measured absolute distances d_1 and d_2 have the form:

$$\begin{aligned} \text{re}\,Y_l &= \frac{1}{2}(\cot\beta d_1 + \cot\beta d_2); \\ \text{im}\,Y_l &= \frac{1}{2}(\cot\beta d_2 - \cot\beta d_1). \end{aligned} \tag{6c}$$

These relations follow from (5c).

As it has already been pointed out the envelope of the standing wave is obtained with the square law taken into consideration whem matched loads are measured in line B, therefore these measurements provide $d_1 = d_2 = \lambda/8$. By inserting these values in (6c) we obtain $\text{re}Y_l = 1$, and $\text{im}Y_l = 0$.

It is possible to find the standing wave ratio from the measured impedance by means of an impedance (admittance) diagram, or more precisely, from formulas relating the admittance with the standing wave ratio [5].

The direct relation of d_1 and d_2 to the standing wave ratio is shown in Fig. 3. This diagram is symmetrical with respect to its diagonal, therefore only the upper part of it is shown in Fig. 3.

Errors in slotless lines. The sources of errors consist of reflections from irregularities including those of probes; of losses, including those introduced by coupling elements, and of variations in the coupling when the short-circuiting device is moved.

Let us examine them separately.

1. The reflection is characterized by the value of its natural standing wave ratio K_0 due to all the irregularities. The error is due to the fact that the standing wave ratio from load K_x differs from that of load K_l. For the worse phase relation in reflections [5] the following expression holds

$$K_x = K_0^{\pm 1} K_l \tag{7}$$

Hence the maximum relative error due to reflections is

$$\delta K_1 = \pm (K_0 - 1). \tag{8}$$

2. The line losses are characterized by the value of the line transfer constant T; the losses in the short-circuiting device are determined by the value of L_k. The losses introduced by the probes decrease $|T|$; the losses due to the loops decreased $|L_k|$ which has the same effect on the error.

Hence from the direction of the load, without considering the reflections from irregularities, we have:

$$|L_x| = |T^2 L_l| < |L_l|. \tag{9}$$

from the direction of the short-circuiting plunger we have $|L_k| < 1$. In the precise expressions for the curves obtained for lines A and B (3a, 3b) the load reflection coefficients appear only in a combination $L_x L_k$, which can be written by taking (9) into consideration as:

$$L_x L_k = L_l T^2 L_k = L_l L_{in} \tag{10}$$

where L_{in} is the reflection factor at the input of the line at the short-circuiting device end. Hence, for any method of determining the standing wave ratio from the measured curves this ratio is equal to

$$K_{ms} = \frac{1 + L_l L_{in}}{1 - |L_l L_{in}|} = K_l \left[1 - \frac{K_l^2 - 1}{K_l (K_{in} + K_l)} \right]. \tag{11a,b}$$

hence the error due to losses is

$$\delta K_2 \simeq - \frac{K_l^2 - 1}{K_l K_{in}}. \tag{12a,b}$$

The input standing wave ratio K_{in} can be determined from the resonance curve of lines whose input is closed by fixed short-circuiting device. In this case $L_l = -1$ and the curve is represented in the region of its resonance maximum x_0 when (3a) and (10) are taken into account equally for all types of lines (see above) in the form of:

$$\alpha = \frac{1}{|1 - |L_{in}| e^{-j2\beta (x - x_0)}|^2}. \tag{13}$$

It follows from (13) that K_{in} is placed along the width of the resonance curve Δx at half the level with respect to α_{max}:

$$K_{in} \simeq \frac{2}{\beta \Delta x} . \tag{14}$$

It is possible to find in lines A and B from the measured K_{ms} and the input K_{in} the standing wave ratio of load K_l:

$$K_l = \frac{K_{ms} K_{in} - 1}{K_{in} - K_{ms}} \tag{15a,b}$$

(15) is derived from (11). Here the error due to losses is excluded.

The error in line B can be written when (3b), (4b), (9), and (10) are taken into account in the form:

$$\delta K_2 \simeq - \frac{1}{2} \quad \frac{K_l^2 - 1}{K_l K_{in}} - \frac{1}{2} \cdot \frac{K_l^2 - 1}{K_l K_T} , \tag{16}$$

where

$$K_T = \frac{1 + |T|^2}{1 - |T|^2} .$$

3. The error due to the instability of coupling is characterized by the relative difference in readings of different maxima in the same manner as in the case of a slotted line:

$$\delta K_3 = \frac{1}{2} \cdot \frac{\Delta \alpha}{\alpha} . \tag{17}$$

The sphere of application of slotless lines. Slotless lines can be made in the form of waveguides or coaxial cables. Waveguides can be used in the case when slotted lines are inapplicable due to the slot interfering with propagation conditions, for instance, in measuring the standing wave ratio in a round waveguide at wave H_{01}. For this application the coupling elements of the line should be chosen according to the structure of the field of the wave. Work in that sphere seems to be fruitful if one considers the growing importance of wave H_{01} for long communication lines.

Coaxial slotless lines A and B were used by the Novosibirsk State Institute of Measures and Measuring Instruments (NGIMIP) for certifying reference loads in the range of 500-3000 Mc. In this application, the width of the resonance curve of a line shorted at the input is first measured and the input standing wave ratio K_{in} (14) is determined. Next, the standing wave ratio is measured with load K_{ms} connected to the line. The standing wave ratio of load K_l is then determined from the values of K_{ms} and K_{in} (15a,b). This method is similar to the one used for measuring the parameters of dielectrics when the Q factor of an unloaded resonator is taken into account. The accuracy of these measurements exceeds that obtain from normal slotted lines for the following reasons. The natural standing wave ratio of slotless lines can be reduced by dispensing with the resting washer in the coupling device. Here the internal conductor is fixed behind the short-circuiting device. The natural standing wave ratio K_0 is of the order of 1.01-1.02. The smallest K_0 is obtained on B lines at frequencies for which the distance between the probes approaches an uneven number of quarter wavelengths. The instability of coupling when the short-circuiting device is moved in slotless lines is smaller than that due to the movement of the probe in slotted lines. The lateral displacements due to the movement do not change the effective area of the loop, but they can vary the effective length of the probe.

The lateral displacements of the internal conductor in the side direction δ_1 and along the probe axis δ_2 (Fig. 4) do not lead to substantial changes in coupling if double probes are used. In this instance the variations of δ_1 are negligibly small like the side displacements of a probe in slotted lines. The displacement along the axis of the probe is compensated by the fact that the coupling with the generator (indicator) is achieved by means of two identical channels through a T – coupling 4 (Fig. 1). The instability due to the use of double probes and loops amounts to 1%.

Line B is exceptional since it has deformations in the transmitting channel between the generator and the moving loop. If the cable length is considerably larger than the travel of the short-circuiting device (thus decreasing the deformation) the variations in the coupling amount to 3%.

Thus the error in certifying loads by means of A and B lines is estimated at 2-3%. The above data characterize the slotless lines as a type of instruments.

LITERATURE CITED

[1] R. Eichaker, Communication of "Rode and Schwartz," (1953) No. 4.

[2] R. W. Beatty, IRE Trans. MTT-7, No. 3 (1959).

[3] J. Kornfeld, Radiotech. 30, No. 10 (1954).

[4] M. E. Gertsenshtein and L. N. Bryanskii, Izmeritel'naya Tekh. No. 1 (1956).

[5] Transmission Lines for Centimeter Wavelengths [in Russian] ("Sovetskoe Radio," 1951).

A STUDY OF HIGH-Q QUARTZ CRYSTAL PLATES

A. G. Smagin

Translated from Izmeritel'naya Tekhnika, 1960, No. 9, pp. 48-51, September, 1960

At the present time, despite the utilization of molecular generators and cesium frequency standards, the work on the improvement of precision quartz crystal resonators for highly stable generators of standard frequencies and quartz clocks has not lost its importance. In the first place, this refers to the investigation of the possibility of a further improvement of the Q-factor of quartz elements which determines to a considerable extent the stability of the quartz generator frequency.

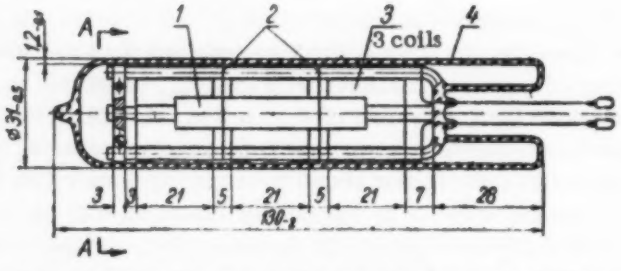

Fig. 1. 1) Quartz plate; 2) fixing threads; 3) electrodes; 4) vacuum bulb.

The All-Union Scientific Research Institute of Physicotechnical and Radiotechnical Measurements has developed Y-cut quartz plates with a Q-factor of $25 \cdot 10^6$. These plates are fixed in the two node planes by means of 20-35 μ diameter threads made of natural silk and tied to four glass rods fused to the base.

The nickel electrodes are round and are fixed to the same glass rods as the plates.

Figure 1 shows the schematic of the quartz plate and the vacuum bulb. Electrodes of a square cross section and those with a circular one inscribed in the square produce the same Q-factor.

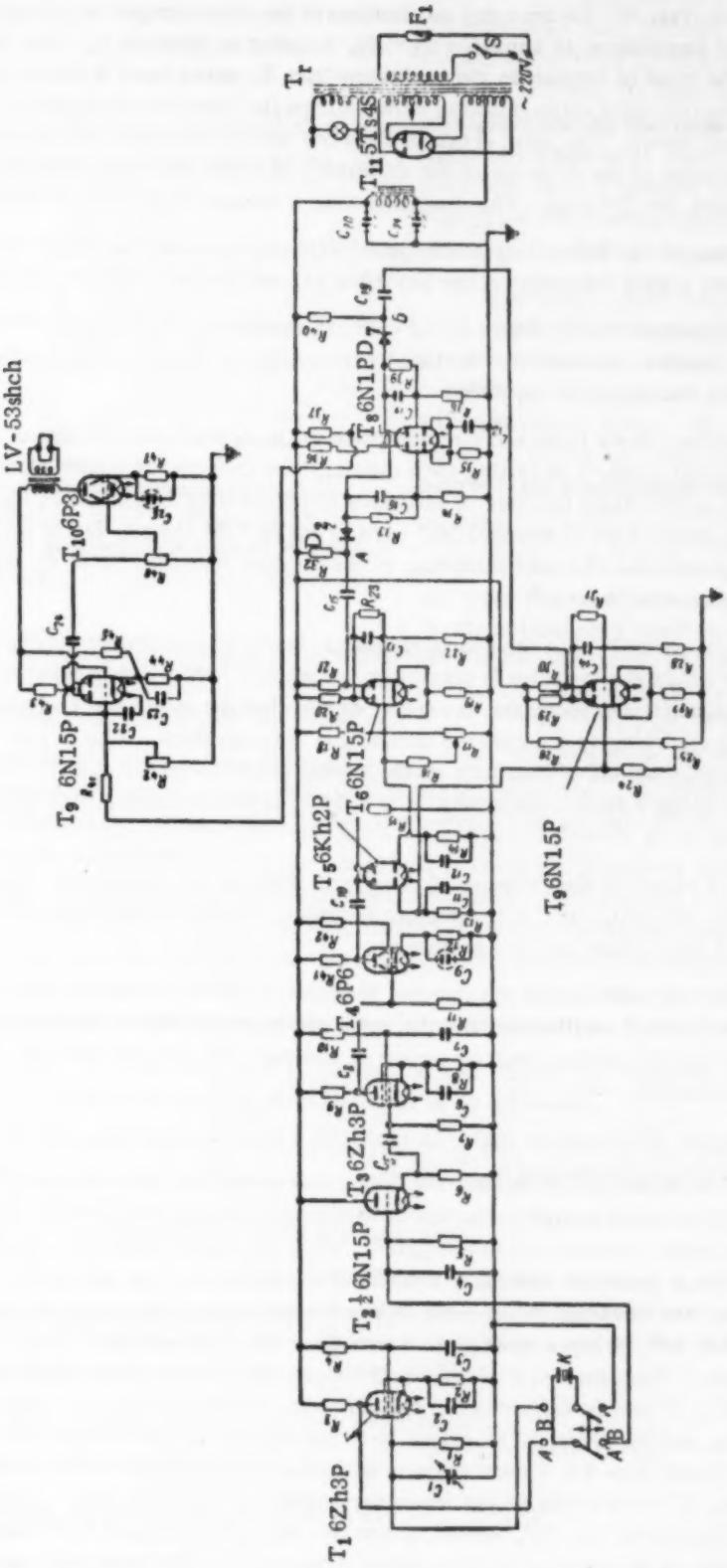
LV-53shch
T10 6P3
T9 6N15P
T8 6N1PD
T6 6N15P
T5 6Kh2P
T4 6P6
T3 6Zh3P
T2 6N15P
T1 6Zh3P
T9 6N15P
Tr
T11 5TS4S
F1
~220V
S
A
B
K

Fig. 2.

The quartz plates are connected in a Pierce circuit operating on a second harmonic at 100 kc. For measurements, the plate is switched over to an automatic meter which measures freely decaying oscillations and has a reactive input impedance (Fig. 2). To decaying oscillations of the resonator are fed through a cathode follower T_2, which has a high input impedance, to amplifier $T_3 - T_4$, and then to detector T_5. The detected signal is fed through two channels to the input of amplitude discriminators $T_6 - T_7$ which have different biasing voltages. The pulse obtained from the discriminator differentiating network trips the first half of trigger T_8. The electronic relay T_9 triggers an electronic timer. The pulse obtained from the second amplitude discriminator disconnects the the timer. From the knowledge of the decrease of the amplitude of freely decaying oscillations by a known factor, it is possible to calculate the Q-factor. This instrument has a measurement error of approximately 1%.

The distinctive feature of this instrument as compared with the one described in [1] is the possibility of measuring the Q-factor over a wide frequency range (50-1000 kc) and the use of an electronic relay.

In [2] quartz crystal plates with a Q-factor of $5.5 \cdot 10^6$ are described. Such a high Q-factor was obtained by carefully cleaning the plates in ammonium fluoride, by increasing the length of the lead-in electrodes and eliminating chamfers along the length of the plate.

The methods of finishing quartz plate surfaces described in [3, 4] provide Q-factors of the order of $4\text{-}5 \cdot 10^6$ without using any other special methods of raising their quality. The Q-factor of quartz plates oscillating at 100 kc and made by the Khar'kov State Institute of Measures and Measuring Instruments (KhGIMIP) in 1957 amounted to $2 \cdot 10^5$ (owing to the work of the KhGIMIP carried out in 1958 their Q-factor was raised at 100 kc to $1.9 \cdot 10^6$). When these plates were finished according to the method described in [3, 4], their Q-factor was raised 20-25 times, i.e., it reached $4\text{-}5 \cdot 10^6$.

It has already been shown in [5] that the quartz resonator, being an anisotropic oscillating system, has an optimum configuration for which the Q-factor is maximum. Moreover, the distance between the fundamental and the partial resonant frequencies is increased to such an extent that the losses due to coupled oscillations in the system are greatly reduced owing to a decreased interaction between them. This is also confirmed by the results obtained in [2]: the grinding off of chamfers on the crystal plates raises the interval between the fundamental frequency and that of the torsion oscillations up to 4.6% (the initial interval was 0.5%) and increases the Q-factor.

For a certain width of chamfers the Q-factor of the quartz plate is at a maximum. It was so far impossible to calculate this effect theoretically. It is therefore necessary to select experimentally the conditions for which the losses in coupled oscillations are at a minimum.

It is however, not only the widening of the interval between the fundamental and partial frequencies which leads to decreased losses in coupled oscillations, but the same effect is attained in decreasing the coupling between the quartz resonator and the driving force by means of widening the gap between the surface of the quartz element and the driving electrodes.

It was possible to excite certain quartz plate samples with a gap between them and the electrodes amounting to 52.2 mm, with the Q-factor increasing to $23\text{-}25 \cdot 10^6$.

The relation of the Q-factor of quartz resonators to various dielectrics placed in the field between the driving electrodes and the quartz element was investigated. When the quartz plate was excited by electrodes of 30×30 mm^2 cross section, a plexiglas plate 1.25 mm thick was placed on one side of the quartz plate between it and the electrode. The Q-factor of the plate before the insertion of plexiglas amounted to $8.9 \cdot 10^6$ and after the insertion of $2.2 \cdot 10^6$. When a glass plate 2 mm thick was inserted the Q-factor dropped to $3.8 \cdot 10^6$; when the thickness of the glass was doubled the Q-factor was halved. When the crystal plate was driven by means of round electrodes 30 mm in diameter, two molybdenum glass mouldings 4.7 mm in diameter were inserted between the crystal and the plates. The crystsl Q-factor without the mouldings was $8.9 \cdot 10^6$ and with $3.2 \cdot 10^6$. When a ground quartz plate 8×8 mm^2 in cross section was inserted in the field between the quartz plate and the electrodes the Q-factor of the quartz resonator dropped to $8.0 \cdot 10^6$, when a similar polished plate was inserted the Q-factor dropped to $8.7 \cdot 10^5$. Hence, quartz has the smallest losses as a dielectric. The external surface of a tube made of such a material is covered by means of cathodic pulverization with electrodes for driving the crystal plate, thus reducing to zero the number of molecules which migrate inside the bulb where the quartz plate is located. It is possible that this effect helped the author to attain [2] a very small aging coefficient of $2.4 \cdot 10^{-12}$ per day.

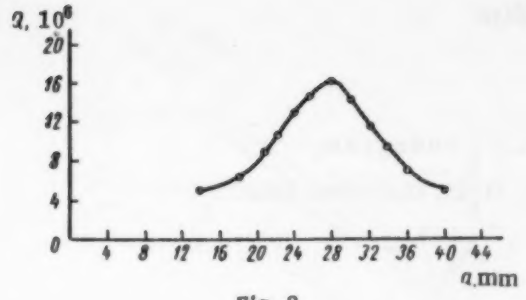

Fig. 3.

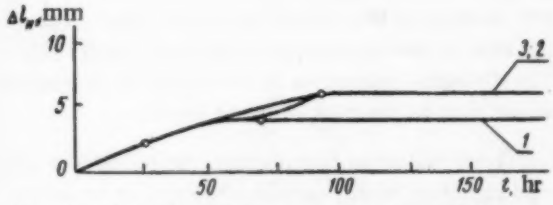

Fig. 4. 1) A load of 20 g-wt; 2) a load of 50 g-wt; 3) a load of 100 g-wt.

The effect of fixing the quartz plates on the Q-factor was studied in the following manner. A quartz plate 112 mm long and 20 x 20 mm^2 in cross section was suspended from its node planes by two natural silk threads which were fixed to plexiglas holders. The distance between the threads was 56 mm. The diameter of the driving electrodes was fixed. Pencil lines spaced by 2 mm were drawn on the quartz plate. The plate was under a pressure $5 \cdot 10^{-2}$ mm Hg. Under these conditions the relation between the Q-factor of quartz plate No. 2 and its fixing were obtained at 48 kc (Fig. 3).

The temperature-frequency coefficient of the above quartz plates is zero in the range of 38-42°C. There are reasons to believe that a zero-temperature coefficient can be obtained for X-cut crystals over a wider frequency range. In a manner similar to quartz lenses [6, 7] this can be attained by varying the cut, gaps and the configuration of the plate.

The relative frequency deviations of the quartz resonator due to variations in the generator supply voltage were measured at a temperature in the zero temperature-frequency coefficient range. In order to prevent the frequency variations due to anode voltage instability to be affected by the heater voltage variations the heaters of the tubes were stabilized. Under these conditions the relation of the frequency to the supply voltages in the Pierce circuit was studied. It was found that $\Delta f/f = 2 \cdot 10^{-10}$ for voltage variations of 1%.

It can be assumed that the finishing methods applied, practically eliminated quartz aging due to surface effects; however aging due to the constant elongation of the hreads by which the crystal plate is fixed should also be reduced to a minimum. Tests were made with three types of threads: those made of natural silk, capron and perlon. The thread diameter was 20-35 μ. First, Hook's curves and hysteresis loops were plotted for the three types of threads. Next, the threads were extended mechanically n times and heated up for a short time to 220°C. Irreversible effects appeared in the threads. Hook's curves and hysteresis loops were plotted again and breaking loads were suspended from the threads thus treated which were each 30 cm long. The aging curve of the silk thread under the effect of loading is shown in Fig. 4. The rate of change in length with respect to time was the highest in the initial period of the perlon thread.

We consider, however, more advisable to use natural silk threads for fixing the quartz plates since their rate of aging does not change with loading from a weight of 50 g upwards.

At present, it is necessary to study not only the raising of the Q-factor as the predominant effect for stabilizing quartz resonators, but also attempt to decrease other instability factors, since their effect may become predominant and reduce the advantages of high-Q oscillating systems to nothing.

LITERATURE CITED

[1] E. D. Novgorodov, Izmeritel'naya Tekhn., No. 4 (1959).*

[2] G. Becker, Arch. Elektr. Ubertragung 12, No. 1 (1958).

[3] A. G. Smagin, Author's Certificate, No. 13449 (1959).

[4] A. G. Smagin, Kristallografiya, No. 6 (1959).

[5] A. G. Smagin, Doklady Akad. Nauk SSSR 118, No. 6 (1958).

[6] E. D. Novgorodov and N. Kh. Neparidze, Izmeritel'naya Tekh. No. 2 (1958).*

[7] A. G. Smagin, Trudy BNIIFTRI, No. 2 (1958).

*See English translation.

MEASURING THE COMPLEX REFLECTION FACTOR OF DIELECTRIC MATERIALS

D. I. Mirovitskii, G. G. Valeev, and I. F. Budagyan

Translated from Izmeritel'naya Tekhnika, No. 9, pp. 51-53, September, 1960

The so-called free space measuring method [1, 2] is being adopted on an increasing scale for determining electromagnetic parameters of various materials. Since the equipment for these measurements consists of waveguide units, and horn and parabolic antennas are used for radiating and receiving electrical energy, their sphere of application is normally limited to milimeter and short wave sections of the centimeter wave range. For longer waves the dimensions of the equipment and the minimum size of material samples increase rapidly [3]. Measuring systems utilizing surface wave transmission lines [4] in the same manner as in the sphere of acoustical measurements [5], make it possible to use much smaller equipment than in the case of space waves.

On the other hand, when only the modulus of the reflection factor has to be determined, the required experimental data is obtained either by measuring samples of the tested material of different thicknesses, or by measuring thin samples and moving during the measurement the shorting device, which is placed behind the sample. It is also possible to measure at different incident angles of vertically and horizontally polarized waves [6]. Owing to the complicated nature of measurements and, in the latter instance, the need for special measuring equipment, it is advisable to utilize free space measurements of the complex reflection factor, and use very simple formulas [7] for computing the electromagnetic parameters of the tested sample.

The instrument (Fig. 1) is designed for measuring complex reflection factors of a plane-parallel sheet material placed in free space in a narrow beam of waves which is produced by an axial radiation antenna [8], and represents a system of surface wave transmission lines consisting of a directional coupler [9] a balancing device and a phase shifter. The balancing device serves to compare the adjustable reference signal with the unknown signal reflected by the sample under test.

The high frequency signal generator 1 is advanced along the line of the surface wave 2 towards the balancing device 3 which consists of crossing surface wave lines and is divided between channels 4 and 6. Section 4 of the basic line consists of a dielectric rod antenna which irradiates sample 5 under test. For greater accuracy of determining the phase of the reflection factor this sample can be pressed against the antenna's external end. Section 6 of the secondary line also consists of a dielectric rod antenna which irradiates a standard reflector 7, consisting of a mesh of plane-parallel thin metallic threads fixed in a circular band. The reflection factor modulus with a slope angle α of the threads (in a plane perpendicular to axis 9-6) is related to the orientation of the incident wave electrical field by the expression $|R_{0\alpha}| = |R_0|\cos\alpha$. The variation of the mesh reflection factor phase with α variations is insignificant, due to its small reactance.

The signals reflected by the sample tested and the standard are added in the balancing device 3, and fed along line 8 through the surface wave directional coupler 9 of the antenna type to the surface wave line segment 10, which is loaded by the null-indicator 11.

The part of the generator energy branched off into the adjustable line 6 depends on the relation between the decelarations of surface wave speeds in the main (2-4) and the adjustable (6-8) lines and the angle between them. By selecting the angle between the lines and the cross sections of the dielectric rods it is easy to obtain the required division of energy between the main and adjustable lines and preserving at the same time a directivity of 45 db in a ± 25% frequency band. Thus, when there is no sample and standard there will be no high frequency energy reaching line 8.

The instrument consists of surface wave lines which are in fact polystyrene rods of 10 × 20 mm cross section (dielectric waveguides).

The reflection factor is measured by comparing the reference signal which is controlled both in magnitude and phase ($U_1 e^{i\varphi_1}$) with the unknown signal $U_2 e^{i\varphi_2}$) reflected by the sample.

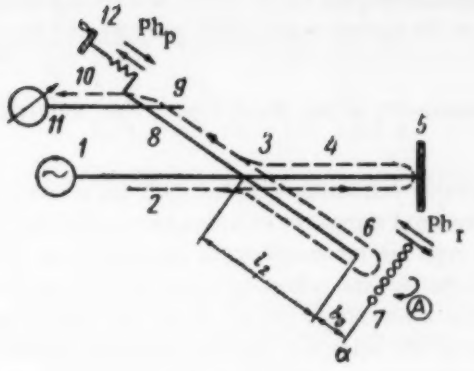

Fig. 1.

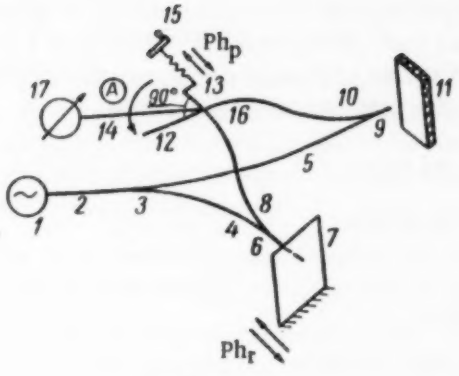

Fig. 2.

The modulus of the reflection factor is determined by the slope angle α of the reference threads, and the phase from the phase shifter rough Ph_r and precise Ph_p readings.

The rough phase measurement is attained by displacing the standard 7 along axis 9-6 (along the direction of the wave propagation). The precise phase measurement of the reference signal is made by means of the so-called electrical vernier, a dielectric waveguide, which is displaced by means of a micrometer screw 12 along the 9-6 axis. When the waveguide is displaced the two interdependent segments of the high frequency line l_2 and l_3 are readjusted with respect to each other. (They stretch from the balancing device to the standard). Their speed of propagation is respectively $v_{ph} = \beta c$ (the dielectric waveguide) and c (the free space segment from the radiating end of antenna 6 to standard 7). With the decelaration of the surface wave phase velocity in line 9-6, i.e., as the value of β tends to unity, the accuracy of phase measurement increases since a phase shift of 180° corresponds to a displacement of dielectric rod 8-6 by $l = \lambda/2\,(1-\beta)$.

The use of an adjustable balancing device (Fig. 2) for equalizing the amplitudes of the reference and the measured signals provides the possibility of excluding from the circuit a standard with a varying reflection factor modulus. The signal fed from the high-frequency generator 1 along the dielectric waveguide 2 is divided in the waveguide splitter 3 between channels 4 and 5 and is fed to the dielectric radiators 6 and 9 which irradiate standard 7 and sample 11. The reflected measured and reference signals are fed through splitters of the antenna type 8 and 10 to the adjustable balancing device 16.

The reflection factor modulus of the sample is determined by the slope angle of the dielectric waveguide 14 of the balancing device. Since the reference 13 and the measured 12 signal arms of this device cross at right angles their decoupling exceeds 40 db, thus providing a very small coupling between the reference and measured signals (less than 1% of the field strength amplitude). When segment 14 is inclined to a position coinciding with the continuation of arm 12, null-indicator 17 only receives the signal reflected from the sample, and when segment 14 is in a position corresponding to arm 13, the null-indicator only receives the signal reflected from the standard. When waveguide 14 is in a balanced position (along the bisector of the angle between arms 12 and 13) the indicator receives both signals with equal transfer constants. The rotation of segment 14 in the direction indicated by the allow leads to a decrease in the amplitude of the signal reflected from standard 7 and an increase in the amplitude of the signal reflected from sample 11 according to an approximate cosine law. The phase of the reflection factor is determined in the same manner as in the instrument shown in Fig. 1 by means of the rough (Ph_r) and precision (Ph_p) scale readings of the phase shifter. In order to reduce multiple reflections the electrical vernier micrometer device 15 is placed outside the irradiation zone.

The measured sample is located in free space thus avoiding the basic defects of measuring in an enclosed system, for instance, in a coaxial measuring line whose errors include those due to gaps between the tested material washer and the internal surface of the line, due to the phase and amplitude irregularities of the sample, since the indicator registers both regularly reflected and dispersed signals, and whose other defects consist of the inconvenient and small dimensions of the washers, a sampling method of control and irreparable damage to the tested material when test washers are made from it.

Moreover, the instrument employs up to date optical methods of measuring materials, thus making it possible to use samples whose dimensions are of the same order as the wave length, to examine parts of large samples

in sections without making contact with the surface and without damaging the material and finally to vary the irradiation area of the sample by changing the deceleration of the surface wave phase velocity and the dielectric radiator.

The high precision of measurement provided by the instruments of the above type is due mainly to two reasons.

1. In order to measure the reflection factor phase in weakly reflecting samples, i.e., the phase of a weak signal, it is necessary in order to decrease the minimum of the total signal, to decrease correspondingly the level of the reference signal. The waveguide devices of this type are inconvenient in use, hence the waveguide impedance meter is only supplied with an adjustable phase shifter for the reference signal [10]. The adjustable balancing device or a standard with a variable reflection factor makes it possible by means of consecutive tuning to equalize with great precision both the amplitude and phase of the reference and the measured signals, which is facilitated by the use of the electrical vernier in the phase shifter.

2. The interaction between the instrument antenna and the standard produces the so-called parcel oscillation of the signal, thus leading to errors in the measurement not only in the modulus but also in the phase of the reflection factor. In order to decrease this error a more complex method of measurement has to be used, i.e., the sample has to be measured repeatedly at varying distances from the antennas [11]. The small interaction with the sample in the instruments of the type here described almost eliminates completely this measuring difficulty which is characteristic of the equipment using waveguide units and ordinary antennas.

LITERATURE CITED

[1] E. G. Goodall and J. A. Jackson, Marconi Rev. 20, 125 (1957).

[2] A. F. Harvey, Proc. IRE 106, B, 26 (1959).

[3] D. I. Mirovitskii, Izmeritel'naya Tekh., No. 2 (1960).*

[4] D. I. Mirovitskii, Author's Certificate, No. 121825 (May 7, 1958).

[5] L. M. Brekhovskikh, Akust. Zhur. 5, No. 1 (1959).

[6] J. S. Seeley, Proc. IRE 105, C, III, 7 (1959).

[7] A. L. Mikaelyan, Radiotekh. i Élektron. 3, No. 7 (1958).

[8] D. I. Mirovitskii and V. D. Dubrovin, Pribor. i Tekh. Éksp., No. 3 (1960).

[9] D. I. Mirovitskii, Author's Certificate No. 124484 (March 18, 1958).

[10] A. I. Zykov, Izmeritel'naya Tekh. No. 3 (1959).*

[11] D. I. Mirovitskii, Pribor. i Tekh. Éksp. No. 4 (1959).

* See English translation.

UTILIZATION OF THE STANDARD FREQUENCY OF 100 kc TRANSMITTED OVER THE RADIO

V. Ya. Volodarskii and A. G. Nikitin

Translated from Izmeritel'naya Tekhnika, No. 9, pp. 53-54, September, 1960

The reception and utilization of the 100 kc reference frequency transmitted over the radio is made difficult due to the lack of special radio receivers. The following two methods of reception are suggested.

1. By using a comparator amplifier intended for checking frequency dividers in standard signal generators type GSS-6. Used as a TRF receiver for the 100 kc signal, this amplifier provides at the output of the last high frequency stage a voltage of 3 v. This signal is fed to the input of the frequency multiplier which then provides frequencies of 100 kc, 1, 10 and 100 Mc. The presence of quartz filters in the multiplying channel raises the quality of the signal waveform. In order to avoid self-oscillations in the receiver, the receiving antenna lead-in is screened.

In order to obtain a set of low reference frequencies (100 cps, 1 and 10 kc) the frequency divider is used, whose input is fed with the 100 kc signal obtained either from the frequency multiplier or the amplifier output. For a stable operation of the circuit it is advisable to connect a simple quartz filter tuned to 100 kc to the input of the frequency divider.

The above equipment can be used in all inspection agencies both under stationary conditions and for mobile tests stations wherever the reception of the 100 kc transmitted frequency is possible.

Thus,the checking of heterodyne frequency meters and other frequency measuring equipment becomes possible under high and medium precision conditions directly in the locations where they are used.

2. By using the reference 100 kc frequency directly in frequency measuring devices (secondary frequency standards) instead of their own 100 kc supply which has an error of $\pm 5 \cdot 10^{-7}$.

The 100 kc unit type 4-UPCh is used in this case as a TRF receiver. An antenna with a screened lead-in is connected to the input of the unit. In order to improve the waveform of the signal all the stages of the unit are tuned to 100 kc without affecting the operation of unit 4-IND.

The amplified signal is fed from the output of unit 4-UPCh to unit 2-ZG to which a special jack is connected for feeding the signal to a frequency amplifier instead of its own master generator of the secondary frequency standard.

Next,the signal is fed from the amplifier normally to all the units of the secondary frequency standard, thus providing fixed frequencies at 100, and 1000 cps, 10 and 100 kc, 1, 10, and 100 Mc with a relative error of the order of $\pm 2 \cdot 10^{-8}$.

Thus, high precision reference frequencies are provided in 3-5 min after switching in without a long heating-up period of the master generator lasting four hours.

The reception of 100 kc by means of the 4-UPCh unit provides a check on the master generator of the secondary frequency standard at any time of the day as distinct from checking it by means of the 1 kc reference frequency which is transmitted by radio only during 15 min each day. The checking of the master generator by means of the 100 kc frequency is done by direct comparison of the reference and the measured frequency (the reference frequency from the output of the 4-UPCh unit and the measured frequency from the output of the 100 kc unit type ZD with the "measure" switch of the 3-IG unit in the "calibrate" position) on an oscilloscope by the Lissajous figures method.

ACOUSTICAL MEASUREMENTS

INVESTIGATION OF SOUNDPROOF COVERINGS FOR SOUND-MEASURING CABINETS

A. N. Rivin and L. Z. Pronenko

Translated from Izmeritel'naya Tekhnika, No. 9, pp. 54-56, September, 1960

In constructing sound-measuring cabinets, great attention is paid to a correct choice of soundproofing coverings. In order to eliminate standing waves inside the measuring cabinet, such coverings should absorb over 99% of the sound energy incident on them, which can only be achieved in practice if the material and dimensions of the coverings are carefully selected. The study of soundproof coverings was made on a special low frequency sound interferometer which measured sound reflection factors in the range of 35-40 to 400 cps. The interferometer horn was made in the shape of a concrete troughof 400×400 mm^2 cross section, 8.5 m long, and covered with lids. A rigid wall which closes the opening of the horn could be displaced by means of a special drive and fixed at a known distance from the surface of the sound absorbing covering sample placed in front of it. The sound vibrations in the horn were generated by means of an electrodynamic loud-speaker placed at the opposite end of the horn. In order to ensure a uniform frequency characteristic of the radiator, the end portion of the horn was deadened by means of fiberglass wedges.

The distribution of pressure nodes and antinodes in the horn and the relation of pressures in the nodes and antinodes was measured by means of a microphone mounted on a highly damped carriage. This equipment could measure the sound amplitude reflection factor with a quadratic mean error of 2%. The first experiments with sound-absorbing coverings were made with normal wool consisting of drawn glass fibers 10 μ thick. Samples made of these coverings consisted of pyramids made of gauze bags which were packed with glass wool of a density of 150 kg/m^3 and a resistance to air blast of 40 rayl/cm.*

These tests showed that the use of such coverings could not provide an absorption exceeding 99% required for the sound measuring cabinets (this absorption corresponds to an amplitude reflection coefficient of 10%) at frequencies below 100 cps.

Glass separator plates made of starch-pasted drawn fiberglass prove to be a more suitable material for making soundproof covering. Samples of such covering in the shape of wedges were cut out of piles of glass separator plates with a specific gravity of 190 kg/m^3 and a resistance to air blast of 30 rayl/cm.

These coverings provide with a cavity of 150 mm as shown in Fig. 1, the required absorption starting at 55-60 cps. However, in this case an additional maximum of reflection arises at higher frequencies and attains 12-15%. In order to eliminate this maximum it is possible to use damping of the cavity between the base of the wedges and the wall by means of glass wool of a density of 125 kg/m^3. Coverings of such a construction provide an absorption over a wide frequency range and can be successfully used in constructing sound-measuring cabinets.

We also studied wedges made of staple fiberglass plates produced by the Merefyansk plant. At a specific gravity of 60 kg/m^3 this material possesses a resistance to air blast of 12 rayl/cm and a sufficient stiffness to be able to make wedges out of it. Samples of covering were made of stapled piles of such laminas and cut

* Translator's note: rayl = rayleigh = acohm/cm^2 = acoustical ohm per square centimeter is a unit of specific acoustical resistance.

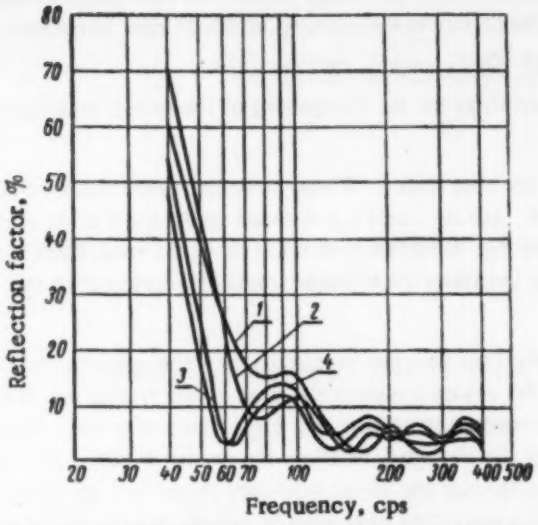

Fig. 1. Sound reflection factor of a soundproof covering made of glass separator plates. Length of wedges is 1 m. 1) Cavity of 30 mm; 2) cavity of 100 mm; 3) cavity of 150 mm; 4) cavity of 200 m.

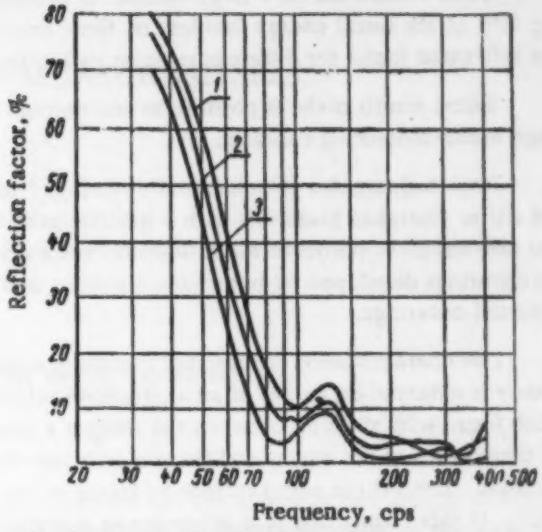

Fig. 2. Sound reflection factor for coverings made of staple fiberglass. Length of wedges 900 mm. 1) Cavity 100 mm; 2) cavity 150 mm; 3) cavity 200 mm.

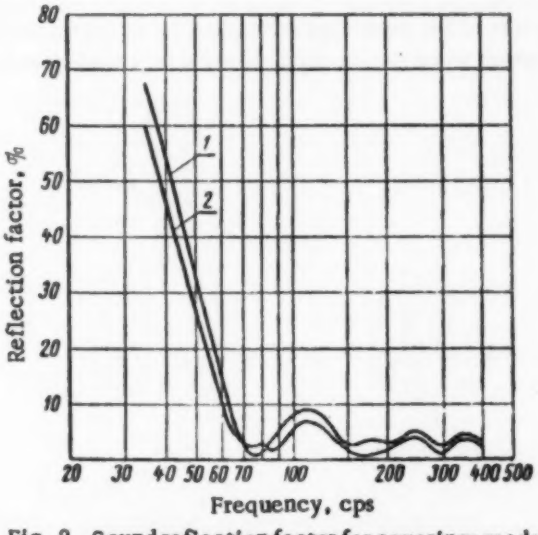

Fig. 3. Sound reflection factor for coverings made of staple fiberglass. Length of wedges 900 mm, cavity width 200 mm, gap between wedges 5 mm. 1) Cavity damped by means of two plates; 2) cavity damped by means of three plates each 60 mm thick.

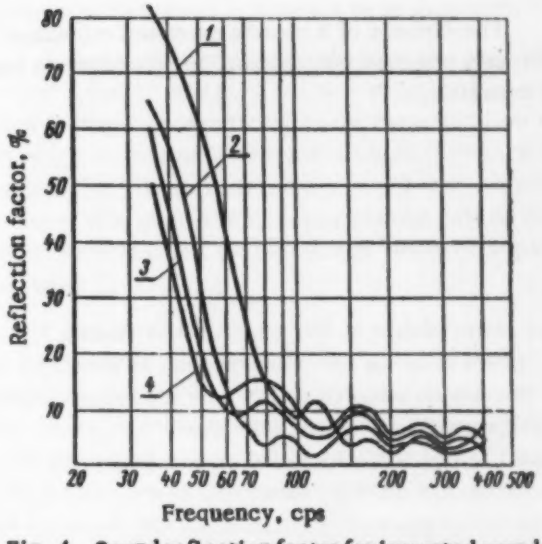

Fig. 4. Sound reflection factor for imported soundproof coverings. Length of wedges 1000 mm, gap getween wedges 5 mm. 1) Without a cavity; 2) a cavity of 100 mm; 3) a cavity of 150 mm; 4) a cavity of 200 mm.

on a tape saw to the shape of separate wedges 400 mm thick. The height of the wedges was 900 mm and their base had a straight portion 100 mm long and a tapering portion 800 mm long thus providing a layout 1 m wide without any loss of laminas. Three wedges were bound into a unit with a foundation of 400 × 400 mm^2. Test results of these coverings are shown in Fig. 2. As a result of these investigations the best type of sound absorbing coverings were selected in the shape of units consisting of three wedges 900 mm long placed at a distance of 100 mm from the wall with the cavity between the wall and the foundation of the wedges filled with three layers of staple fiberglass of a total thickness of 180 mm. Test results for these coverings are shown in Fig. 3.

Tests carried out on a large number of samples showed that such coverings provide an absorption exceeding 99% of the sound energy incident on them over a wide frequency range starting at 60-62 cps. Moreover, the reflection factor for different samples varied by less than 2%.

These results make it possible to recommend these coverings for the equipment of the newly manufactured large sound-measuring cabinets.

Imported samples of soundproof coverings 1 m long were also tested. These coverings were made of denser and stiffer fiberglass materials with a specific gravity of 150 kg/m^3 and a resistance to air blast of 40 rayl/cm. The measurement results of the reflection factor are given in Fig. 4 and show that for an equal total thickness the coverings developed by us provide a similar and in some instances even better sound absorption than the imported coverings.

The characteristics of imported coverings consist in the fact that the required sound absorption at low frequency is obtained by means of an appropriate selection of the cavity between the base of the wedge and the wall which forms with the slots between the wedges a peculiar acoustical resonator of a high figure of merit. When the dimensions of the cavity and the gap between the wedges are changed, or when the cavity is filled with sound absorbing material the sound reflection factor at low frequencies and the lower boundary frequency are sharply raised. In this connection it is necessary in manufacturing and installing coverings to adhere strictly to the dimension of the cavity and the gaps between the wedges, which it is not always possible to attain in mass production and installation of coverings in a sound measuring hall.

Coverings made of staple fiberglass owing to the use of softer and less blast-resisting material do not produce in the cavity between the base of their wedges and the wall a clearly expressed resonance and the variation of their size as well as the gaps between the wedges do not lead to considerable variations in absorption. This peculiarity facilitates the manufacture and installation of sound-absorbing coverings and the achievement of the uniformity of their characteristics.

The absence of a clearly expressed resonance in the cavity of the coverings developed by us confirms the previously observed considerable improvement in sound absorption when the cavity is filled with sound-absorbing materials.

LIQUID AND GAS FLOW MEASUREMENTS

SYMMETRICAL CONSTANT PRESSURE-DROP FLOW GAUGE

D. N. Ulezko

Translated from Izmeritel'naya Tekhnika, No. 9, pp. 56-57, September, 1960

In the Khar'kov State Institute of Measures and Measuring Instruments the author of this article developed a new design for a piston flow meter, with a constant pressure drop, type SRPP (see figure, where on the right the sensing part of instrument PPÉ is shown for comparison purposes).

In the SRPP instrument, the liquid, having passes damper 2, lifts piston 1 by flowing under it until the speed of the jets at the output of both ports, which are then opened, drops to a value when the static pressure applied to the piston from above and transmitted (along channels 3) to the liquid in the cavity above the piston, together with the weight of the piston in the liquid, balances the pressure on it from below.

The piston remains in a balanced condition with an equal pressure on it from above and below, i.e., with a constant pressure difference at the ports (the weight of the piston in the liquid is assumed to be constant).

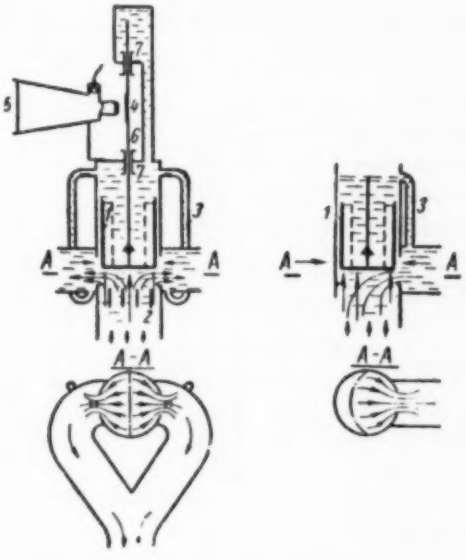

Owing to the rectangular shape of the ports with vertical sides, the height of the port uncovered by the piston is roughly proportional to the measured flow; this height is measured on scale 4 which is projected on to screen 5. The scale is fixed to string 6 which rests by means of a groove in its lower heavier part on the ball of the piston and passes through bushes of a gland-less outlet 7.

Contrary to flowmeter PPÉ in which, owing to the existence of one port only, the piston is always pressed against the wall of the cylinder on the port side, in the instrument SRPP the radial efforts applied to the piston are always balanced. The jets of liquid through the ports of flowmeter SRPP are symmetrical and therefore provide a resultant force applied to the center of the piston along its axis, whereas in flow-meter PPÉ the resulting pressure on the bottom of the piston is sharply displaced to one side and tends to twist the piston.

The upper measuring limit of an instrument with a heavy piston amounts to 10 m^3/hr and with a light piston to 2.5 m^3/hr.

The instrument is supplied with a scale 40 mm long with calibrations of 0.1 mm. The scale is amplified optically by a factor of 62 to 2.5 m.

The 70 mm screen of a small projector which forms a component part of the instrument covers approx-imately 1/35 part of the scale which corresponds to 1 mm movement of the piston.

The symmetrical flowmeter was used for checking 30 mm oilmeters. The meter readings were simultaneously checked by a weighing method.

The tests have shown that in order to provide the required accuracy of checking those meters by means of symmetrical flowmeters it is sufficient to measure them for 15 sec on the first check discharge, for 20 sec on the second and 30 sec on the third (a timer with a calibration of 0.01 sec, for instance, an electrical timer can be used) thus reducing the total duration of testing to 1/10 as compared with the volume measuring method.

The instrument can be constructed in the form of a commercial flowmeter for liquid oil products or as an indicating or recording instrument.

PHYSICOCHEMICAL MEASUREMENTS

AN ULTRASONIC RECORDER OF THE LEVEL OF LIQUIDS

B. A. Syvak and V. A. Nosov

Translated from Izmeritel'naya Tekhnika, No. 9, pp. 57-58, September, 1960

With the development of production automation the requirement in simple and reliable level meters is increasing.

The instrument described in this article is a recorder of the level of liquids made by the Institute of Automation of the State Planning Committee of the Ukr. SSR. It is simple in construction and provides level measurements of liquids in both metallic and nonmetallic containers of any shape for a distance between the transducers not exceeding 1.5-2 m* and in pipes not less than 30 mm in diameter. This makes it possible to use the instrument under the most diverse production conditions. The principle of operation of the instrument is based on utilizing the difference in the acoustical properties of air and liquids. The attenuation of ultrasonic vibrations in air is considerably greater than in liquids. Moreover, the reflection factor of ultrasonic waves from the walls of the container is considerably larger in the metal-air section than in the metal-liquid section. Hence, there is practically no transmission of ultrasonic waves through the walls of the container or inside it above the level of the liquid. Below the level of the liquid, however, part of the ultrasonic energy of the radiator is transmitted to the receiver.

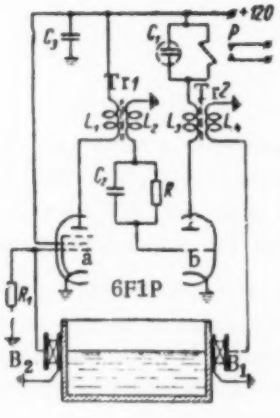

In the above level meter, two barium titanate transducers B_1 and B_2 which operate at 1 Mc are placed on opposite sides of the tank facing each other at the height of the controlled level of the liquid so that a highly directional beam of ultrasonic waves is transmitted from transducer B_1 to transducer B_2, which receives its maximum amplitude. The maximum acoustic coupling between transducers B_1 and B_2 is established experimentally by selecting the position and the slope angle of one transducer with respect to the other.

Transducers B_1 and B_2 are connected to the input and the output of a two-stage amplifier, which is transformer coupled (see figure). The amplifier operates in a self-oscillatory condition which is maintained by an acoustical feedback through the layer of liquid by the barium titanate transducers B_1 and B_2. If there is no liquid in the path of the ultrasonic waves, the amplifier stops oscillating. When the level of the liquid lowers and passes below the transducers B_1 and B_2 the oscillation of the amplifier stops, and relay P operates signalling that the level of the liquid has dropped.

Tests have shown that the error in estimating the level of the liquid in the tank does not exceed 0.5 mm.

The signal from transducer B_2 is amplified by tube 1/2 6F1P (a) and transmitted through coupling transformer Tr1 to the second stage of the amplifier, tube 1/2 6F1P (b). Owing to the large time constant of the RC_2 circuit, the oscillations are intermittent and the current through tube 1/2 6F1P (b) does not exceed 0.2 ma.

* The sounding of containers larger than 1 m in diameter is possible by means of a series connection of two level recorders described in this article.

When the oscillations stop, the current rises to 8 ma. Relay P, which is connected to the anode circuit of the tube, has an operating current of 2 ma and a releasing current of 1 ma. As compared with the current in the tube, this amounts to a four-five fold margin of safety and provides a stable operation of the instrument with the supply voltage changing in the range of 180-240 v.

The transmission of the signal to the barium titanate transducer and its matching anode circuit of tube 1/2 6F1P (b) is done by means of transformer Tr2.

The instrument is mounted on a panel of 110 × 220 mm.

ESSAYS AND REVIEWS

AN AUTOMATIC MEASURING CONVERTER BASED ON THE HALL EFFECT*

Translated from Izmeritel'naya Tekhnika, No. 9, pp. 58-69, September, 1960

Figure 1 shows a circuit for comparing the effective value of an alternating current $I_{\sim}$ with a direct current $I_{_}$. Hall's transducer H_1 has the same alternating current $I_{\sim}$ flowing through it as winding F_1 which provides the magnetic field for the transducer. Moreover, the output of the transducer has a voltage U_1, proportional to:

$$I^2_{max} \sin^2 \omega t = \frac{1}{2} I^2_{max} (1 + \cos 2\omega t), \quad (1)$$

whose direct current component is proportional to $I^2_{max}/2$, where I_{max} is the maximum value of current $I_{\sim}$.

Hall's transducer H_2 is connected in the same manner as transducer H_1, but into the direct current $I_{_}$ circuit. A voltage U_2 proportional to $I^2_{_}$ appears at its output.

Voltages U_1 and U_2 are connected in opposition to each other. When the deflection of the dc galvanometer coil is zero, and hence, $U_1 = U_2$ we have

$$I_{_} = \frac{I_{max}}{\sqrt{2}}, \quad (2)$$

i.e., the value of the direct current is equal to the effective alternating current. Thus, the circuit of Fig. 1 can be used for the same purposes as the thermoelectric, electromechanical and other comparators are being used at the present time. The defect of the circuit in Fig. 1 consists in the use of two Hall's transducers, which may produce errors due to a difference in their characteristics.

This defect can be overcome by using the circuit shown in Fig. 2. This circuit has only one Hall's transducer placed in the field of coil F. The transducer and the coil are traversed simultaneously both by an alternating and a direct current; moreover if at any given time the currents $I_{_}$ and $I_{\sim}$ are flowing in the same direction through coil F, they will flow in opposite direction in transducer H; and coversely if they are opposing each other in the coil they are in the same direction in the transducer. Thus, the voltages produced at the output of the transducer by the direct and the alternating currents are at any instant opposed to each other, and providing condition (2) is observed, their total value at the output of the transducer is zero, i.e., the galvanometer coil will not be deflected. The separation of the dc and the ac circuits is achieved in the circuit of Fig. 2 by means of inductance L and capacitance C. The circuit of Fig. 2 has the advantage of the Hall transducer characteristics, including its relation to temperature, not having any effect on the accuracy of comparing the direct and alternating current.

Figure 3 shows the schematic of the comparator device with an automatic adjustment of the alternating current to a given value of the direct current. The circuit uses one Hall's transducer H and two excitation coils

*An article from the journal: Archiv für technisches Messen und industrielle Messtechnik, No. 290 (March, 1960).

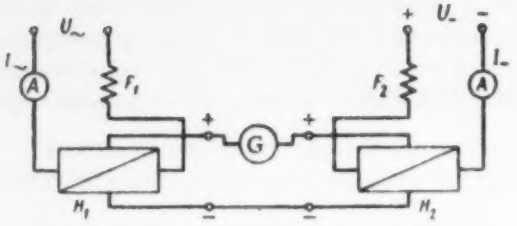

Fig. 1.

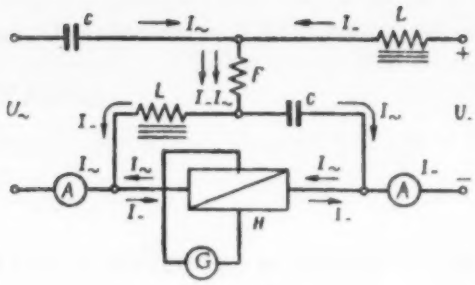

Fig. 2.

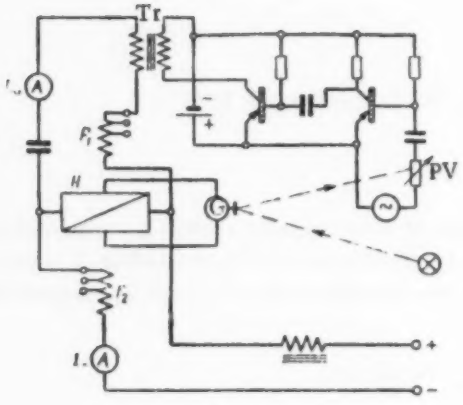

Fig. 3.

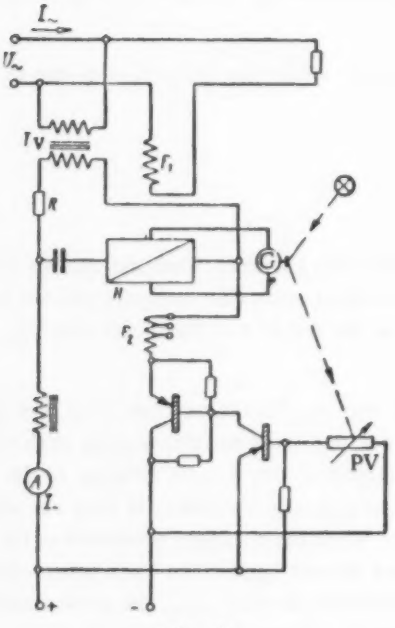

Fig. 4.

F_1 and F_2. An alternating current flows through coil F_1 and a direct current through coil F_2. This provides a simple separation of the dc and ac circuits. If the currents $I_\sim$ and I_- are unequal, the galvanometer G coil is deflected from its zero position thus changing the illumination of the photovaristor provided by the beam, which is reflected from the mirror of the galvanometer. The voltage difference thus produced is amplified by means of a transistor and fed through transformer Tr to coil F_1. The adjustment of current $I_\sim$ will continue until it becomes equal to I_-.

A similar circuit can be used for automatic adjustment of a direct current to the value of a given alternating current.

Figure 4 shows a circuit for automatic conversion of ac to dc power. Contrary to the normal methods of measuring power by means of a Hall's transducer the circuit in Fig. 4 uses a zero balance method which provides certain advantages. The current of the circuit whose power is measured flows through coil F_1. The controlling current is fed to the transducer through a voltage transformer VT. A building-out resistor R is connected in series with the transducer. The value of the direct current which feeds coil F_2 depends on the illumination of the photovaristor PV, i.e., on the position of the galvanometer G coil. The circuit is balanced if the condition shown below is fulfilled:

$$I_-^2 = kU_{max} I_{max} \cos\varphi, \qquad (3)$$

where k is the coefficient of proportionality.

Thus, the circuit provides a conversion of the alternating current power to the square of the direct current. If it is required to obtain a linear relation between the direct current and the alternating current power, coil F_2 should be fed from a direct current stabilized source. Then, the value of the direct current through the transducer will be proportional to the alternating current power. Moreover, by changing the current through coil F_2 it will be possible to change the coefficient of proportionality between the current and the power.

The circuit in Fig. 4 makes it possible to convert to direct current, not only the effective, but also wattless power. For this purpose the phase of the current through coil F_1 should be rotated through 90°. The same effect can be obtained by shifting the phase of the alternating current flowing through transducer by 90°.

An experimental investigation of the above circuits was carried out with a Siemens Halske Hall's transducer type JC24 with an internal resistance of 1.5 ohms. Measurements have shown that in using the circuit in Fig. 2 with manual control of the comparator an accuracy of the order of 0.1-0.2% can be easily attained with currents varying from 25 to 250 ma. Circuits with automatic comparison provide an accuracy of 0.2-0.5%, in the range of 20 to 2000 cps. The Hall's transducer used had a ferrite core with an air gap of 2 mm. It will be probably advisable in future to use the transducers whose coils which provide the magnetic field do not have a ferromagnetic core. This will raise the accuracy of comparisons and conversion.

MATERIAL RECEIVED BY EDITORIAL BOARD

EXPERIENCE OF DEVELOPING DEPARTMENTAL INSPECTION NETWORKS AND INSTRUMENT REPAIR DEPOTS

M. S. Bril'

Translated from Izmeritel'naya Tekhnika, No. 9, pp. 60-61, September, 1960

The coming into force of regulations 12-58 requires an extension and strengthening of the departmental inspection network and instrument repair depots in all the branches of our national economy.

The extension of the types of repaired instruments by the operating inspection agencies, and the establishment of new laboratories, measuring instrument workshops, control and inspection centers and workshops depend to a great extent on the intiative and the organizing ability of the State Inspection Laboratories for measuring equipment.

During the transition period to the new type of State Inspection of Measurement Equipment the Administration of the Plenipotentiary Committee attached to the Council of Ministers of the UkSSR has considered it necessary to reorganize the work of departmental inspection in a planned manner. The inspection laboratories of the Ukraine were set the task of extending in the next 2-3 years efficient departmental and technical supervision to all measures and measuring instruments used in the Republic.

In order to deal with this problem, the State inspection laboratories (GKL) adopted measures as long ago as 1958 for the compiling by all the plants and organizations of plans for developing depaıtmental and technical inspection and repair of instruments.

In order to unify these plans, the administration of the Committee printed special forms. These forms provided information of the types of existing measuring instruments and the extent to which they were covered by inspection, the number and type of instruments which should be additionally covered by inspection in 1959-61 and on the organizational inspection methods.

The organizational and technical work of the laboratories was carried out in stages. In the first place, closer relations were established with the Sovnarkhoz (Councils of National Economy), the Soviet Regional Executive Committees and other regional organizations which, following the advice of the GKL, instructed their subordinated organizations to draft plans for developing instrument inspection. State inspectors were allocated to each large plant and regional organization for helping to develope these plans and advising on all the questions connected with inspection organization.

The plans submitted by the plants and organizations were analyzed in detail by the GKL on the basis of the economic advisability of establishing or extending the inspection and repair agencies. These plans were then summarized on departmental lines. They were then further corrected in conjunction with Sovnarkhoz representatives and regional organizations. The plans outlined the establishment of depot laboratories and their assignment to areas for servicing plants and organizations.

Finally, decisions were made by the Sovnarkhozes, instructions issued by the Soviet regional committees and other regional organizations approving the summarized draft plans for the development of instrument inspection and repairs.

By the end of 1958 the drafting and approval of these plans was in the main completed,and the laboratories began checking their execution. During 1959,new inspection agencies were established in the regions, new depot laboratories and instrument repair plants and centers organized. The technical equipment of the previous existing inspection agencies and repair plants was considerably improved: the areas covered by the control and inspection instrument workshops were extended, the laboratories were supplied with new equipment and reference instruments, the training of the workers engaged in the checking and repair of instruments was improved.

For instance, in the Kiev region in 1959 new inspection agencies were established in 25 plants and organizations, the types of instruments inspected were extended in six enterprises, four new depot laboratories were organized, in 18 factories, center and workshops for repairing instruments were set up.

The Zaporozh'e Sovnarkhoz established depot inspection and instrument repair laboratories in five large plants.

In the republic as a whole 30% more instruments were submitted to departmental and technical inspection in 1959, whereas in the previous years this increase did not exceed 3-4%.

We should draw particular attention to the organization of inspection in agriculture. At first,an attempt was made to entrust technical inspection of instruments to the permanent weighing instrument workshops of the local industry. However,this attempt did not go beyond a formal conclusion of agreements. In this connection, the administration of the committee decided to use the experience gained by the Sadgorsk Tractor Repair Station (RTS) of the Chernovitsy region in organizing instrument repair workshops and extend this experience to the rest of the Ukraine.

The Ministry of Agriculture of the republic issued an order in 1959 for the purpose of improving the organization of repairs instructing the heads of regional agricultural administrations, heads of regional technical supply agencies and directors of RTS to organize in 1959-60 interconnected instrument repair workshops attached to the RTS in sufficient numbers to provide full servicing of collective and State farms and other agricultural establishments and organizations; it also provided for the supply of trucks, equipment and means for purchasing the required apparatus for mobile workshops.

In 1959 with the active assistance of GKL interconnected RTS,instrument repair workshops were established in 15 regions of the Ukraine. In eight regions they are now being established.

The State inspection laboratories have compiled a list of standard equipment required by the RTS instrument repair workshops, supplied them with measuring instruments they could spare and helped in training service mechanics according to a syllabus which included both theoretical and practical instruction in laboratories and instrument repair plants.

The strengthening and improvement in the work of departmental interconnected RTS workshops will make it possible to improve the condition of the measuring equipment in the rural areas of the republic.

ORGANIZING THE WORK OF SECTIONS ACCORDING TO THE TYPE OF MEASUREMENTS

N. V. Malinin

From the experience of the Gor'kii State Inspection Laboratory for Measurement Equipment
Translated from Izmeritel'naya Tekhnika, No.9, p. 62, September, 1960

The Gor'kii State Inspection Laboratory (GKL) for measuring equipment systematically holds meetings of sections of workers engaged in measurments. The radiotechnical section,in whose work the head of the Central Factory Laboratory (TsZL) takes part,meets most often.

The first meetings of the sections dealt with exchanging their most recently gained experiences.

Among other things the radiotechnical section discussed the principle of operation, circuit and technical data of an instrument for determining cable faults (with an accuracy of 0.5 m).

Com. Paul'man, head of the TsZL, stated that his plant developed and introduced a centralized system of supply of a standard frequency to the benches of workers engaged in adjusting and tuning. Previously,each bench carried several instruments which had to be repaired, checked and removed for repairs, whereas now all these instruments have been taken off the benches, much useful space has been made available, and the workers who used to service these instruments have been transferred to other activities. The test frequency is distributed from a single highly stable source and the required frequencies at the benches are obtained by dividing or multiplying the basic frequency by well known methods, thus making it possible to substitute instruments by sockets. As a result of this measure,the saving in the plant amounted to more than 400,000 rubles.

Com. Spiridonov stated that his TsZL has developed and introduced a compensation method of checking ratio transformers at all the specified points. Hand operations in this equipment have been reduced to a minimum, the operator has only to connect the colored ends of the transformer windings to the appropriate terminals, further testing is carried out automatically by switching circuits. The rejection of transformers was very consistent, i.e., the dispersion of measurements amounted to 0.05% and the productivity of labor was raised 12-15 times. The use of this equipment provided a saving of more than one million rubles per annum.

The members of this section were able to obtain all the required information including the circuit and computations referring to this equipment.

After the first few meetings the interest in the work of the radiotechnical section greatly increased. The representatives of the Sovnarkhoz (Council of National Economy) were invited to one of the section meetings. They were told about the deficiencies in the supply of reference radio equipment to the plants and suggestions were made by the Sovnarkhoz and TsZL workers about introducing new measurement equipment and up-to-date technology.

At several meetings scientists read papers on the principles of operation of new instruments, their circuits and technical characteristics.

For instance, a detailed account was given of the technical characteristics of a source of stabilized voltage with a dc and ac output of 0-1500 v, 0-50 amp dc, and 0-100 amp ac. The ac voltage and current are supplied at 50, 400, and 1000 cps. It is possible by means of this instrument to check by the comparison method grade 0.2 instruments and supply potentiometers, thus dispensing with storage batteries.

Our GKL recommended the Sovnarkhoz to supply interested organizations with 27 such instruments.

Lecturers of the industrial electrical equipment department of the A. A. Zhdanov Gor'kii Polytechnic Institute rendered active assistance in the work of the section.

Lectures were also given at the section on the use of transistors in radio instruments, on the types and basic characteristics of radio instruments produced by our industry on the modern efficient ways of raising $\cos \varphi$ in factories and on the repair of electrical measuring instruments.

The section is systematically informed on the instructions of the Committee of Standards, Measures, and Measuring Instruments, on the new instruments entered on the State register, tested and approved for general use and also on the obsolete instruments whose production is discontinued.

We are aiming for each TsZL to have at first a small and simple organizational plan of technical measures for introducing new equipment, means of automatic control and progressive technology, and we discuss the best of these plans. We note in the departmental inspection documents the degree to which the plan has been fulfilled.

The members of the section are keen to adopt the new equipment in their own factories. Thus TsZL workers of one of the plants took part in developing and producing a conveyor 300 m long with automatic addressing of details.

Other sections work in a similar manner to the radiotechnical one including the section on electrical and magnetic measurements.

INFORMATION

MEASUREMENT EQUIPMENT AT THE INDUSTRIAL EXHIBITION OF THE HUNGARIAN PEOPLE'S REPUBLIC

Translated from Izmeritel'naya Tekhnika, No. 9, pp. 63-64, September, 1960

At the industrial exhibition of the Hungarian People's Republic which was held in Moscow from August 12 to September 4, 1960, the production of the instrument-making industry was well represented.

The exhibited radio-measuring instruments covered a range from dc to UHF. The overwhelming majority of them consisted of instruments intended for tuning and checking radio equipment under laboratory, workshop and field conditions.

These instruments include both those of general use (oscillators, universal oscilloscopes, tube voltmeters, etc.), and specialized instruments (television signal generators, special oscilloscopes, "reference" television receivers, etc.). In mentioning radio measuring instruments one should include servicing equipment intended for checking definite pieces of apparatus and exhibited together with these objects. Thus,the equipment of a 24 channel radio-relay station includes seven servicing instruments: a generator of UHF signals and noise with different types of modulation; an intermediate frequency sweep generator, an intermediate frequency noise generator, a harmonic and noise signal meter, a tuned amplifier, a tube test set and an oscilloscope. All these instruments are light-weight and small in dimension. Their accuracy is adequate for checking the equipment and ajusting it in case of failures.

Among the instruments intended for measuring wire communication equipment the transistorized low-frequency oscillator type TH-11 should be noted. Its range is 20 cps to 100 kc; frequency error ± 2%; output voltmeter error ±3%; attenuator error ±2% at a loss of 80 db; its frequency stability is better than ±0.01% with supply voltage variations of +20 to −35% of the nominal voltage with a load varying between infinity and 400 ohms; its coefficient of nonlinear distortions at a level of 1 v does not exceed 0.5%. The weight of the instrument with its batteries is 3.6 kg and its overall dimensions are 203 × 261 × 163 mm.

Many oscilloscope models intended for various purposes were also exhibited.

Orion EMG 1548 is a universal instrument with frequency scanning from 20 cps to 200 kc and a driven sweep from 5 to 10000 μsec. Its vertical amplifier has a range of 5 cps to 8 Mc. The distinctive feature of the instruments consists of a very accurate measurement of time intervals of 0.05 to 1000 μsec. This accuracy is due to the use of a precision delay system with an error of setting not exceeding ± 1%.

Orion KTS 1581/S is intended mainly for tuning television sets, it can however,be used for other work, since it is made for a sufficiently universal application. It has both periodic scanning of 15 cps to 300 kc and a driven sweep of 10 to 1000 μsec. The time markings have periods of 1, 10, and 100 μsec ± 5%. The vertical channel calibrator errors do not exceed ±5%. The vertical amplifier range is 20 cps to 7 Mc and that of the horizontal amplifier 20 cps to 2 Mc. The instrument's characteristic consists in its small overall dimensions (170 × 270 × 385 mm) and light weight (12 kg).

Orion EMG 1538 is used for studying relatively slow processes. It has a periodic scanning of 0.1 cps to 10 kc and a vertical amplifier range of 0.1 cps to 10 kc. A special photographic attachment (Orion EMG 1578/1)

can be supplied with the instrument for recording periodic phenomena directly on a photosensitive tape at a speed of 30, 90 and 200 mm/sec and time markings of ± 0.02 sec ± 2%.

The oscillographic method is used in instrument type 1158/S for determining faults in cables 150 m to 150 km long. This method is also used in equipment KTS 2780/S for recording and observing, by means of piezoelectric transducers rapidly changing pressures and accelerations.

Several types of tube voltmeters and instrument amplifiers were exhibited. The most interesting of these exhibits consisted of a tube microvoltmeter with an instrument amplifier of a range of 10 cps to 300 kc (Orion ÉMG 1316). The lower measuring limit of 30 μv has an error not exceeding ± 2% (at a frequency of 1000 cps); the variation of gain with frequency does not exceed ± 0.5 db; the input impedance is 2 meg with 30 μμf in parallel. When used as an instrument amplifier, the device has a coefficient of nonlinear distortion not exceeding 1% at an output voltage of 2.5 v.

The exhibited UHF instruments included several types of generators, measuring lines, matching devices and sets of coaxial and waveguide channel units.

Signal generator Orion FMV 1271. Its range is 1800-4000 Mc; its output power is 0.5 mw. The peculiarity of this instrument consists in its accurate frequency setting on the scale with an error not exceeding 0.5% and its small stray frequency deviations (less than 0.1 Mc).

Standard signal generator Orion ÉMG 1176. Frequency range of 1800-4000 Mc, output power 10^{-3} to $2 \cdot 10^{-16}$ w, error of power setting ± 2 db; attenuator error ± 1 db, and frequency setting error ± 1%. The generator can work under conditions of continuous oscillations or with frequency or pulse modulation. Its peculiarity consists in dispensing with the use of an output power versus frequency calibration curve. This advantage is attained by a careful balancing of the coupling between the generator tuned circuit, the thermistor cell and the output, as well as a good matching of the cell output to the channel.

Waveguide measuring line type 1762-58. Frequency range of 3300-8180 Mc is covered by two exchangeable waveguides with cross sections of 58 × 29 and 34 × 15 mm. Its natural voltage standing-wave ratio does not exceed 1.03. The line is distinguished by its simplicity of construction and good parameters.

Matched, tunable waveguide moving load type 1765-58 with a waveguide cross section of 29 × 58 mm. Frequency range 3300-4900 Mc. The load includes a matching transformer with a separate adjustment of the modulus and phase of the reflection factor, which provides a standing-wave ratio better than 1.02. Since the load is detachable it can be easily tested for certification and is convenient for checking measuring lines.

The greater part of the electrical measuring instruments shown at the exhibition consisted of grade 1.5 rack-mounted instruments for dc or commercial frequency measurements, as well as laboratory grade 0.2 instruments.

Millivolt-milliammeters type LDA with top ranges of 75 mv and 15 ma. The voltage measuring range is extended up to 750 v by means of external multiplying resistors type RP grade 0.1. The current range is extended to 750 amp by means of external shunts type RP grade 0.2.

Multirange astatic ammeters and voltmeters types LEA and LEV grade 0.2 are produced in the form of ammeters with two, and voltmeters with four measuring ranges.

Reference dc potentiometers type YKA for checking ammeters and voltmeters. The measured voltage is 1 μv to 600 v, and the measured current up to 100 amp. The errors in the value of potentiometer steps amount to 0.02% for decades exceeding 1 ohm and to 0.1% for those of less than 1 ohm.

Of the dosimetric instruments shown at the exhibition the most interesting one was radiometer type 1877. Its range amounted to 0-10000 pulses/sec in 8 bands. Its error is ±2%. Its time constant is 0.2, 1, 5, 20, and 100 sec. The discriminator resolution is less than 2 μsec. The level of discrimination can be set continuously in the range of 5-50 v. The high voltage at the instrument output can be varied in the range of 300-2000 v. The voltage stability is ± 0.5% for supply voltage variations of ± 10%.

Stabilized rectifier type 1842/B. Its output voltage is controlled in the limits of 300 to 3000 v. Its load current must not exceed 0.5 ma. The output voltage stability is ±0.02% with supply voltage variations of +5 to −15% of the nominal voltage.

The measuring equipment shown at the exhibition points to the great successes achieved by the Hungarian Instrument-making industry which is one of the leading industries in the Hungarian People's Republic.

COLLECTION "NEW MEASURING INSTRUMENTS AND METHODS OF CHECKING THEM" (No. I)

Translated from Izmeritel'naya Tekhnika, No. 9, p. 64, September, 1960

A collection of the All-Union Scientific Research Institute of the Committee of Standards, Measures, and Measuring Instruments entitled "New Measuring Instruments and Methods of Checking Them" (No. I) has just appeared in print. The collection contains information about new measuring instruments which are being produced by our instrument-making industry, and indicates their technical characteristics and methods recommended for their checking. Information on instruments of foreign firms is also provided. High precision measuring equipment and instruments which are produced by our scientific research institutes are described. A separate section deals with the data on the exchange of information on rationalization of methods and means for measuring and checking instruments. The measuring methods used abroad are described. A bibliographical note on new publications dealing with measuring techniques is appended.

The publication of this collection aims at introducing in industry and the scientific research institutions new, up to date measuring methods which would ensure unified and precise measures and measuring instruments in the USSR.

Orders for the coming issues of the collection should be addressed to the Distribution Department of the Standartgiz, 4 Shchusev Street, Moscow, K-1.